

# Measurement report: Long-term measurements of surface ozone and trends concentrations in semi-natural sub-Saharan African African ecosystems

- 5 Hagninou Elagnon Venance Donnou<sup>1</sup>, Aristide Barthélémy Akpo<sup>1</sup>, Money Ossohou<sup>2,3</sup>, Claire Delon<sup>4</sup>,  
Véronique Yoboué<sup>3</sup>, Dungall Laouali<sup>5</sup>, Marie Ouafu-Leumbe<sup>6</sup>, Pieter Gideon Van Zyl<sup>7</sup>, Ousmane  
Ndiaye<sup>8</sup>, Eric Gardrat<sup>4</sup>, Maria Dias-Alves<sup>4</sup>, and Corinne Galy-Lacaux<sup>4</sup>

<sup>1</sup>Laboratoire de Physique du Rayonnement, Faculté des Sciences et Techniques,

- 10 Université d'Abomey-Calavi, Cotonou, 01 B.P. 526, Benin

<sup>2</sup>Department of Physics, University of Man, Man, Côte d'Ivoire

<sup>3</sup>Laboratoire des Sciences de la Matière, de l'Environnement et de l'Energie Solaire,  
Université Félix Houphouët-Boigny, Abidjan, Côte d'Ivoire

<sup>4</sup>Laboratoire d'Aérologie, Université Toulouse III Paul Sabatier, CNRS, Toulouse, 31400, France

- 15 <sup>5</sup>Laboratoire de Climat-Environnement et Matériaux-Rayonnement, Université Abdou Moumouni,  
Faculté des Sciences et Techniques, Niamey, BP 10662, Niger.

<sup>6</sup>Department of Earth Sciences, Faculty of Sciences, University of Douala, Douala, P.O. Box 2701, Cameroun

<sup>7</sup>Atmospheric Chemistry Research Group, Chemical Resource Beneficiation, North-West University,  
Potchefstroom, 2520, South Africa

- 20 <sup>8</sup>Centre de Recherches Zootechniques de Dahra, Institut Sénégalais de Recherches Agricoles, Dahra, Senegal

Correspondence to: H. E. Venance Donnou (donhelv@yahoo.fr) and Corinne Galy-Lacaux (corinne.galy-lacaux@aero.obs-mip.fr)

- 25 **Abstract.** For nearly 30 years, in the framework of the International Network to study Deposition and Atmospheric chemistry  
in Africa (INDAAF) program, we present has measured surface ozone from 14 sites in Africa the seasonal variability of  
atmospheric ozone concentrations at the regional scale. The correlations of local atmospheric chemistry and meteorological  
parameters to ozone photochemistry are investigated, as are long-term trends in ozone concentrations. Fourteen measurement  
sites were identified for this study, representative of the main African ecosystems: dry savannas (Banizoumbou, Niger;  
30 Katibougou and Agoufou, Mali; Bambey and Dahra, Senegal), wet savannas (Lamto, Côte d'Ivoire; Djougou, Benin), forests  
(Zoétélé, Cameroon; Bomassa, Republic of Congo) and semi-agricultural/arid savanna (Mbita, Kenya; Louis Trichardt,  
Amersfoort, Skukuza and Cape Point, South Africa). The data are collected with passive samplers and archived as monthly  
averages; quality assurance is maintained by INDAAF's calibration and intercomparison protocols with other programs  
employing the same systems. This analysis reports on correlations of INDAAF ozone time-series (1995-2020) with local  
35 meteorological parameters and with ozone precursors, biogenic volatile organic compounds (BVOC) and nitrogen oxides  
(NO<sub>x</sub>), derived from standard global databases. As part of several study programmes, validation and intercomparison tests of  
passive samplers at remote sites have been carried out to ensure controlled quality measurements and to provide reliable long-  
term gases concentrations. Over the period 1995-2020, monthly ozone concentrations were measured at these sites using  
passive samplers. Mean annual Monthly averages of surface ozone range from 3.94.7±1.14 ppb (Bomassa) to 30.84.0±8.040.5  
40 ppb (Louis Trichardt), reflecting a general positive gradient from West Central Africa to South Africa. Ozone levels in the wet

season (in dry savanna) are higher and in the same order of magnitude to concentrations in the dry season (in wet savanna). In East Africa, ozone levels show no marked seasonality. We established a positive gradient of mean annual O<sub>3</sub> concentrations from West Central Africa to South Africa. In the dry savanna, under the influence of temperature, ozone concentrations are closely linked to Biogenic Volatile Organic Compound (BVOC) emissions ( $0.51 < r < 0.95$ ). It is also sensitive to nitrogen monoxide (NO) emissions in the presence of high precipitation and humidity. Biogenic VOC emissions, anthropogenic NO<sub>x</sub>, temperature and radiation exhibit a good correlation ( $0.49 < r < 0.92$ ) with O<sub>3</sub> in wet savannas and forests. At the southern African sites, the photochemistry of O<sub>3</sub> is influenced by humidity, rainfall, temperature, NO<sub>x</sub> emissions (anthropogenic and biogenic) and VOC. At the decade scale, from 2000 to 2020, Katibougou and Banizoumbou sites (dry savanna) experienced a significant decrease in ozone concentrations respectively around -2.4 ppb decade<sup>-1</sup> (with a very high certainty) and -0.8 ppb decade<sup>-1</sup> (with a medium certainty) at 95% confidence interval. Seasonal Kendall statistical tests revealed with a high certainty decreasing trends of -0.7 ppb decade<sup>-1</sup> in Banizoumbou and -2.4 ppb decade<sup>-1</sup> in Katibougou. These decreasing trends are consistent with those observed for nitrogen dioxide (NO<sub>2</sub>) and biogenic VOCs. An increasing trend is observed in Zoéétéélé (2001-2020), estimated with the Sen slope estimated at +0.7 ppb decade<sup>-1</sup> and at Skukuza (2000-2015; Sen slope = +3.4 ppb decade<sup>-1</sup>). The increasing trends are consistent with the increase in biogenic emissions at Zoéétéélé and NO<sub>2</sub> levels at Skukuza. Very few surface O<sub>3</sub> measurements exist in Africa, and long-term results presented in this study are the most extensive for the studied ecosystems. The importance of maintaining long-term observations like INDAAF cannot be overstated. The data can be used to assess ozone impacts on African crops. For Tropospheric Ozone Assessment Report (TOAR II), they provide invaluable constraints for models of chemical and climate processes in the atmosphere.

## 60 1 Introduction

Ozone (O<sub>3</sub>) is a greenhouse gas, difficult to observe and quantify on a global scale due to its acute spatial variability resulting from its variable photochemical lifetime (between 20 and 25 days) (Cooper et al., 2020; Young et al., 2013). It has phytotoxic effects altering key plant physiological processes that can significantly reduce the productivity of agricultural crops and ecosystems (Dufour et al., 2021; Lelieveld et al., 2015; Mills et al., 2018; Monks et al., 2015). At the local scale, its presence in high concentrations in the lower troposphere is harmful to human health, notably through irritation of the upper airways (Camredon and Aumont, 2007; Schultz et al., 2017). Ozone is a secondary air pollutant, meaning that it is not emitted directly but formed in the troposphere as a result of oxidative chemical reactions of precursor gases such as nitrogen oxides (NO<sub>x</sub>), carbon monoxide (CO) and volatile organic compounds (VOCs) (Lu et al., 2019; Schultz et al., 2017). It is chemically lost by photodissociation or by surface deposition and uptake by plant stomata (Silva and Heald, 2018), or by heterogeneous reactions involving aerosols. Stomatal uptake of O<sub>3</sub> and subsequent damage to plants can lead to changes in biosphere-climate interactions (Sadiq et al., 2017). Mitigating its negative impacts on health requires reducing both pollutant concentrations and population exposure (Petetin et al., 2022). These changes are compounded by the variation of O<sub>3</sub> precursors, which in recent decades have shifted from high and mid-latitudes to low latitudes, where O<sub>3</sub> production efficiency is greater (Zhang et al., 2016). These variations are particularly significant in tropical regions, where seasonal cycles linked to natural and anthropogenic sources of gas and particle emissions are well marked (Adon et al., 2010). Zhang et al. (2016) indicate that both modeling and observational studies about ozone trends are not uniform regionally or seasonally, i.e. even in the tropics where a number of sites with ozonesonde profiles exhibit no trend (Thompson et al., 2021). A study with sondes over equatorial southeast Asia by Stauffer et al. (2024), shows no definite ozone trend annually but a 6-8% decade<sup>-1</sup> increase limited to 3 months.yr<sup>-1</sup>. Air quality forecasts could therefore be used to warn the population of the potential occurrence of a pollution episode (Petetin et al., 2022). Its long-term importance for atmospheric chemistry has been investigated by several studies on air quality (Monks and Leigh 2009) and atmosphere-biosphere interactions (Fowler et al., 2009).

International Global Atmospheric Chemistry Project (IGAC) has produced the Tropospheric Ozone Assessment Report (TOAR) on the global measures for Climate Change, Human Health and Crop/Ecosystem Research

(www.igacproject.org/TOAR). This report stated that free tropospheric O<sub>3</sub> has increased during the industrial era and in recent decades (Gaudel et al., 2018; Tarasick et al., 2019). Despite these years of regional and global surface O<sub>3</sub> research and monitoring, many regions of the world such as Africa, South America, the Middle East and India, remain under sampled, leading to incomplete knowledge of the horizontal, vertical and temporal distribution of O<sub>3</sub> (Cooper et al., 2014; Lin et al., 2015; Mills et al., 2018; Oltmans et al., 2013; Sofen et al., 2016). Although Africa is considered as one of the most sensitive continents to air pollution and climate change, it is one of the least studied (Laakso et al., 2012; Swartz et al., 2020a).

From this perspective, long term measurement programs play a vital role in studies of air pollution and the various changes in the chemical composition of the atmosphere. These long-term assessments are crucial for posing the most topical research questions on atmospheric chemistry (Vet et al., 2014), in order to provide the right answers for relevant decision-making at local and global scale. In situ, satellite, O<sub>3</sub>-sonde and aircraft observations (IAGOS research infrastructure) provide a substantial amount of information on the current distribution of tropospheric O<sub>3</sub>, its variability and trends (Gaudel et al., 2018; Tarasick et al., 2019). They are well suited to improve our understanding of emissions, transport, chemical reactions, deposition processes and the impacts of atmospheric species on human health, vegetation and climate change (Lefohn et al., 2018). Numerous projects and programs long-term have therefore sprung up in several places around the world, for decades. In Africa, the International Network to Study Deposition and Atmospheric Composition in AFrica (INDAAF; <https://indaaf.obs-mip.fr>), operational since 1995, is dedicated to study the evolution of the chemical composition of the atmosphere and deposition fluxes. INDAAF is a national observatory (Service National d'Observation, SNO) of the Institut National des Sciences de l'Univers (INSU) of the Centre National de Recherche Scientifique (CNRS) and of the Institut de Recherche pour le Developpement (IRD), and a labelled component of the European research infrastructure Aerosols, Clouds and Trace gases Research Infrastructure (ACTRIS). The INDAAF long term monitoring network is also labelled by Global Atmosphere Watch (GAW) program of the World Meteorological Organization (WMO) as a contributing network and is a component of the DEBITS (Deposition of Biogeochemically Important Trace Species) activity of IGAC (International Global Atmospheric Chemistry).

Previous studies have considered surface ozone levels in Africa. Indeed, many large African field international campaigns (EXPRESSO, SAFARI/TRACE-A, ORACLES, SAFARI-2000, MOZAIC, AMMA) have been performed over the past 30 years on African air quality and environment. The links to dynamical factors affecting ozone seasonality (Diab et al., 2003, 2004), the interannual variability in ozone related to ENSO and ~~NO<sub>x</sub>NO<sub>x</sub>~~ (Balashov et al., 2014) over the South African Highveld, regional convective influence, and the [El Niño–Southern Oscillation \(ENSO\)](#) transition (Thompson et al., 2003b) and widespread impact of biomass burning and domestic fires in southern Africa occurring several months each year are well established (Thompson et al., 2003b). The mean ozone profile in the lower troposphere over the coast of Gulf of Guinea (December-February) and over Congo (June-August) in the burning season is characterized by systematically high ozone (Sauvage et al., 2005). The combination of high ~~NO<sub>x</sub>NO<sub>x</sub>~~ emissions from soil north of 13°N and northward advection by the monsoon flux of VOC-enriched air masses contributes to the ozone maximum simulated at higher latitudes (Saunio et al., 2009). Adon et al. (2010) characterized the ozone concentration levels (together with several atmospheric pollutants), from 2002 to 2007, at seven remote sites in West and Central Africa, while Martins et al. (2007) investigated O<sub>3</sub> concentrations in Southern Africa over a period of 9 to 11 years (1995-2005). The high ozone values recorded in southern Africa by Martins et al. (2007) are linked to the anthropogenic effect on the chemical species recorded in the atmosphere of the region. Biogenic emissions are the main contributor to ozone production, through the emission of ~~NO<sub>x</sub>NO<sub>x</sub>~~ as precursors during the wet season in the dry savanna region (Adon et al., 2010). This result is consistent with the observations made by Saunio et al. (2009) during the AMMA programme. In the dry season (wet savanna), biomass burning is the dominant factor as mentioned by Sauvage et al. (2005). As for the tropical forests of Central Africa, they appear to be a major O<sub>3</sub> sink. In South Africa, Swartz et al. (2020a) assessed long-term seasonal and interannual trends of O<sub>3</sub> based on a 21-years (1995-2015) dataset at the Cape Point station. This work was continued at 3 historic IDAF-DEBITS sites (Amersfoort, Louis Trichardt, Skukuza, Swartz et al., 2020b). No trends of O<sub>3</sub> were observed at these four sites and the concentrations remained relatively constant over the sampling

130 period. The ~~El Niño–Southern Oscillation (ENSO)~~ made a significant contribution to modelled O<sub>3</sub> levels at Amersfoort, Louis Trichardt and Skukuza confirming thus the studies of Balashov et al. (2014) and Thompson et al. (2003b). The influence of local and regional meteorological factors ~~were/was~~ also evident. Laban et al. (2018) reported O<sub>3</sub> levels in northeastern South Africa, and characterized the links between observed ~~NO<sub>x</sub>/NO<sub>x</sub>~~ and O<sub>3</sub> concentrations. These studies were completed by the effect of precursor species and meteorological conditions on ozone formation (Laban et al., 2020). The critical role of regional-scale O<sub>3</sub> precursors such as high anthropogenic emissions of ~~NO<sub>x</sub>/NO<sub>x</sub>~~ (under a limited regime of VOC), coupled with meteorological conditions are well emphasised and is agreement with Swartz et al. (2020a,b). ~~Further work has been carried out in different locations in Africa to characterise O<sub>3</sub> levels. Other works were carried out by Bencherif et al. (2020), Brown et al. (2022), Gaudel et al. (2020), Hamdun and Arakaki (2015), Ihedike et al. (2023), Josipovic et al. (2010), Khoder (2009), Lannuque et al. (2021), Lee et al. (2021), Ngoasheng et al. (2021), Tsvilidou et al. (2023) and Zunckel et al. (2004) in different locations in Africa to characterize O<sub>3</sub> pollution levels.~~ The conclusions of these studies reported that an increase of tropospheric column with a mean of 1.2 nmol mol<sup>-1</sup> decade<sup>-1</sup> (2.4 % decade<sup>-1</sup>) above Gulf of Guinea and +3.6% over South Africa (Bencherif et al., 2020; Gaudel et al., 2020). A strong diurnal variation of O<sub>3</sub> is observed with a maximum in the mid-day time or afternoon due to the local photochemical production (Hamdun and Arakaki, 2015; Ihedike et al., 2023; Khoder, 2009; Zunckel et al., 2004). The low surface ozone concentrations recorded at ~~many sites the studied sites~~ could be caused by titration of O<sub>3</sub> by ~~NO<sub>x</sub>/NO<sub>x</sub>~~ (Hamdun and Arakaki, 2015; Ngoasheng et al., 2021) but the higher ~~NO<sub>x</sub>/NO<sub>x</sub>~~ concentrations lead to increased O<sub>3</sub> chemical production (Brown et al., 2022). The influence of local climate ~~ie~~ as harmattan, temperature, humidity and radiation on ozone formation have been also raised (Balashov et al., 2014); Ihedike et al., 2023; Khoder, 2009). ~~Using aircraft based measurements of O<sub>3</sub> and a range of its precursors in African wildfire outflow over Senegalese, Ugandan savanna and over the North Atlantic Ocean near Cape Verde, Lee et al. (2021) suggested that the contribution of biomass burning to O<sub>3</sub> burden over the Atlantic could be underestimated. Surface emissions from biomass burning contribute of 24% to boundary layer ozone over Africa (Lee et al., 2021).~~ In the studies of Lannuque et al. (2021), Sauvage et al. (2007), Tsvilidou et al. (2023), it appears clearly that tropical meteorology particularly impacts the O<sub>3</sub> distributions through the movement of air masses in the Intertropical Convergence Zone (ITCZ) by the north-easterly Harmattan flow (January) or the southeasterly winds and monsoon flow (July). Other projects such as POLCA (POLution des Capitales Africaines) and DACCIWA (Interactions Dynamique-Aérosols-Chimie-Nuages en Afrique de l'Ouest), have also been implemented in African capitals such as Bamako, Dakar and Yaoundé (Adon et al., 2016), Abidjan, Cotonou (Bahino et al., 2018) and have provided O<sub>3</sub> concentration surface measurements. These studies confirmed that in cities where NO<sub>2</sub> is high, O<sub>3</sub> is less abundant than in rural areas as reported in Hamdun and Arakaki (2015) and Ngoasheng et al. (2021). However, despite many African studies about ozone and air quality, it should be noted that these campaigns for the most part are only snapshots in time. The number of measurements publicly available is very small and INDAAF is among the few long-term datasets that are available to the scientific community. With the exception of South Africa, O<sub>3</sub> variability is not yet sufficiently documented and very little information is available on the long-term evolution of O<sub>3</sub> chemistry in Africa (Fleming et al., 2018; Gaudel et al., 2018; Mills et al., 2018). ~~Studies on the isoprene emissions changes, the temperature sensitivity of NO<sub>x</sub> and O<sub>3</sub> chemistry (Brown et al., 2022) as well as meteorological changes involved in the seasonality and spatial patterns of ozone trends in the tropics (Stauffer et al., 2024) are therefore recommended. The constraints of the climate response of isoprene emissions, the temperature sensitivity of NO<sub>x</sub> and O<sub>3</sub> chemistry (Brown et al., 2022) on the one hand and on the other hand the meteorological changes meteorological changes when diagnosing regional tropospheric ozone trends and potential shifts in the timing and spatial patterns of biomass burning and ozone precursor emissions in the tropics (Stauffer et al., 2024) are recommended by these authors.~~ The impact of meteorological parameters (temperature, humidity, rainfall, radiation) and atmospheric chemistry (~~NO<sub>x</sub>/NO<sub>x</sub>~~ and VOCs concentrations) on the seasonality of O<sub>3</sub> concentrations, and the analysis of long-term O<sub>3</sub> trends are only partially explained. Further work is therefore needed to fill the data gaps in Africa, and better understand the mechanisms of O<sub>3</sub> formation as a function of ecosystems and their long-term evolution.

As part of the INDAAF program, this study aims to improve the long-term assessment of surface O<sub>3</sub> in the western, central, eastern and southern African regions. In the first objective, we document the long-term (1995-2020 depending on the site) monthly, seasonal and interannual variability of O<sub>3</sub> concentrations on a regional scale at fourteen sites grouped by ecosystem (dry savannas, humid savannas, forests and agricultural/semi-arid savannas), followed by a comparative study with existing references. The study goes further by discussing the seasonal architecture of anthropogenic and biogenic O<sub>3</sub> precursors based on meteorological parameters and emission inventories and the correlation between O<sub>3</sub> and these factors. In the third objective, we use non-parametric statistical tests to assess long-term seasonal and annual trends in O<sub>3</sub>, and discuss the results according to trends in anthropogenic and biogenic emissions of precursors and several new trend studies that include African data. For the first time, the chemical evolution of tropospheric O<sub>3</sub> is examined over the long term at all INDAAF and companion sites. This study provides a robust regional mapping of the long-term seasonal cycle O<sub>3</sub> formation at the continental scale.

## 2. Materials and methods

### 2.1 Sampling sites

Fourteen O<sub>3</sub> measurement sites located in different African ecosystems have been selected for this long-term study of tropospheric O<sub>3</sub> chemistry (Fig. 1), among which 8 stations of the INDAAF long-term monitoring network located in 7 West and Central Africa countries (Mali, Niger, Ivory Coast, Senegal, Benin, Congo and Cameroon). These sites are characteristic of dry savanna, wet savanna, forest, agricultural and semi-arid ecosystems (Table 1). A detailed description of INDAAF monitoring stations and land use classes is available in Adon et al. (2010, 2013). Other sites implemented through INDAAF's companion projects and using the same O<sub>3</sub> measurements protocols were also selected for this study. The site of Dahra in Senegal, part of the 'Cycle de l'Azote entre la Surface et l'Atmosphère en afriQUE' (CASAQUE) project is located in dry savanna and used for grazing (Bigaignon et al., 2020). The site of Mbita, part of the Integrated Nitrogen Management system (INMS) is located in East Africa. In South Africa, four long-term DEBITS sites (Louis Trichardt, Skukuza, Cape Point and Amersfoort) are considered. They are regionally representative of the specific ecosystems of southern Africa. Full descriptions of these South African sites can be found in the works of Conradie et al. (2016), Laakso et al. (2012) and Swartz et al. (2020a,b). All study sites are representative of semi natural rural sites in remote regions. Table 1 presents geographical coordinates and some ecological and climatological characteristics of the sites. In the remainder of the text, the measuring stations will be referred to using the following abbreviations: Banizoumbou (Ba), Katibougou (Ka), Agoufou (Ag), Bambey (Bb), Dahra (Da), Lamto (La), Djougou (Dj), Zoetele (Zo), Bomassa (Bo), Mbita (Mb), Louis Trichardt (LT), Skukuza (Sk), Cape Point (CP) and Amersfoort (Af).

**Table 1.** Geographical, ecological and climatic characteristics of the study sites

Ecosystem	Station	Latitude, Longitude	Country	Land cover classes	Climate
Dry savanna	Banizoumbou (Ba)	13°18' N, 02°22' E	Niger	Open grassland with sparse shrub and culture	Sahelian
	Katibougou (Ka)	12°56' N, 07°32' W	Mali	Deciduous shrubland with sparse trees	Sudano-Sahelian
	Agoufou (Ag)	15°20' N, 01°29' W	Mali	Open grassland with sparse shrub and trees	Sahelian
	Bambey (Bb)	14°42' N, 16°28' W	Senegal	Cultivated grass land with sparse trees	Sahelian
	Dahra (Da)	15°24' N, 15°26' W	Senegal		Sahelian

				Open grassland with sparse shrub and trees, sylvopastoral area	
Wet savanna	Lamto (La)	06°13' N, 05°02' W	Cote d'Ivoire Benin	Mosaic forest/savanna	Guinean
	Djougou (Dj)	09°39' N, 01°44' E		Deciduous open woodland	Sudano-Guinean
Forest	Zoetele (Zo) Bomassa (Bo)	03°10' N, 11°49' E 02°12' N, 16°20' E	Cameroun Congo	Dense evergreen lowland forest	Guinean Guinean
Agricultural field	Mbita (Mb)	0°25' S, 34°12' E	Kenya	Tropical agricultural area	Subtropical
Regional savanna/ Semi-arid	Louis Trichardt (LT)	22°59' S, 30°01' E	South Africa	Cultivated/Semi-arid regional savanna	Subtropical
	Skukuza (Sk)	24°59' S, 31°35' E		Semi-arid regional background site surrounded by natural bushveld in a protected area	Subtropical
	Cape Point (CP)	34°21' S, 18°29' E		Southern Hemispherical marine background site, rocky and sparsely vegetated, Fynbos biome	Mediterranean
	Amersfoort (Af)	27°04' S, 29°52' E		Semi-arid regional savanna, impacted by anthropogenic activities	Warmtemperate

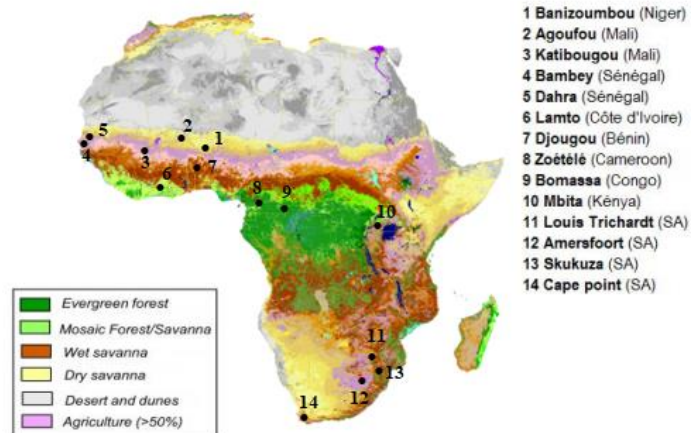


**Figure 1.** Location of the 14 measurement studied sites in Africa on a vegetation map (adapted from Mayaux et al., 2004)

## 2.2 Passive sampling and chemical analysis

### 2.2.1 Sampling procedure

O<sub>3</sub> concentrations were measured using passive samplers developed at the Laboratoire d'Aérodologie (LAERO) in Toulouse in the framework of the INDAAF program, and at the North West University in Potchefstroom in South Africa. They are based on the passive sampling technique, which relies on laminar diffusion and the chemical reaction of the atmospheric pollutant under consideration (Adon et al., 2010; Ferm, 1991 and Martins et al., 2007). These sensors have been tested and validated in different tropical and subtropical regions (Carmichael et al., 2003; Martins et al., 2007). The measurement protocols including passive samplers deployment, analysis by Ionic chromatography and the calculation method of concentrations have been widely described in previous studies (Adon et al., 2010; Bahino et al., 2018; Carmichael et al., 2003; Ferm and Rodhe, 1997; Galy-Lacaux et al., 2009; Galy-Lacaux and Modi, 1998; Osohou et al., 2019; Swartz et al., 2020b). Sampling periods at the measurement sites were coordinated and passive samplers are exposed on a monthly basis using the calendar months. One blank dedicated to ozone is included in the expedition of samplers each two months on sites. In this way, the delay between field deployment and analysis are the same both blanks and exposed samples. All data presented in this paper are blank corrected. A total of 1,317 blanks were assessed at the 14 sites over the studied period. In this paper, we use a monthly database of O<sub>3</sub> concentrations. The concentration measurement period runs from the start date of measurements at each site to 2015-2020 (Table 2). Ozone concentration collection efficiency (%) on the sampling period (ratio of the number of valid concentrations to the number of filters analysed) was assessed at each of the 14 sites (Table 2). All wet and dry seasons duration are indicated in Table 2. These proportions are fairly representative of high quality measurements as indicated in the work of Laakso et al. (2008, 2012), Laban et al. (2018) and Petäjä et al. (2013). Measurements of O<sub>3</sub> concentrations are continuing at the most of sites and are referenced in the INDAAF website (<https://indaaf.obs-mip.fr>).

**Table 2.** Sampling period and concentration data collection efficiency

Ecosystem	Station	Sampling period	Detection limit (ppb)	Data collection efficiency (%)	Total of samplers	Season	Measurement altitude (m)
Dry savanna	Ba	2000-2020	0.1	93.5	248	Dry season: Oct-May Wet season: Jun-Sep	1.5
	Ka	2001-2020		86.7	240		
	Ag	2005-2018		82.6	132		
	Bb	2016-2020		94	50		
	Da	2012-2020		83.7	104		
Wet savanna	La	2001-2020		94.2	240	Dry season: Nov-Mar Wet season: Apr-Oct	1.5
	Dj	2005-2020		92.5	186		
Forest	Zo	2001-2020		86.7	240	Dry season: Dec-Feb and July-Aug Wet season: Mar-Jun and Sep-Nov	3
	Bo	2001-2020		68.3	240		

Agricultural field	Mb	2017-2020		95.3	43	Dry season: Jun-Oct and Jan-Feb Wet season: Mar-May and Nov-Dec	1.5
Regional savanna/semi-arid	LT	1995-2015	0.02	95.2	248	Dry season: Apr-Sep Wet season: Oct-Mar	1.5
	Sk	2000-2015		86	192		
Af	1997-2015	85.5		221			
CP	1995-2020	90.7		248	Dry season: Oct-Mar Wet season: Apr-Sep		

### 230 2.2.2 Validation and quality control of INDAAF passive samplers

To ensure the reliability of the ozone concentrations measurements carried out by the passive sampling monitoring network in West, Central, East and Southern Africa, several validation and quality control tests were carried out as part of the IGAC-DEBITS program and other collaborations with the Swedish Environmental Research Institute (IVL), the AMMA program, the pilot program for measuring urban meteorology and the environment (GURME) launched by the WMO/GAW and the National University of Singapore. These various performance tests were carried out in Africa at the Banizoumbou (Niger), Zoetele (Cameroon), Lamto (Côte d'Ivoire), Djougou (Benin) and Cape Point (South Africa) sites, in France at Toulouse and in Asia (Singapore). In this assessment, the precision and accuracy of the passive samplers used for O<sub>3</sub> monitoring by the various institutions were determined. Ozone<sub>3</sub> detection limits were calculated on the basis of laboratory blank samples. Comparison of gas concentrations measured by passive samplers (integrated over 15 days) and active analysers was carried out at various sites in Toulouse (1998-2020). The test results indicated a good correlation between the two measurement methods, with an average comparative ratio of 1:0.8 for ozone and a correlation coefficient R<sup>2</sup>=0.8 (Adon et al., 2010). During the 2007 AMMA campaign in Djougou, an intercomparison between measurements from passive samplers and active analysers during the wet season from April to September 2006 revealed that the maximum difference observed between the two techniques (passive/active) was around 6% (Adon et al., 2010). In Banizoumbou, Zoétéélé, Lamto and Cape Point, INDAAF and IVL passive samplers were co-located and exposed for a period of one year. The correlation was good between the two types of measurements (Adon et al., 2010; Carmichael et al., 2003). The most recent evaluation of the University of the North West passive samplers used at the South African sites was an international comparison study organised by the National University of Singapore in 2008 (Swartz et al., 2020b). Results indicated that the passive sensors used and operated in INDAAF compared very well with active samplers and had better accuracies. Data quality of the analytical facilities is also ensured through participation in the World Meteorological Organization (WMO) bi-annual Laboratory Intercomparison Study (LIS) (Swartz et al., 2020a,b). The recovery of each ion in standard samples was between 95 % and 105 % (Conradie et al., 2016) and the analysed data were also subjected to the Q test, with a 95 % confidence threshold to identify, evaluate and reject outliers in the datasets (Swartz et al., 2020a). Diffusive samplers have many advantages in the field, including no need for calibration, sampling tubing, electricity or technicians and are small, light, reusable, costefficient and soundless (Adon et al., 2010).

### 2.3 Meteorological parameters and leaf area index

In order to characterize each measurement site, classical meteorological parameters are used such relative humidity, ambient air temperature, rainfall, radiation and leaf area index (LAI). At Ba, Bb, La, Dj and Zo sites, the data on ambient air temperature,



relative humidity and rainfall are extracted from the AMMA-CATCH database (Analyse Multidisciplinaire de la Mousson Africaine - Couplage de l'Atmosphère Tropicale et du Cycle Hydrologique; [www.amma-catch.org/](http://www.amma-catch.org/)) and the Observatoire de recherche en environnement "Bassins versants tropicaux expérimentaux" (SO BVET; [bvet.obs-mip.fr/](http://bvet.obs-mip.fr/)) (Ossouhou et al., 2019). The measuring devices used at Ka, La and Bo is described in the same work (Ossouhou et al., 2019). At Bb site, relative humidity, temperature and rainfall are collected in the INDAAF database (<https://indaaf.obs-mip.fr/>). At Da site, measurements of meteorological parameters come from a measuring station installed by the University of Copenhagen (Bigaignon et al., 2020). In Ka, Ag, Bo, Mb, LT, Af, Sk and CP, the meteorological data are provided by the intermediate reanalysis archive (ERA 5) of the European Center for Medium-Range Weather Forecasts (ECMWF). The time series of global solar radiation used in this study at all sites except Dahra are also ERA 5 reanalysis data obtained from ECMWF. To ensure the reliability of the ERA5 data on the study sites, we determined the estimation errors (RMSE) and the correlation between the reanalysis data and those measured in situ. We chose the Banizoumbou site in Niger (2000-2020), which hosts a meteorological station that provides temperature, humidity and rainfall data, and the Dahra site, where radiation data are measured. We obtained a low error estimate (RMSE) of the order of  $9.9 \times 10^{-3} \text{ }^\circ\text{C}$  for temperature,  $4.8 \times 10^{-3} \%$  for humidity and  $2.3 \times 10^{-1} \text{ mm}$  for rainfall in Niger. At the Bambeï site in Senegal, the estimated errors are of the order of  $6.4 \times 10^{-2} \text{ J/m}^2$  for radiation. The correlation between in situ and ERA5 data for these two sites is very good and is about of 0.96 for rainfall, 0.99 for humidity, 0.80 for radiation and 0.99 for temperature. LAI data are obtained from MODIS (Moderate Resolution Imaging Spectroradiometer) with a resolution of  $0.25 \text{ km}^2$  for an 8-day time scale centred around each station (Ossouhou et al., 2019). All these parameters are collected at the same sampling period as  $\text{O}_3$  concentrations, with the exception of LAI measurements, which began in 2000 (<https://modis.ornl.gov/data.html>).

280

#### 2.4 ~~$\text{NO}_x$~~ and VOC emissions

The emissions of ~~volatile organic compounds (VOCs)~~ and ~~nitrogen oxides ( $\text{NO}_x$ )~~ from biomass combustion were downloaded from the ECCAD (Emissions of atmospheric Compounds and Compilation of Ancillary Data) database in the GFED4 inventories for  $0.25^\circ \times 0.25^\circ$  grid cells. BVOC emissions are extracted from the MEGAN-MACC inventory in the ECCAD database ([eccad.aeris-data.fr](http://eccad.aeris-data.fr/)). The biogenic  $\text{NO}$  fluxes used are model outputs in reference to the work of Delon et al. (2010, 2012). They were filtered in the eastern grid from  $5^\circ\text{S}$  to  $20^\circ\text{N}$  in latitude, and  $20^\circ\text{W}$  to  $30^\circ\text{E}$  in longitude over the period from 2002 to 2007 and cover only the Ba, Ka, Ag, La, Dj, Zo and Bo sites. ECCAD platform is the emissions database of the international GEIA project (Global Emission Initiative: [geiacenter.org](http://geiacenter.org)) has been developed within the framework of the French atmospheric data center AERIS (<http://www.aeris-data.fr/>) (Darras et al., 2022). The GFED4 inventory is based on satellite data of fire activities and vegetation productivity observed since 1997 ([eccad.aeris-data.fr](http://eccad.aeris-data.fr/)). MEGAN (Model of Emissions of Gases and Aerosols from Nature) inventory quantifies net biogenic emissions of isoprene and other gases emitted by vegetation into the atmosphere (Guenther et al., 2006; Sindelarova et al., 2014). The determining variables of MEGAN are derived from models and satellite and ground observations, enabling simulations to be carried out on a regional and global scale. They take into account the emission factor, which represents the emission of a compound in the canopy under standard conditions, the emission activity factor, which included changes in emission due to deviations from standard conditions, and the factor that explains production and losses within the plant canopy (Guenther et al., 2006). Isoprene,  $\alpha$ -pinene and  $\beta$ -pinene, which account for the largest proportion of BVOCs emitted by vegetation in Africa (Ferreira et al., 2010; Jaars et al. 2016; Liu et al., 2021; Saxton et al., 2007; Serça et al., 2001), were identified and used in this study. A more detailed description of these emission inventories is discussed in the work of García-Lázaro et al. (2018), Guenther et al. (2006) and Vitolo et al. (2018). For each emission category,  $\text{NO}_x$  ( $\text{kg m}^{-2} \text{ s}^{-1}$ ) and VOC ( $\text{kg m}^{-2} \text{ s}^{-1}$ ), we use the sum of fluxes from all biomass combustion sources (agricultural, waste combustion, savanna, grassland, scrubland, boreal forest, temperate forest, tropical deforestation, peat degradation and peat fires) at a monthly scale and over the study period for each site. These inventories emissions are widely used and Global Fire Emissions Database GFED have been recommended by Stauffer et al. (2024) to study potential shifts in the timing and spatial patterns of biomass burning and ozone precursor emissions in the tropics.

300

## 2.5 Statistical analysis

The Mann-Kendall and seasonal Kendall tests, associated with the calculation of Sen's slope (Sen, 1968) is applied to all sites with at least 10 years of measure using XLSTAT 2022.2.1.1313 software at 95% confidence intervals. In the case of Kendall's seasonal test, the seasonal nature of the series is taken into account. The literature provides extensive information on Mann Kendall trends calculations (Frimpong et al., 2022; Hirsch et al., 1982; Kendall, 1975; Merabtene et al., 2016). Vectors with p-values less than 0.05 exhibit a very high certainty to obtain the trend, while vectors with p-values in the range of 0.05–0.10 give a [medium](#) indication of a trend (Gaudel et al., 2018). Vectors with p-values in the range of 0.10–0.34 provide a weak indication of change, and p-values greater than 0.34 indicate [very](#) weak or no change. The vectors with p-values in the range of 0.05–0.34 are very useful for understanding regional trends as they typically follow the same pattern as the very high certainty vectors (Chang et al., 2017; Gaudel et al., 2018). Another non-parametric breakpoint test (Pettitt test) is carried out using Khronostat 1.01 software to assess possible breaks in homogeneity in the O<sub>3</sub> concentration series and for optimal application of the trend test.

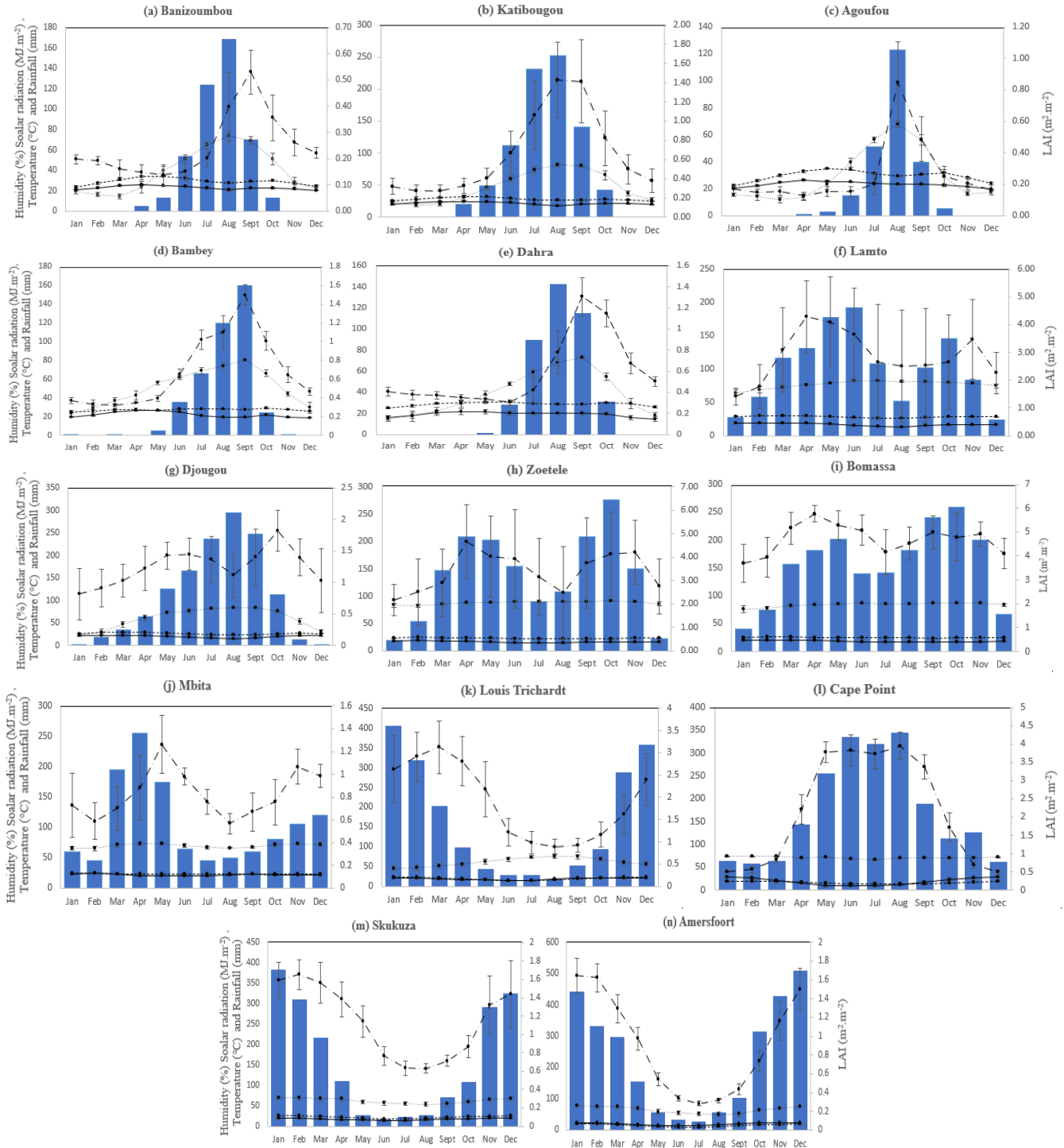
## 3. Results and discussion

### 3.1 Meteorological and biophysical parameters variation

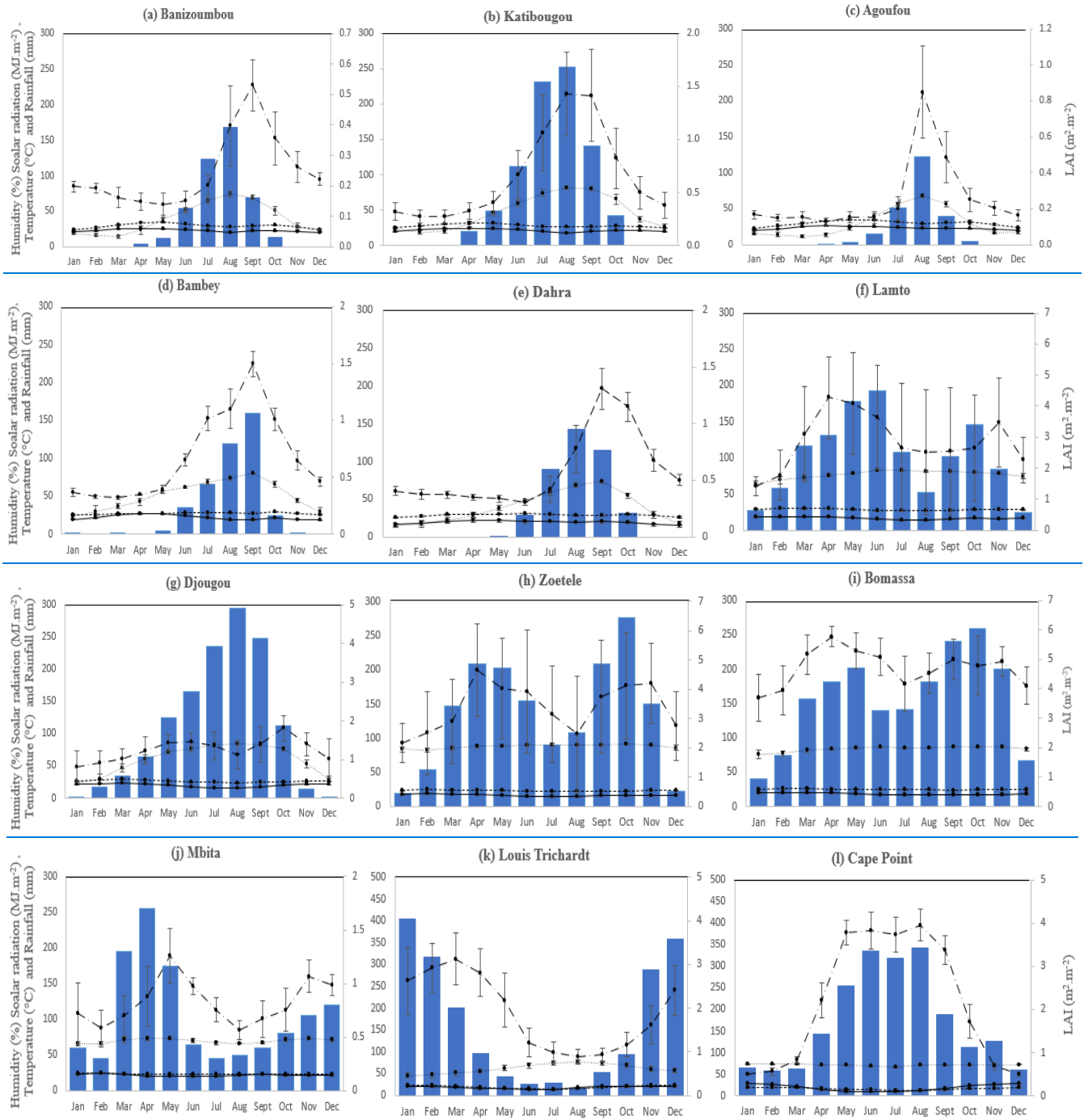
The monthly variations of meteorological parameters and leaf area indexes (LAI) are shown in Fig. 2 for all sites. In dry savanna, the rainfall regime is unimodal, with the greatest amounts of rain recorded from July to September corresponding at the maxima of LAI. Mean air temperature ranged from  $22.1 \pm 0.9^\circ\text{C}$  to  $34.9 \pm 0.4^\circ\text{C}$ , with air relative humidity from 68% to 82%. The most elevated solar radiation is found at Ag ( $23.1 \pm 0.5 \text{ MJ}\cdot\text{m}^{-2}$ ). In wet savanna and forest sites, the rainfall pattern and LAI follow a quasi-bimodal distribution. The mean annual LAI varies from  $1.2 \pm 0.3 \text{ m}^2\cdot\text{m}^{-2}$  (Dj) to  $4.7 \pm 0.7 \text{ m}^2\cdot\text{m}^{-2}$  (Bo). The most significant monthly variations in relative humidity are found in Dj (23.2 - 84.1%). At Mb site, the maximum rainfall occurs between March and May, reaching 255 mm in April. The vegetation cover is denser at the end of the first wet season ( $1.3 \pm 0.3 \text{ m}^2\cdot\text{m}^{-2}$  in May) with an average value of humidity around 70%. In Southern Africa, the humidity varies from 13% to 22% year-round except at CP where variations are very low. The maximum of rain is collected between December and January (432 mm on average) at LT, Af and Sk sites and in August at CP (343 mm). LAI maxima are of the order of  $1.6 \pm 0.2 \text{ m}^2\cdot\text{m}^{-2}$  at Af ;  $3.1 \pm 0.6 \text{ m}^2\cdot\text{m}^{-2}$  at LT;  $4.0 \pm 0.1 \text{ m}^2\cdot\text{m}^{-2}$  at CP and  $1.7 \pm 0.2 \text{ m}^2\cdot\text{m}^{-2}$  at Sk in wet season. In wet savanna and forest, the temperature variations are low, as well as in Mb ( $23.6 \pm 0.5^\circ\text{C}$ ). On the other hand, at the South African sites, the temperature reaches amplitudes ranging from  $6^\circ\text{C}$  to  $10^\circ\text{C}$ . From wet savanna to semi-arid savanna (South Africa), the average solar radiation is below at  $22 \text{ MJ}\cdot\text{m}^{-2}$ . Along the north-south transect for the study sites, the gradient of humidity, leaf area index and rainfall are positive, whereas it is negative for temperature and radiation. The variations in meteorological parameters are strongly influenced by the alternating seasons. These characteristics are dependent on the type of climate. Indeed, in West and Central African climate (and its variability) is a function of the position of the [Inter-Tropical Convergence Zone \(ITCZ\)](#), which is a band separating the hot and dry continental air coming from the Sahara desert (Harmattan) from the cooler, humid maritime air masses (Monsoon) originating from the equatorial Atlantic Ocean (Adon et al., 2010; Lannuque et al., 2021; Sauvage et al., 2005). Its geographical shift from the Northern Hemisphere during the boreal summer to the Southern Hemisphere during the boreal winter with different positions throughout the year (for example in January, around  $5^\circ\text{N}$  and in August, around  $22^\circ\text{N}$ ) define the seasons in this region of Africa and explain the marked seasonal variations observed in West and Central Africa (Sauvage et al., 2005). The position of the convergence zone gives rise to the “wet” seasons. Compared with West Africa, East Africa exhibits slightly different regimes due to the topography and the proximity of the Indian Ocean. The climate of southern Africa is characterized by alternating wet and dry periods which are also modified by the position of the ITCZ (Lannuque et al., 2021). Within the ITCZ warm and humid surface air masses converge and are convectively uplifted into the upper troposphere. The uplifted air masses are then advected polewards in the upper branches of the Hadley cells. The

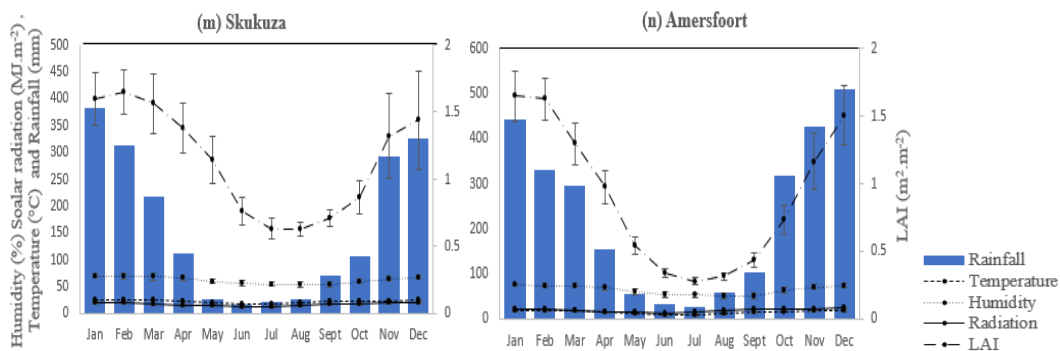
dry air in the descending branches of these cells creates the conditions for wildfires and the resulting emission of ozone precursors (Lannuque et al., 2021).

350



355





365 **Figure 2.** Mean monthly variation in air temperature ( $^{\circ}\text{C}$ ), rainfall (mm), relative humidity (%), solar radiation ( $\text{MJ}\cdot\text{m}^{-2}$ ) and  
 370 leaf area index ( $\text{m}^2\cdot\text{m}^{-2}$ ). The mean absolute deviation is represented by the vertical bars.

### 3.2 Characterization of $\text{O}_3$ levels

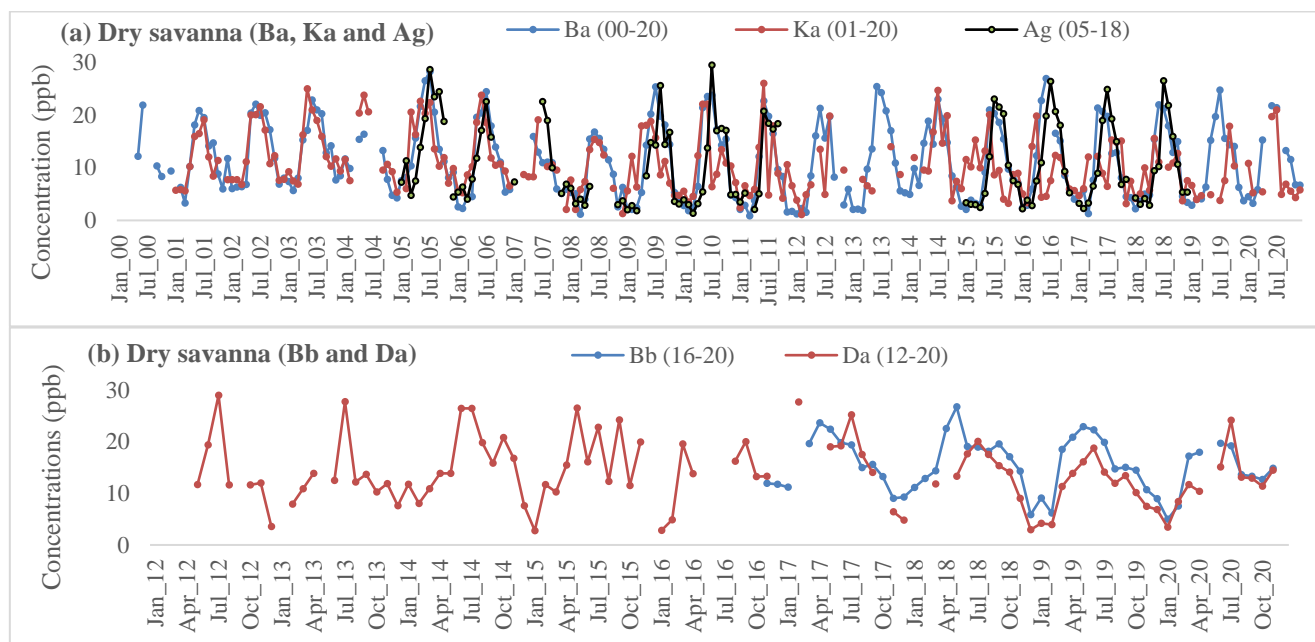
#### 370 3.2.1 Seasonal and annual variation in $\text{O}_3$ levels

##### 3.2.1.1 Dry savanna

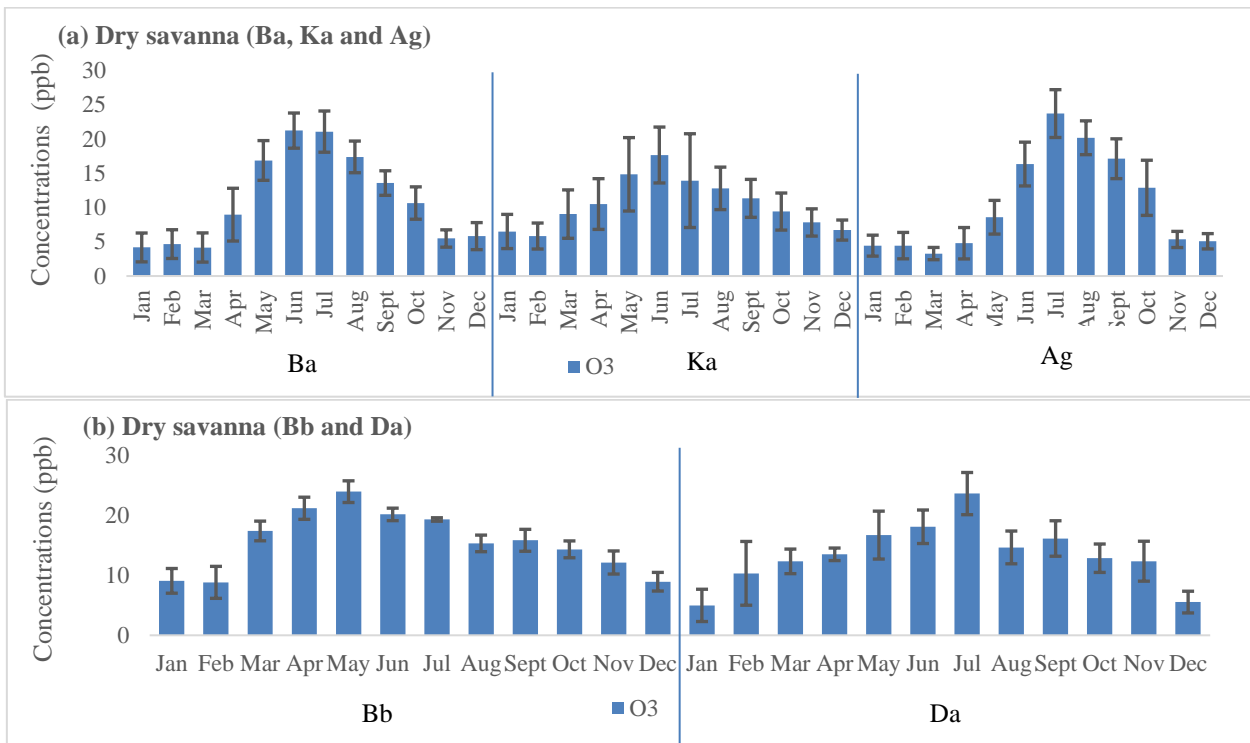
Figure 3 presents monthly  $\text{O}_3$  surface concentrations measured in Ba, Ka, Ag (Fig. 3a), Bb and Da (Fig. 3b) representative of  
 375 dry savannas in Niger, Mali and Senegal. The seasonal variability of  $\text{O}_3$  is well marked:  $\text{O}_3$  levels during the wet season are  
 higher than in the dry season (Table 3). On most sites, from January to May, the  $\text{O}_3$  concentrations gradually increase to finally  
 380 reach annual peaks at the start of the wet season (May-June-July). The mean annual cycle of monthly  $\text{O}_3$  concentrations at Ba,  
 Ka, Ag (Fig. 4a), Bb and Da (Fig. 4b) are obtained from averages of monthly in situ measurements over the whole studied  
 period. The annual distribution is similar to the regional rainfall pattern.  $\text{O}_3$  concentrations decrease as the rainy season  
 progresses, but remain at higher levels compared to the dry season. At dry savanna sites, monthly average surface  $\text{O}_3$   
 385 concentrations range from  $6.1 \pm 2.4$  ppb to  $14.5 \pm 2.6$  ppb during the dry season, and from  $13.9 \pm 5.1$  ppb to  $19.4 \pm 3.9$  ppb during  
 the rainy season (Table 3). From dry to wet season,  $\text{O}_3$  levels increased from 18.7% to 68.5%. The annual  $\text{O}_3$  concentrations  
 ranged from  $10.5 \pm 5.4$  ppb at Ka to  $14.8 \pm 4.3$  ppb at Bb (Table 3).

The high  $\text{O}_3$  concentrations observed at the start of the rainy season are due to soil humidification during this period, which  
 generates biogenic NO emissions pulses in the region. Indeed, the accumulated nitrogen in soils (in the form of ammonium  
 and nitrate ions) from traditional agricultural practices, such as grazing, manure spreading and decomposition of crop residues  
 385 (Delon et al., 2015; Laville et al., 2005) is released to the atmosphere when the first rains fall on dry soils. Bacterial nitrification  
 is thus activated, leading to nitrogen consumption and consequent release of large pulses of NO (Adon et al., 2010; Delon et  
 al., 2015; Jaegle et al., 2004; Laville et al., 2005; Ludwig et al., 2001; Ossouhou et al., 2019). During the wet season, the  
 decrease in  $\text{O}_3$  levels may be attributed to a decrease in  $\text{NO}_x$  concentrations. Indeed, soil mineral N is used by plants  
 during their root growth phase, and is therefore less available for the production of NO to be released to the atmosphere  
 390 (Homyak et al., 2014). On the Fig. 5, which presents the monthly variation of  $\text{NO}_x$  and VOCs (natural and anthropogenic  
 emissions) in dry savanna, biogenic NO fluxes (Fig 5e, f and g) show a bell-shaped variation, peaking in August (wet season).  
 We observe a good dependence of  $\text{O}_3$  with NO ( $0.73 < r < 0.92$ ) at Ba, Ka and Ag in the presence of high relative humidity  
 and precipitation ( $0.64 < r < 0.95$ ) (Table 4), that is agreement with the high values of  $\text{O}_3$  observed in wet season over these  
 sites. Monthly profile of BVOC fluxes (isoprene,  $\alpha$  pinene and  $\beta$  pinene) in dry savanna (Fig. 5) shows a maximum at the end  
 395 of the dry season/beginning of wet season at Ba, Ka and Ag (Fig. 5e, f and g), or during the wet season at Bb and Da (Fig. 5h  
 and i). Isoprene fluxes are more obvious at Da ( $214.2 \pm 30$ )  $\text{ng}\cdot\text{m}^{-2}\cdot\text{s}^{-1}$  whereas  $\alpha$  pinene, and  $\beta$  pinene exhibit larger values at  
 Ka site ( $11.2 \pm 1.8$ ;  $5.2 \pm 0.8$ )  $\text{ng}\cdot\text{m}^{-2}\cdot\text{s}^{-1}$  respectively). The fluxes of  $\beta$  pinene ( $0.70 < r < 0.79$ ) and isoprene ( $r = 0.79$ ) correlates  
 well with  $\text{O}_3$  respectively at (Ba, Ka, Ag) and (Bb, Da) under the influence of the humidity, rainfall in Mali and Niger and the  
 temperature, radiation and humidity ( $0.50 < r < 0.76$ ) in Senegal (Table 4).

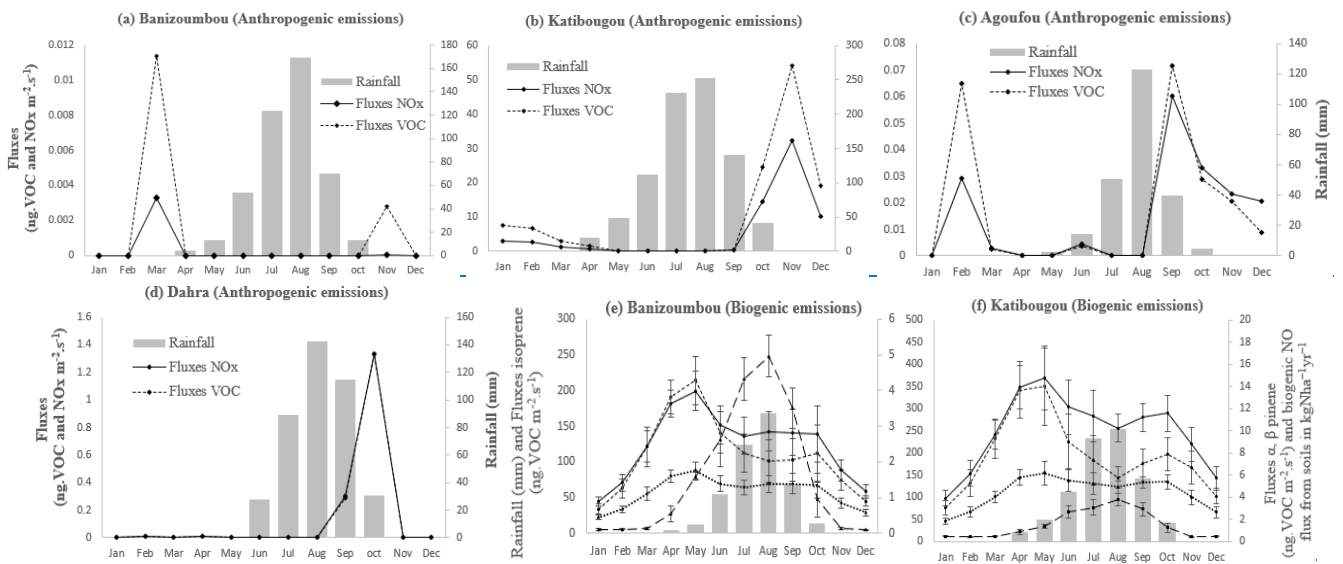
400 These observations in dry savanna are confirmed by Stewart et al. (2008) who correlated O<sub>3</sub> production in the Sahel during the wet season with high NO<sub>x</sub>NO<sub>x</sub> concentrations attributed to biogenic emissions during the AMMA (Analyse Multidisciplinaire de la Mousson Africaine) campaign. In the dry savanna, Oluleye et al. (2013) estimated that rain was responsible for 62% of the O<sub>3</sub> distribution in the West African region, excluding the precursors NO, CO and hydrocarbons, as also illustrated in our results. Saunois et al. (2009) have shown that soil NO<sub>x</sub>NO<sub>x</sub> emissions, combined with the northward advection of volatile organic compounds (VOCs), play a key role in O<sub>3</sub> production in dry savanna regions. This large-scale impact of biogenic emissions has also been verified by Williams et al. (2009), who estimate that 2-45% of tropospheric O<sub>3</sub> over equatorial Africa may originate from NO<sub>x</sub>NO<sub>x</sub> emissions from African soils. All these works are in agreement with the results of this study. Monthly variation in anthropogenic NO<sub>x</sub>NO<sub>x</sub> and VOC emissions (Fig. 5a, b, c and d) indicates during the wet season, NO<sub>x</sub>NO<sub>x</sub> and VOC fluxes are very low. On the other hand, maxima are observed in the dry season with the highest emissions found in Ka and could be the cause of ozone production in the dry season. Indeed, the monthly averaged biomass combustion emissions (GFED4) over the 18-year period (1998-2015) in the Sahel show that Ka is significantly affected by the biomass combustion source in November (Ossouhou et al., 2019).



415 **Figure 3.** Monthly evolution of O<sub>3</sub> concentrations (ppb) in dry savanna (a) Ba (Niger), Ka, Ag (Mali) and (b) Bb, Da (Senegal).



420 **Figure 4.** Mean monthly averages of O<sub>3</sub> concentrations (ppb) in dry savanna (a) Ba (Niger), Ka, Ag (Mali) and (b) Bb, Da (Senegal). Mean monthly averages are calculated from the long ozone data series of Fig. 3. Bars represent mean absolute deviation.



425

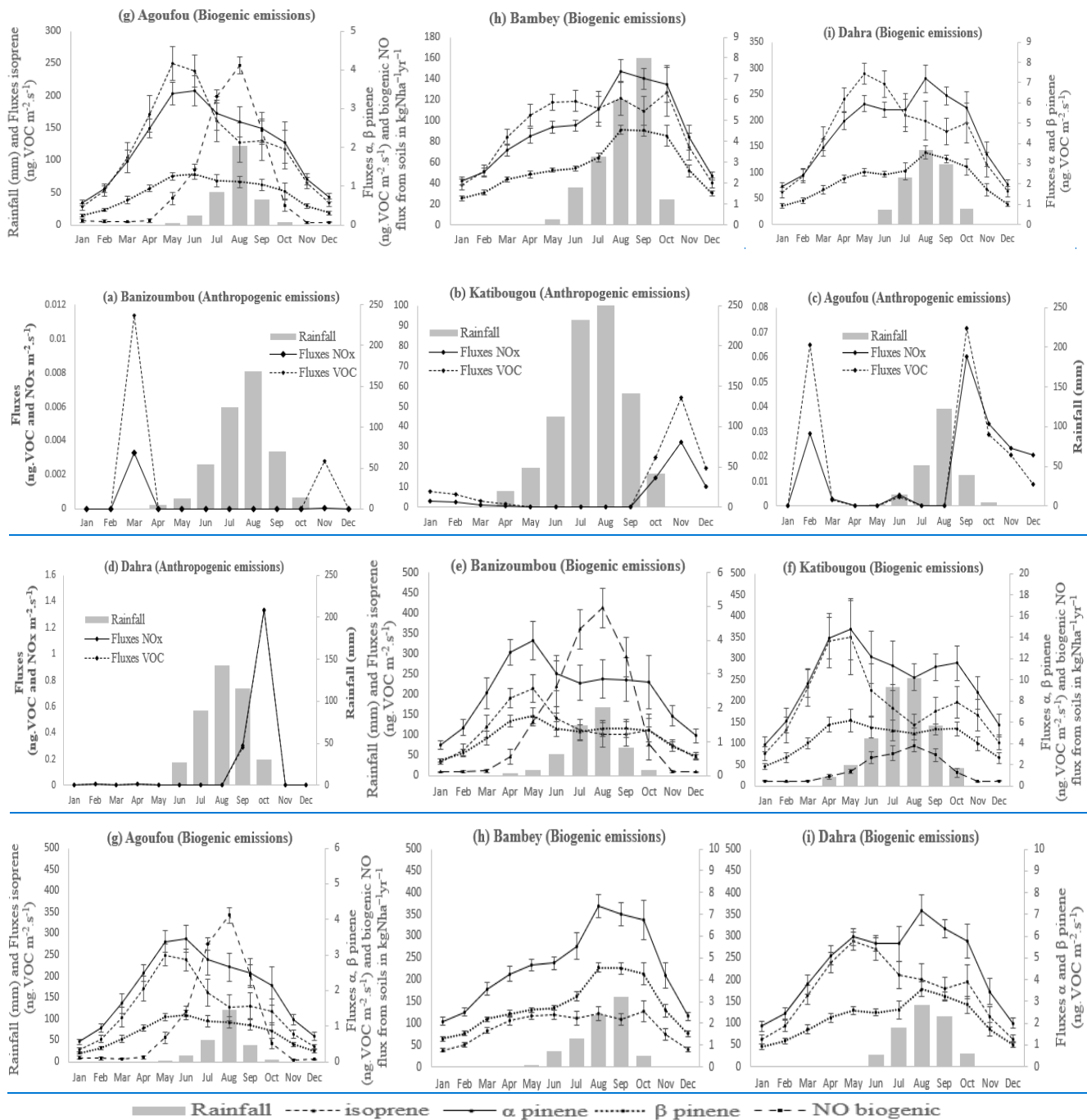


**Figure 5.** Mean monthly fluxes of natural and anthropogenic  $\text{NO}_x$ ,  $\text{NO}_x$  and VOC estimated by the GFED4 and MEGAN inventories for  $0.25^\circ \times 0.25^\circ$  grid cells centered on each of dry savanna.

430

435



**Table 3.** Minimum, maximum and average of monthly, annual and seasonal O<sub>3</sub> concentrations at all sites (1995-2020)

Ecosystem		Monthly		Annual	Dry season			Wet season		
		min	max	Avg	min	max	Avg	min	max	Avg
Dry savanna	Ba	0.9	28.3	11.2±6.9	4.2±2.7	16.9±3.7	7.6±2.9	13.6±2.5	21.2±3.5	18.3±3.2
	Ka	1.2	26.1	10.5±5.4	5.8±2.6	14.9±6.6	8.8±3.7	11.3±3.8	17.7±5.4	13.9±5.1
	Ag	1.4	29.5	10.5±7.3	3.3±1.1	12.9±4.6	6.1±2.4	16.4±3.8	23.7±4.6	19.4±3.9
	Bb	4.96	26.7	14.8±4.3	8.8±3.5	24.0±2.4	14.5±2.6	15.4±1.9	20.2±1.4	17.7±1.6
	Da	2.8	29.0	13.9±6.3	5.0±3.8	16.7±5.4	11.1±4.0	14.7±3.1	23.7±4.8	18.2±4.0
Wet savanna	La	4.25	20.6	10.8±3.3	9.9±1.4	15.1±2.3	13.5±2.3	6.7±1.1	12.2±1.9	9.0±1.5
	Dj	3.3	24.8	13.5±4.8	10.8±4.5	18.7±2.7	14.1±4.0	9.0±2.0	18.4±2.4	13.2±2.8
Forest	Zo	1.2	11.1	5.2±2.1	7.1±2.1	7.8 ±1.6	7.5±2.1	3.5±1.3	6.6±1.9	4.6±1.6
	Bo	1.5	8.3	3.9±1.1	4.0±1.0	5.2±1.2	4.7±1.4	2.8±1.0	5.4±1.0	3.7±1.0
Agricultural or semi-arid savanna	Mb	10.5	30.2	19.9±4.7	13.8±3.4	25.7±5.7	20.9±4.0	14.1±5.0	22.5±2.7	18.5±3.9
	Sk	6.3	64.1	22.8±7.3	23.0±9.6	30.2±6.0	25.9±7.3	14.5±1.9	29.2±5.6	20.3±5.4
	Af	3.2	55.5	26.9±6.3	19.9±6.2	31.2±7.6	24.5±6.3	23.8±4.9	34.4±7.4	29.0±7.3
	CP	3.3	67.4	26.8±6.2	17.3±5.3	30.4±6.0	23.4±5.6	25.9±6.3	32.1±5.7	29.8±6.1
	LT	9.0	86.6	30.8±8.0	24.7±7.9	40.1±10.8	32.0±8.9	21.3±5.2	36.0±9.1	28.3±8.2

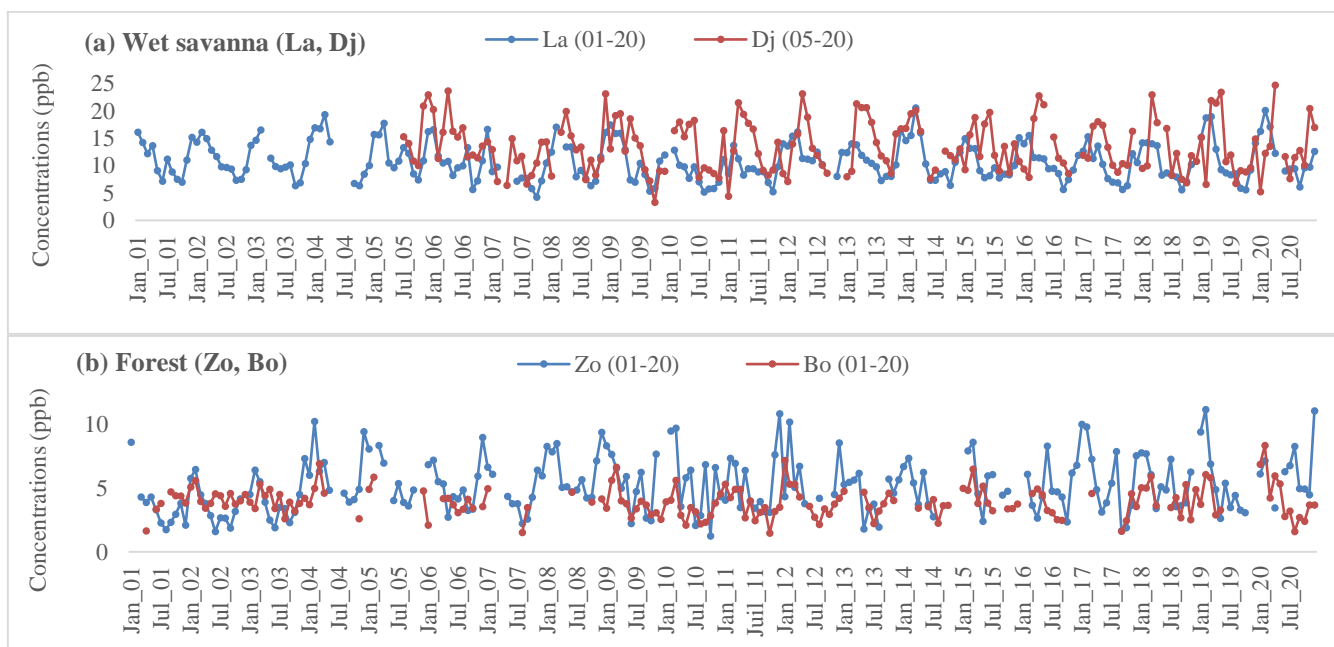
### 3.2.1.2 Wet savanna and forest

440 Figure 6 presents the mean monthly surface O<sub>3</sub> concentrations in Dj, La (Fig. 6a), Zo and Bo (Fig. 6b). Ozone concentrations present a seasonality during the year. The maximum of the data series in La is 20.6 ppb in March (dry season) and the minimum is 4.3 ppb in October (wet season). In Dj, the O<sub>3</sub> levels are higher than in La. The monthly highest value recorded in Dj is 24.8 ppb in April (start of the wet season). At the forested ecosystems sites, O<sub>3</sub> concentrations are lower than in dry, wet and semi-agricultural/semi-arid savannas (Table 3). In Zo and Bo, the highest annual peaks are found in February (11.1 ppb and 8.3 ppb respectively). Monthly averages in the dry season ranged from 4.7±1.4 ppb (Bo) to 14.1±4.0 ppb (Dj), and in the wet season from 3.7±1.0 ppb (Bo) to 13.2±2.8 ppb (Dj) (Table 3). The O<sub>3</sub> mean annual cycle is shown in Fig. 7.

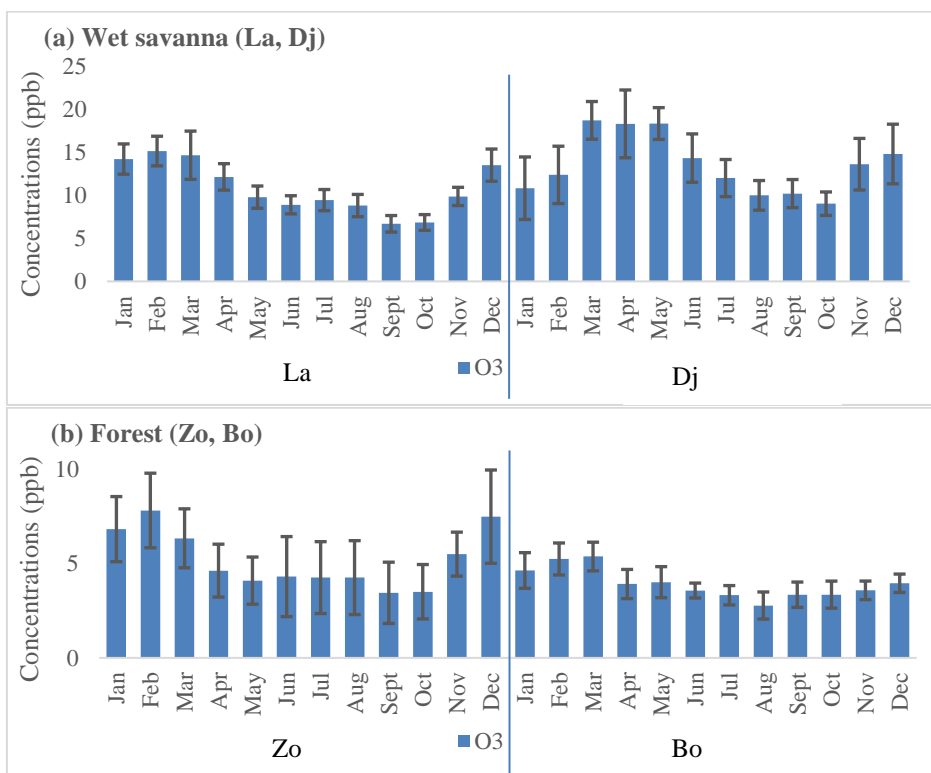
450 The high O<sub>3</sub> concentrations in dry season in these two ecosystems could be related to the biomass burning source, which is generally recorded during the months of December-February in rural tropical environments and BVOC emissions. Indeed, in wet savannas (La, Dj), and forest (Zo) (Fig. 8), NO<sub>x</sub> and VOC anthropogenic fluxes reach their maxima during the dry season. The mean flux estimates are respectively 14.5; 24.2; 4.9 ng.m<sup>-2</sup>.s<sup>-1</sup> for NO<sub>x</sub> and 26.8; 29.4; 5.5 ng.m<sup>-2</sup>.s<sup>-1</sup> for anthropogenic VOCs at La, Dj and Zo (Fig 8a, b and c). BVOC maxima fluxes are obtained at the end of the dry season/beginning of the wet season (Fig. 8e, f, g and h). A drop in these fluxes is then observed during the wet season. Strong Pearson correlations are observed between O<sub>3</sub>, NO<sub>x</sub> and the VOCs (0.49 < r < 0.92) (Table 4). Temperature and radiation are also well correlated with O<sub>3</sub> (0.54 < r < 0.89) in these two ecosystems. These results are corroborated by the literature. 455 Indeed, radiation and humidity facilitate the propagation of radical chain reactions and the production of hydroxyl radicals (OH) at these sites (Graedel and Crutzen, 1993). According to several authors, O<sub>3</sub> levels tend to increase under warm, sunny conditions favorable to photochemical O<sub>3</sub> production (Hamdun and Arakaki, 2015; Morakinyo et al., 2020). Moreover, Aghedo et al. (2007), Mari et al. (2011), Saunois et al. (2009) and Saxton et al. (2007) have reported that vegetated areas emit large quantities of biogenic organic compounds that influence O<sub>3</sub> production in the presence of light and temperature. Others authors 460 such as Abbadie (2006), Adon et al. (2010), Galanter et al. (2000) and Tsvilidou et al. (2023) have linked the high O<sub>3</sub> concentrations recorded in the dry season to the presence of NO<sub>x</sub> emitted by biomass combustion in the wet savanna (Gulf of Guinea). According to Adon et al. (2010), Baldy et al. (1996), Clain et al. (2009), Cros et al. (1992), Hamdun and Arakaki

(2015), Martins et al. (2007), Oluleye et al. (2013) the biomass burning is likely to contribute significantly to O<sub>3</sub> production through precursor emissions (NO<sub>x</sub>, NO<sub>x</sub> and CO) in the dry season (wet savanna) with nearly 30% to 80% of the savanna ground surface burnt annually between December and February. The high O<sub>3</sub> concentrations measured in Tranquebar (India) have been linked to increased emissions of NO<sub>x</sub>, NO<sub>x</sub> and other precursors from various sources (Debaje et al., 2003). Compared to wet and dry savannas, forest sites recorded the lowest O<sub>3</sub> amounts due to significant dry deposition of O<sub>3</sub> on the ground, on foliage and trees (Mari et al., 2011; Rummel et al., 2007; Saunois et al., 2009). Tropical forests are shown to be important O<sub>3</sub> sinks. A strong gradient of O<sub>3</sub> between forest and dry savanna in West Africa has been observed from aircraft measurements (Saunois et al., 2009).

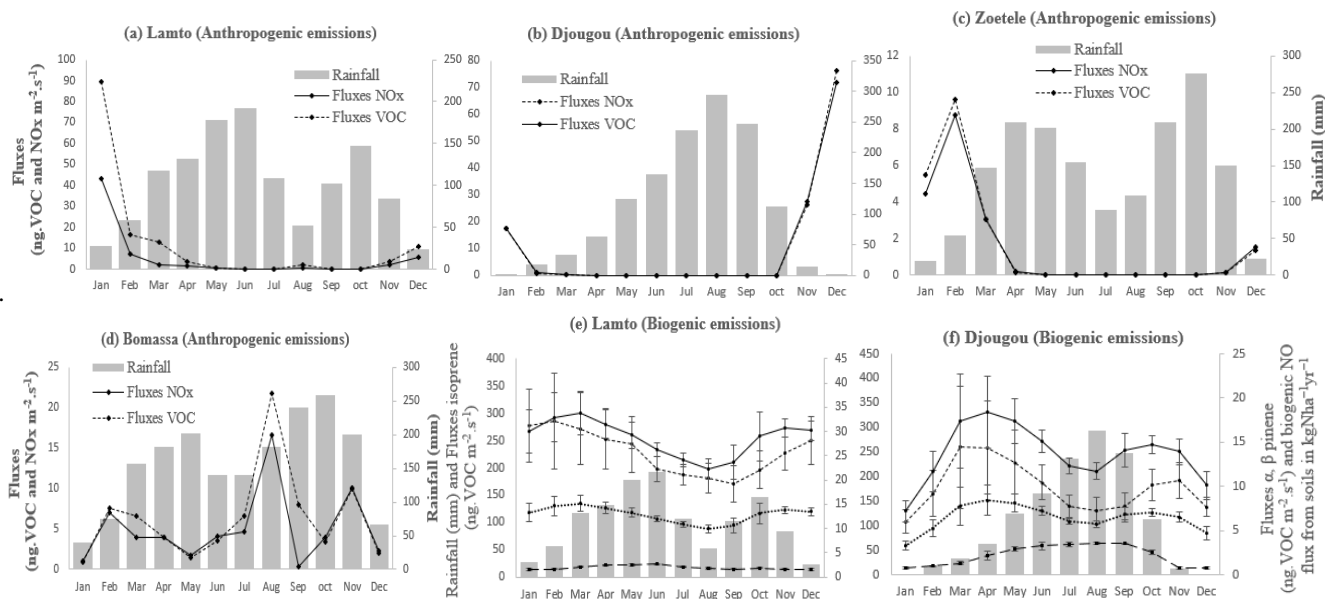
In Bo, high NO<sub>x</sub>, NO<sub>x</sub> and VOC fluxes are observed in the wet season (Fig. 8d), unlike in Zo (Fig. 8c) and corroborated by Ossohou et al. (2019) over the period 1998-2015. The source of these recorded anthropogenic during this period of year at Bo emissions could be biomass combustion. According to the work of Sauvage et al. (2005), the period from August to September corresponds to a peak in biomass burning activity in the southern African countries (Mozambique, Zimbabwe, South Africa). Moving air masses over Central Africa via the northern edge of the continental anticyclone could explain such high emissions at Bo in August-September.



480 **Figure 6.** Monthly evolution of O<sub>3</sub> concentrations (ppb) in (a) humid savanna, La (Cote d'Ivoire) and Dj (Benin) and (b) in forest, Zo (Cameroon) and Bo (Congo).



485 **Figure 7.** Mean monthly averages of O<sub>3</sub> concentrations (ppb) in (a) humid savanna, La (Cote d'Ivoire) and Dj (Benin) and (b) in forest, Zo (Cameroon) and Bo (Congo). Mean monthly averages are calculated from the long ozone data series of Fig. 6. Bars represent mean absolute deviation.



490

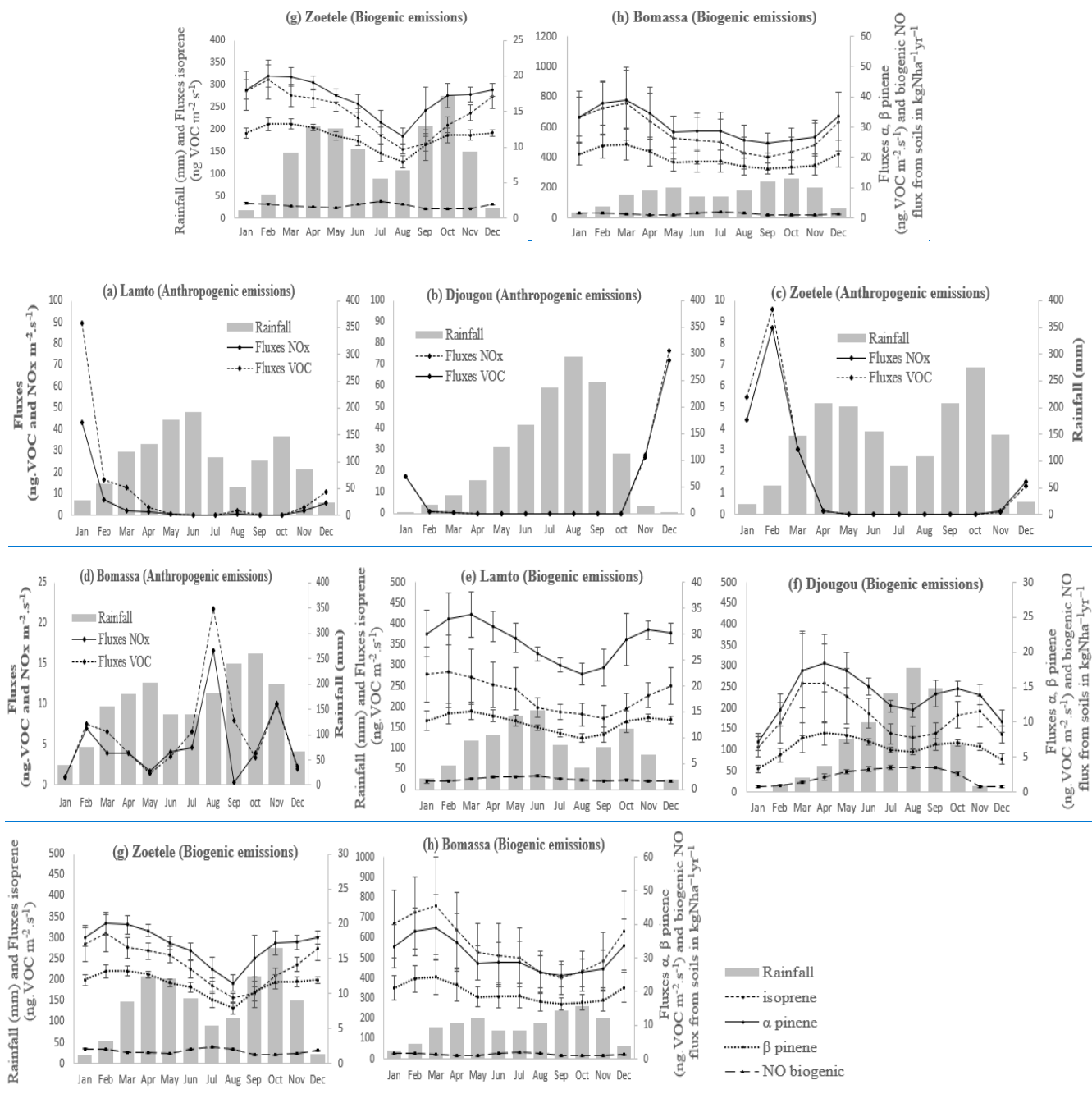


**Figure 8.** Mean monthly fluxes of natural and anthropogenic  $\text{NO}_x$ ,  $\text{NO}$  and VOC estimated by the GFED4 and MEGAN inventories for  $0.25^\circ \times 0.25^\circ$  grid cells centered on each of wet savanna and forests.

**Table 4.** Correlation  $r$  between  $O_3$ , its precursors and meteorological variables at different sites. Blank spaces in the table indicate the absence of data on this site for the precursor concerned over the study period

Ecosystem	Dry savanna					Wet savanna		Forest		Agricultural/semi-arid savanna				
Sites	Ba	Ka	Ag	Bb	Da	La	Dj	Zo	Bo	Mb	LT	CP	Af	Sk
	$O_3$													
NO biogenic	0.85	0.73	0.92	-	-	-0.15	-0.24	0.43	$-10^{-3}$	-	-	-	-	-
NO <sub>x</sub> _C	-0.33	-0.43	0.04	-	0.001	0.49	0.059	0.80	-0.33	0.31	0.37	-0.67	0.62	0.61
VOC_C	-0.40	-0.47	-0.003	-	$-5.10^{-4}$	0.54	0.05	0.79	-0.40	0.31	0.60	-0.87	0.52	0.65
isoprene	0.51	0.54	0.46	0.79	0.78	0.92	0.81	0.80	0.92	0.42	-0.39	-0.91	0.29	-0.64
$\alpha$ pinene	0.67	0.76	0.66	0.45	0.77	0.74	0.64	0.63	0.90	0.36	-0.45	-0.86	0.29	-0.67
$\beta$ pinene	0.70	0.79	0.72	0.34	0.72	0.70	0.56	0.60	0.89	0.33	-0.48	-0.85	0.27	-0.71
Temperature	0.45	0.47	0.42	0.51	0.76	0.72	0.69	0.68	0.89	0.47	-0.46	-0.90	0.49	-0.62
Humidity	0.82	0.64	0.95	0.52	0.70	-0.85	-0.19	-0.89	-0.79	-0.61	-0.79	-0.68	0.1	-0.80
Rainfall	0.74	0.64	0.75	0.15	0.51	-0.48	-0.39	-0.76	-0.54	-0.18	-0.49	0.74	0.53	-0.69
Radiation	0.16	0.15	0.26	0.75	0.69	0.73	0.54	0.65	0.87	0.21	-0.19	-0.76	0.71	-0.43

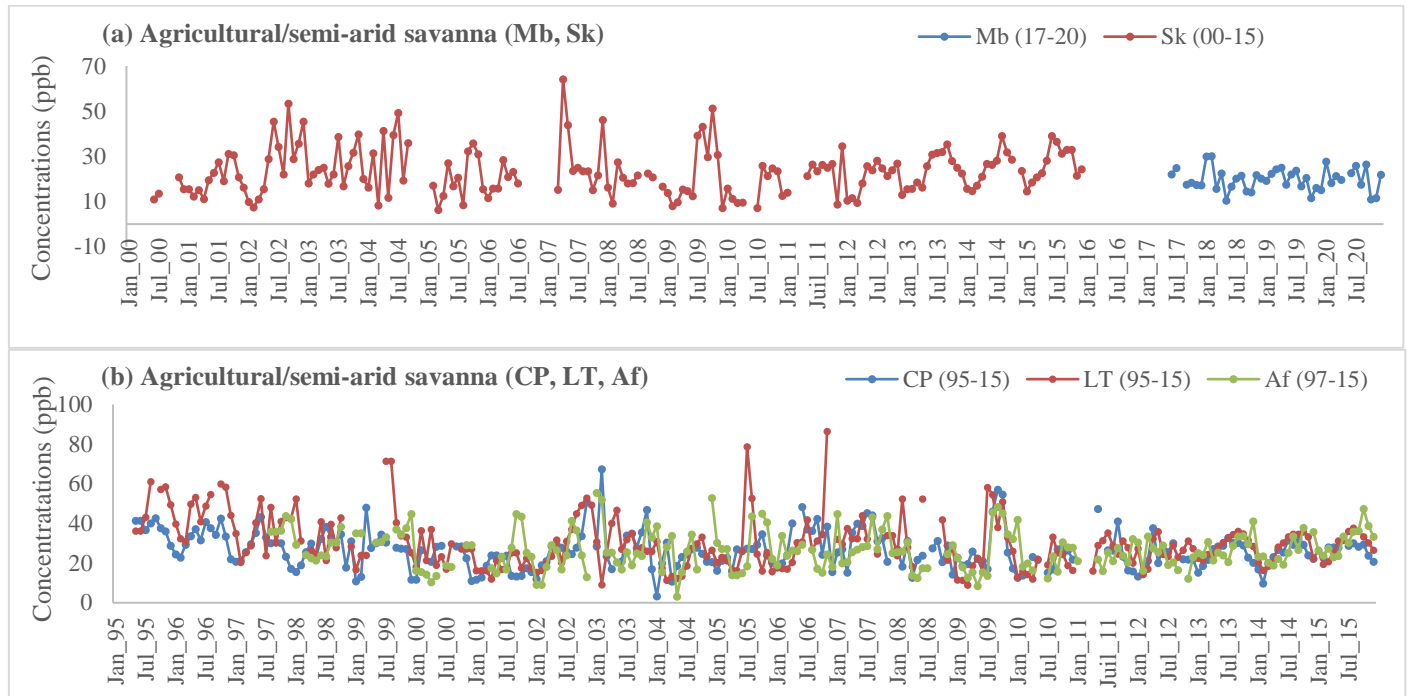
### 505 3.2.1.3 Agricultural and semi-arid savanna

Figure 9 presents the monthly evolution of surface  $O_3$  concentration in agricultural site (Mb) and semi-arid savanna sites (LT, CP, Sk and Af). At Mb site, monthly  $O_3$  concentrations do not exceed 30.2 ppb (Table 3). At the CP, LT, Sk and Af sites,  $O_3$  levels are almost twice as high as in West African sites. The mean annual cycle of  $O_3$  concentrations (Fig. 10a and b) shows that at Mb,  $O_3$  levels are almost similar between seasons (Table 3). In southern African ecosystems, dry-season  $O_3$  concentrations are the highest at LT and Sk. The annual averages are around  $19.9 \pm 4.7$  ppb at Mb;  $22.8 \pm 7.3$  ppb at Sk;  $26.9 \pm 6.3$  ppb at Af;  $26.8 \pm 6.2$  ppb at CP and  $30.8 \pm 8.0$  ppb at LT (Table 3).

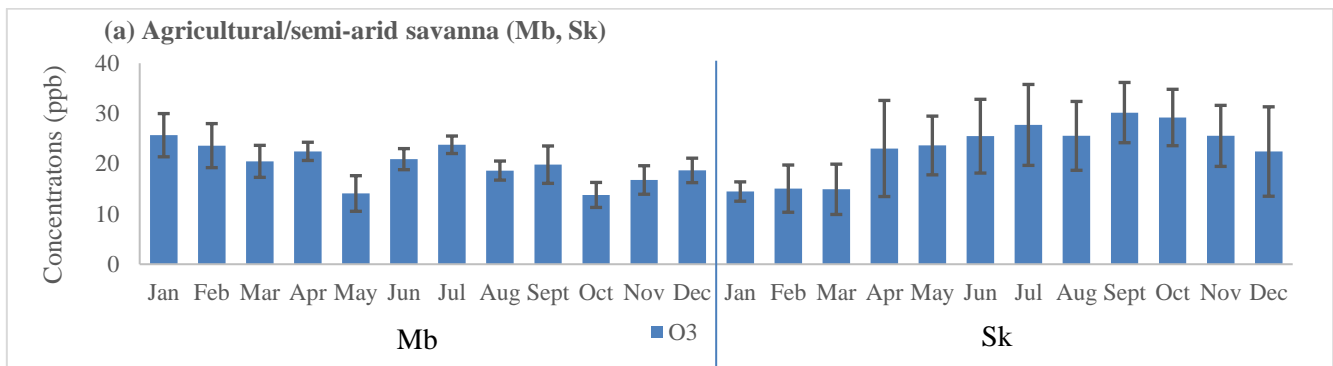
These  $O_3$  levels observed could be associated at the combustion sources and natural emissions. Indeed, on the Fig. 11a, we observe ~~NO<sub>x</sub>~~ and VOC fluxes are quantifiable in February (dry season) at Mbita. Based on the analysis of burned surface areas, Bakayoko et al. (2021) indicated that Mb is strongly influenced by biomass burning from northern and southern sides during both dry seasons. High  $O_3$  levels measured at Mb site during the dry season show similar values as in Nairobi, Kenya, during the same months (Kimayu et al., 2017). At the South African sites, the Fig. 11b, c, d and e shows the mean fluxes of anthropogenic emissions vary from  $0.3 \text{ ng.m}^{-2}.\text{s}^{-1}$  (LT) to  $10.2 \text{ ng.m}^{-2}.\text{s}^{-1}$  (Sk) for ~~NO<sub>x</sub>~~ and from  $2.9 \text{ ng.m}^{-2}.\text{s}^{-1}$  to  $11.8 \text{ ng.m}^{-2}.\text{s}^{-1}$  (Sk) for VOCs with the maxima recorded in dry season. As for the BVOC emissions (Fig. 11 g, i and j), more specifically at LT, Af and Sk, the highest values are reached in the wet season. At CP (Fig. 11h), the maximum emissions are measured in the dry months of January/February. The calculations of correlation indicate ozone is linked to anthropogenic combustion sources at LT, Af and Sk and are anti-correlated with temperature, humidity, and radiation ( $-0.90 < r < -0.43$ ) at LT, CP and Sk (Table 4). High  $O_3$  concentrations are therefore measured at these sites during the driest and coldest months (Swartz et al., 2020b). Except at Af where  $O_3$  has a weak link with BVOC, the increase of isoprene,  $\alpha$  pinene,  $\beta$  pinene emissions rate is positively correlated with  $O_3$  decrease at the others sites. At the CP and Af sites, rainfall and  $O_3$  are correlated ( $0.53 < r < 0.74$ ) and ozone production could therefore also be linked to microbial activity of soils on these two sites. At CP site during the same study period, Swartz et al. (2020b) emphasised higher  $NO_2$  concentrations were attributed to increased microbial activity in the wet season and  $O_3$  seasonal pattern corresponded to the  $NO_2$  seasonality, which was attributed to their related chemistry. The importance of humidity and temperature in  $O_3$  photochemistry observed at almost all South African sites has been highlighted by Balashov et al. (2014) and Laban et al. (2018, 2020).

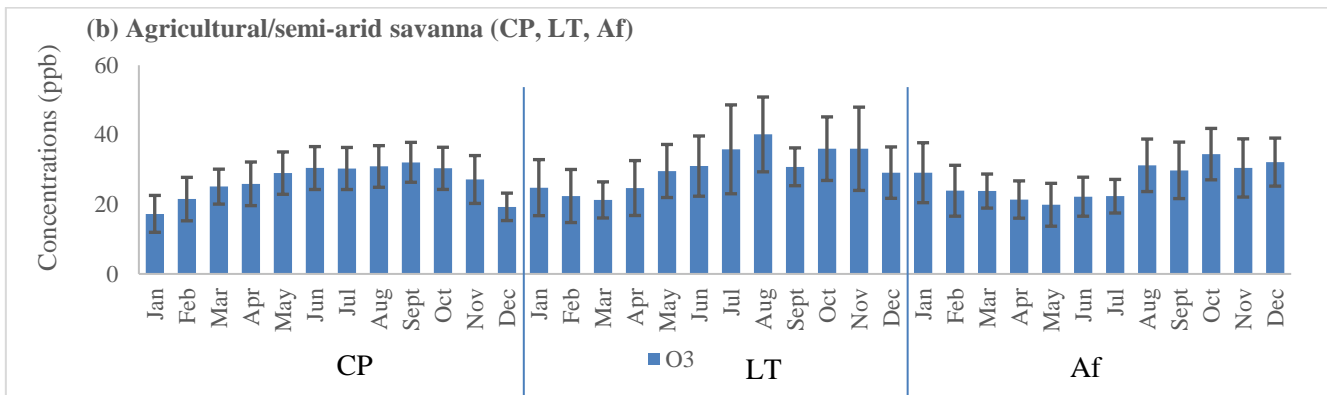
At southern African sites,  $O_3$  levels could be also attributed to a combination of regional and local influences, including emissions from industrial, vehicular and domestic biomass combustion to biomass combustion events in sub-Saharan Africa

(Mozambique, Zambia, Zimbabwe and Angola) recirculated by anticyclonic air mass processes (Baldy et al., 1996; Laban et al., 2018; Martins et al., 2007; Swap et al., 2003; Tiitta et al., 2014; Josipovic et al., 2010). Biomass combustion is considered as a major source of O<sub>3</sub> precursors in South Africa (Ngoasheng et al., 2021; Vakkari et al., 2013) and in Southern Africa (Heue et al., 2016) and may explain the O<sub>3</sub> levels observed in dry season at LT and Sk. The high O<sub>3</sub> levels in the wet season (at Af and CP) due to soil microbial activity (Swartz et al., 2020a) could be also explained by long-range transport of air pollutants emitted from the industrialized Highveld region (Abiodun et al., 2014; Ojumu, 2013). During the austral winter, O<sub>3</sub> concentrations in the boundary layer are higher (e.g. at CP and Af) due to a systematic increase in O<sub>3</sub> precursors from households, combustion for space heating (Bencherif et al., 2020; Laban et al., 2018; Lourens et al., 2011; Oltmans et al., 2013; Swartz et al., 2020b). The high concentrations measured at Af could also be due to industrial activities located near this site (Lourens et al., 2011).

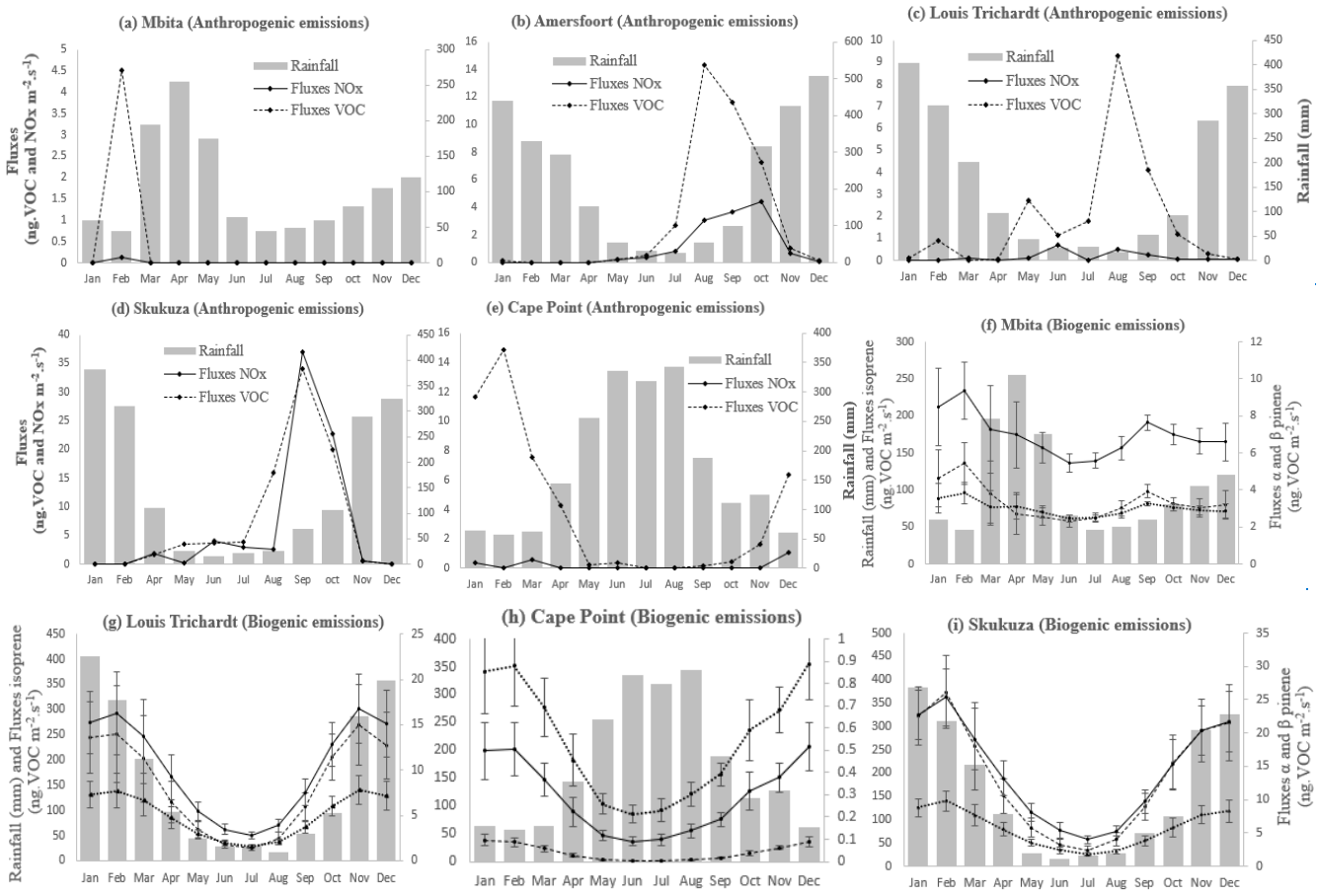


545 **Figure 9.** Monthly evolution of O<sub>3</sub> concentrations (ppb) in Agricultural/semi-arid savanna (a) Mb (Kenya) and Sk (South Africa) and (b) CP, LT and Af (South Africa).

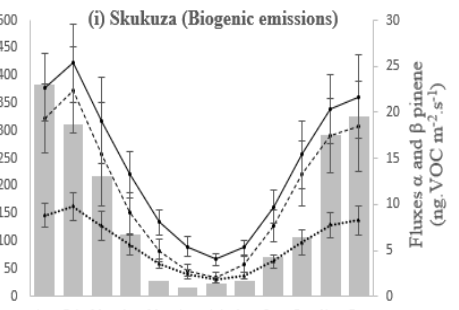
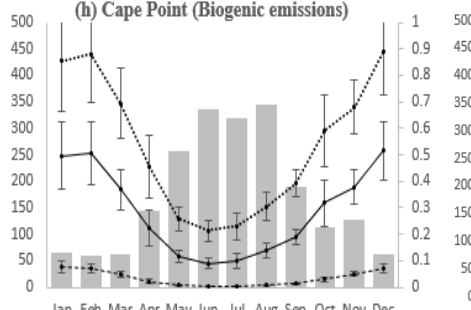
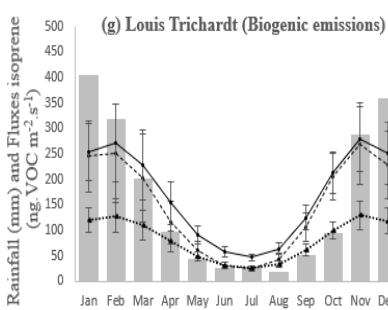
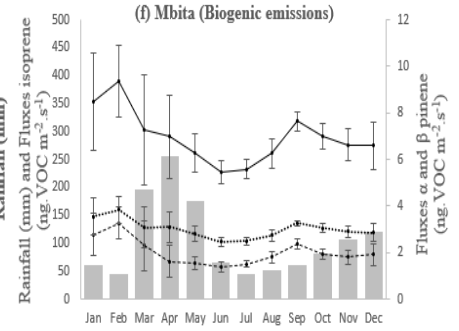
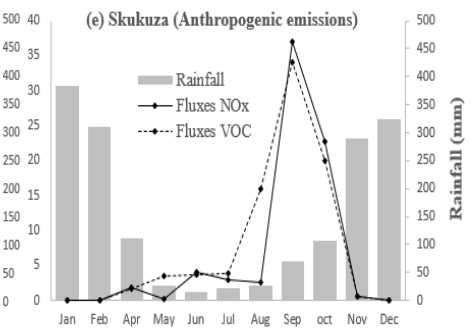
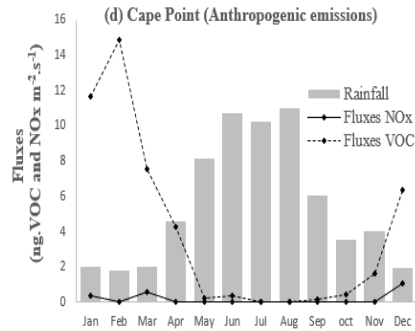
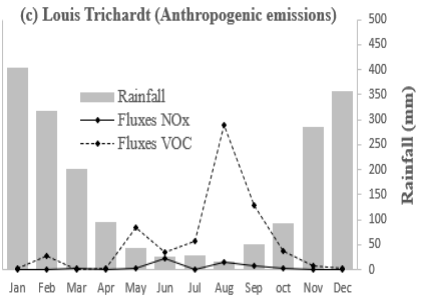
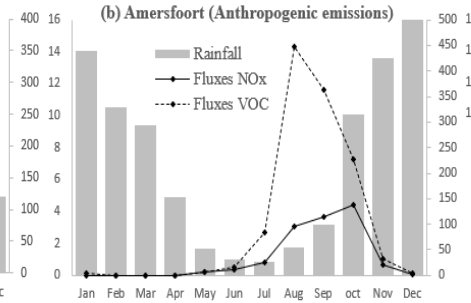
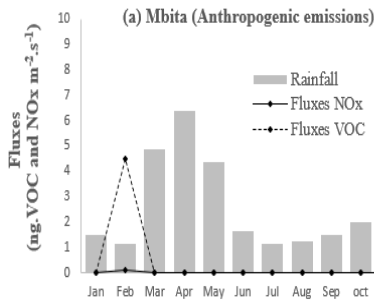
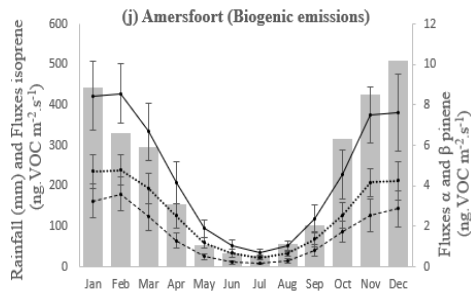




550 **Figure 10.** Mean monthly averages of O<sub>3</sub> concentrations (ppb) in Agricultural/semi-arid savanna (a) Mb (Kenya) and Sk (South Africa) and (b) CP, LT and Af (South Africa). Mean monthly averages are calculated from the long ozone data series of Fig. 9. Bars represent mean absolute deviation.



555





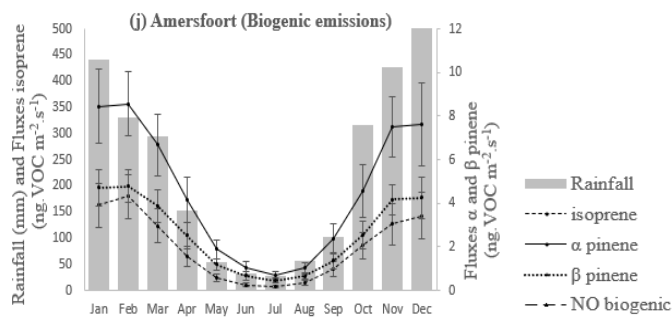
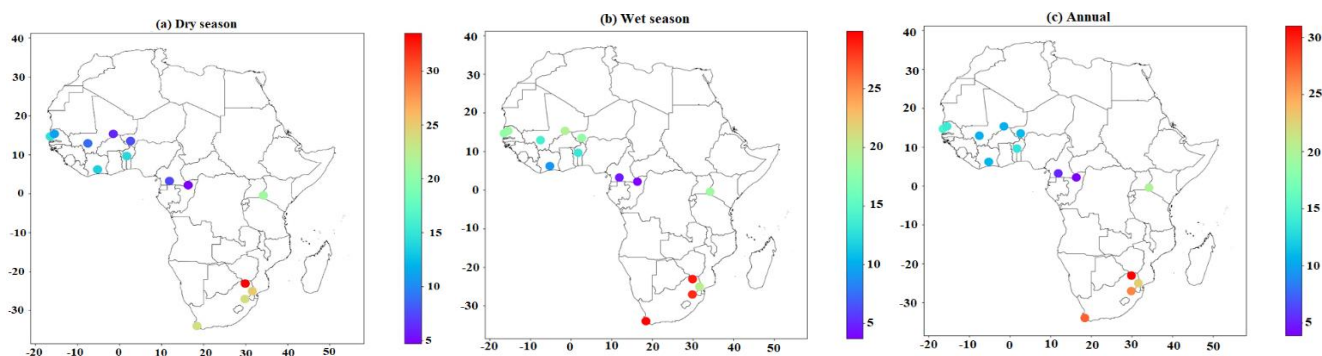


**Figure 11.** Mean monthly fluxes of natural and anthropogenic  $\text{NO}_x$ ,  $\text{NO}_x$  and VOC estimated by the GFED4 and MEGAN inventories for  $0.25^\circ \times 0.25^\circ$  grid cells centered on each of agricultural/semi-arid savanna sites

565

### 3.2.2 $\text{O}_3$ levels in Africa, set in a global context

$\text{Ozone}_3$  concentrations measured at the 14 studied site are mapped on a seasonal and annual scale (Fig. 12).



570 **Figure 12.** Seasonal and annual mapping of  $\text{O}_3$  concentration levels in (a) Dry season (Ba, Ka, Ag, Da and Bb: October to  
 575 May ; La and Dj: November to March ; Zo : December to February and July to August ; Bo: December to February ; Mb: June  
 to October and January to February ; LT, Sk and Af : April to September; CP: October to March), (b) Wet season (Ba, Ka,  
 Ag, Da and Bb: June to September; La and Dj: April to October ; Zo : March to June and September to November ; Bo: March  
 to November ; Mb: March to May and November to December ; LT, Sk and Af : October to March ; CP : April to September)  
 and (c) Annual over the 14 studied sites.

We compared African ozone levels related in this study with studies carried out in Africa and around the world over the last  
 20-years (Table 5, Fig. 13). The bibliographical synthesis takes into account studies where data measurement methodology has  
 been clearly described. Sites where concentrations have been measured by passive samplers are listed. We have identified  
 among others, sites in Nepal, North America, North-Eastern Europe, Asia and Africa. Figure 13 focuses more on  $\text{O}_3$  monitoring  
 studies in Africa.

580

585

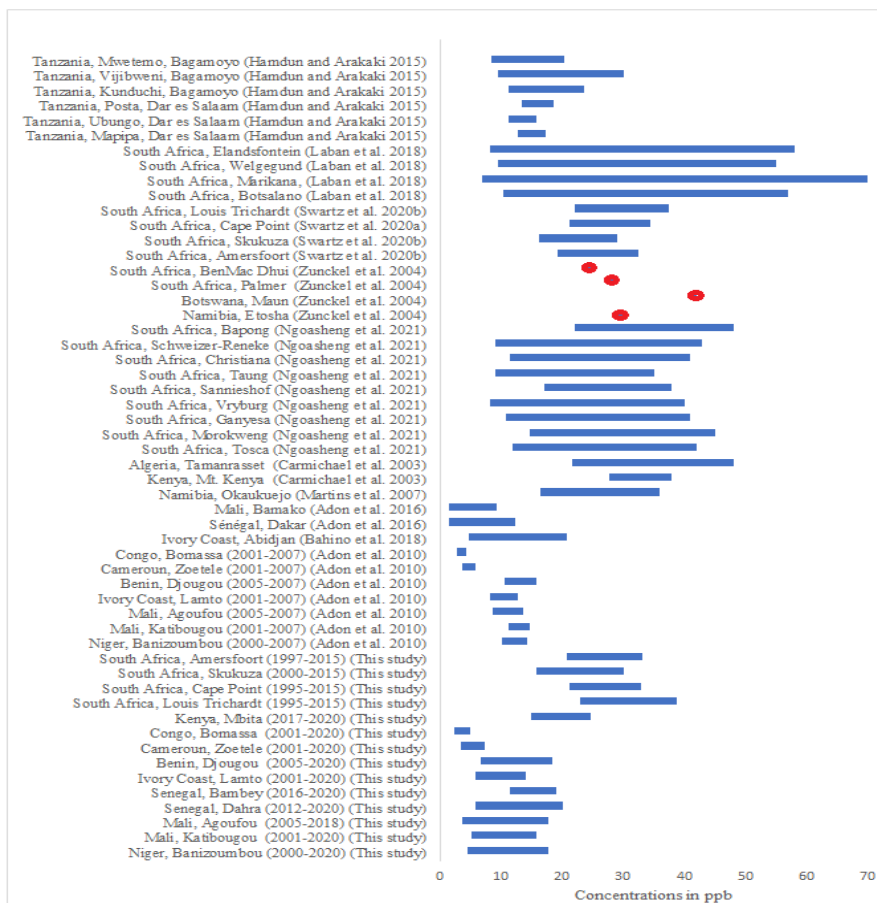
**Table 5.** O<sub>3</sub> concentrations at various sites worldwide as reported in literature

Sites	Type	Period	O <sub>3</sub> (ppb)	References
India, Tranquebar	Rural	May 1997 -Oct 2000	17±7 - 23 ± 9	Debaje et al. (2003)
Sweden, Malmö (20 sites)	Rural	(16–24 Apr 2012 ; 28 May–4 Jun; 20–27 Aug 2012	37.0±5.4	Hagenbjörk et al. (2017)
	Urban		35.0±3.9	
	Traffic		33.6±3.5	
Sweden, Umeå (20 sites)	Rural		27.7±8.4	
	Urban		26.7±7.3	
	Traffic		25.2±6.9	
China, Waliguan mountain	Rural	Sept 99-May 2001	44.9	Carmichael et al. (2003)
Taiwan, Shui-Li	Rural		25.0	
Malaysia, Tanah Rata	Rural		16.0	
Indonesia, Bukit Kototabang	Rural		10.7	
Inde, Agra	Rural		30.8	
Argentina, Isla Redonda	Rural		15.9	
Brazil, Arembepe	Rural		19.2	
Turkey, Camkoru	Rural		35.4	
Arab Emirates, Al-Ain	Rural	Apr 2005-Apr 2006	8.7	Salem et al. (2009)
	Industrial		5.9	
	Traffic		4.4	
	Commercial		5.9	
	Residential		7.3	
American Samoa Island, Tutuila	Urban and Rural	1990-2015	13.7 ± 1.0	Lu et al. (2018)
Chili, El Tololo			32.0 ± 1.3	
South Africa, Cape point			24.3 ± 1.1	
Australia, Cape grim			24.9 ± 0.8	
New Zealand, Baring head			21.4 ± 1.6	
Syowa			25.2 ± 0.9	
Neumayer-G			24.3 ± 1.5	
Arrival heights			25.9 ± 1.5	
South Pole			28.4 ± 1.7	
Barrow Atmospheric Baseline Observatory	Remote site	1973-2015	15-44	Cooper et al. (2020)
Mauna Loa Observatory (MLO)	Remote site	1973-2015	26-65	
American Samoa Observatory	Remote site	1973-2015	5-20	
South Pole Observatory	Remote site	1973-2015	17-40	
China	Rural site	2014-2017	34	Dufour et al. (2021)
Central East China			36	
Beijing–Tianjin–Hebei region			39	
Yangtze River Delta			35	
Pearl River Delta			31	
North America, Europa and Est Asia (Korea et Japan)	3136 Rural sites	2010-2014	0-56 and more	Gaudel et al. (2018)
North America, Europa and Est Asia	3348 Rural sites and 1453 urban sites	2010-2014	0-100 and more	Fleming et al. (2018)

North America, Europa and Est Asia	Rural site	1996-2005	15-55	Young et al. (2018)
North America, Europa and Est Asia	Rural and urban site	2010-2014	10-60	Schultz et al. (2017)
Eastern North America	Rural site	2000-2014	26-38	Chang et al. (2017)
	Urban site		28-38	

590 Several sites reported in Table 5 and Fig. 13 are exposed to high O<sub>3</sub> concentrations. These different levels observed in Africa and around the world are in most cases above values displayed in this study, with the exception of sites in southern Africa. Indeed, in Africa particularly, the earlier studies investigated have mentioned high ozone concentrations measured in southern Africa. Laban et al. (2018) have observed the elevated surface ozone (O<sub>3</sub>) concentrations over four sites in South Africa (Botsalano (2006-2008), Marikana (2008-2010), Welgegund (2010-2015) and Elandsfontein (2009- 2010)) with an annual mean ranging around from 5 to 70 ppb. The temporal O<sub>3</sub> patterns observed at the four sites resembled typical trends for O<sub>3</sub> in continental South Africa, with O<sub>3</sub> concentrations peaking in late winter and early spring (Laban et al., 2018). The assessment of long-term seasonal and inter-annual trends of a 21-year ozone passive sampling (monthly means) dataset collected at the Cape Point Global Atmosphere Watch (CPT GAW) station indicated that annual mean ozone level at this coastal area is of 26 ppb (Swartz et al., 2020b) while at Louis Trichardt (1995-2015), Amersfoort (1997-2015) and Skukuza (2000-2015) the level ranging from 22 ppb to 31 ppb (Swartz et al., 2020a). Over the sites of Botswana (1999-2001) and the Mpumalanga highveld, Zunckel et al. (2004) emphasized the springtime maximum of O<sub>3</sub> concentrations is between 40 and 60 ppb, but reached more than 90 ppb as a mean in October 2000. At the background stations at Cape Point (2000-2002), in Namibia (2000-2002) and areas adjacent to the highveld the maximum concentrations are between 20 and 30 ppb with minimums between 10 and 20 ppb. Ngoasheng et al. (2021) have investigated on the surface ozone concentrations during the period from 2014 to 2015 and 2018 to 2019 over ten sites located at North West in South Africa (8 ppb à 48 ppb). In addition, a more intensive campaign was conducted in June, July and August 2019 during whichat, 15 additional sites were also monitored. During the campaign from September 1999 to June 2001 of the newly established WMO/GAW Urban Research Meteorology and Environment (GURME) project, the mean values of ozone concentrations over the sites of Elandsfontein (35.1 ppb), Cape point (24.2 ppb) in South Africa, Tamanrasset in Algeria (33.2 ppb), Mt. Kenya (31.5 ppb) ~~were evaluated and~~ indicated high values over many sites (Carmichael et al 2003). Over a period of nine to 11-year (1995-2005) at four remote sites: Louis Trichardt (South Africa), Cape Point (South Africa), Amersfoort (South Africa) and Okaukuejo (Namibia) in southern Africa, Martins et al. (2007) exhibited a fairly constant high mean value of ozone about 27 ppb throughout the region except for the Louis Trichardt site, with a relatively high 10-year mean of 35 ppb. These values are approximately two times higher compared to Western and Central Africa INDAAF ozone data. The main reason could be the proximity of South Africa sites to O<sub>3</sub> precursor sources. They are generally located close to industrial, commercial and residential areas, not far from road traffic, garbage dumps, etc., where precursor emissions are high. Some sites may also be influenced by continental air masses containing gaseous pollutants. From 2012 to 2015, Hamdun and Arakaki (2015) measured surface ozone levels at three urban sites (Mapipa, Ubungo, and Posta) and two suburban sites (Kunduchi and Vijibweni) in the city of Dar es Salaam and in the village of Mwetemo, a rural area of Bagamoyo, Tanzania. Ozone levels at suburban (7.9-23.6) ppb sites were generally higher than at urban sites (10.3-18.6) ppb. In the context of the POLCA (~~Pollution of African Capitals~~) program, O<sub>3</sub> was measured using a passive sampling technique from Jan. 2008 to Dec. 2009 at Dakar and from Jun. 2008 to Dec. 2009 at Bamako (Adon et al., 2016). The mean annual concentrations of O<sub>3</sub> are 7.7 ppb in Dakar and 5.1 ppb in Bamako, respectively. At Abidjan during an intensive campaign within the dry season (15 December 2015 to 16 February 2016), using INDAAF (International Network to study Deposition and Atmospheric chemistry in AFrica) passive samplers exposed in duplicate for 2- week periods (Bahino et al., 2018), the highest O<sub>3</sub> concentration measured is at the two coastal sites of Gonzagueville and Félix-Houphouët-Boigny International Airport located in the southeast of the city, with average concentrations of 19.1 ± 1.7 and 18.8 ± 3.0 ppb,

respectively. At urban sites such as Al-Ain, Bamako, Dakar, Abidjan and Cotonou, the low O<sub>3</sub> levels are due to the saturated NO<sub>x</sub>-NO<sub>x</sub> regime observed at these sites, which limits photochemical O<sub>3</sub> production (Adon et al., 2013; Bahino et al., 2018; Salem et al., 2009). At most INDAAF sites, concentrations are lower because of their rural characteristics, generally far from anthropogenic sources, and much more influenced by biogenic activities from soils and vegetation. In the framework of IDAF program, Adon et al. (2010) analysed ozone concentrations from 2000 to 2007 over the sites of Banizoumbou (Niger), Katibougou and Agoufou (Mali), Djougou (Benin), Lamto (Cote d'Ivoire), Zoetele (Cameroon) and Bomassa (Congo). Annual mean O<sub>3</sub> concentrations are lower for all ecosystems and range from 4.0±0.4 ppb (Bomassa) to 14.0±2.8 ppb (Djougou) and are the same order of magnitude over period 2000-2020 (INDAAF program) where concentrations ranging from 3.9±1.1 ppb (Bomassa) to 14.8±4.3 ppb at Bambej in Western and Central Africa. Results are fairly illustrative of the various mitigation or vigilance measures that need to be adopted to ensure the environmental well-being of each ecosystem. ~~The a~~Additional efforts must therefore be made, through ~~projects or~~ programs, to enhance the density of monitoring networks for polluting gases in general and O<sub>3</sub> in particular, especially in Africa, where very few long-term monitoring exist.



640 **Figure 13.** Overview of O<sub>3</sub> monitoring studies in Africa. Blue bars represent lower and upper range of means if reported. Red  
 645 points represent average concentration of O<sub>3</sub>.

### 3.3 Annual and seasonal trends of O<sub>3</sub> and its precursors

#### 3.3.1 Annual trends

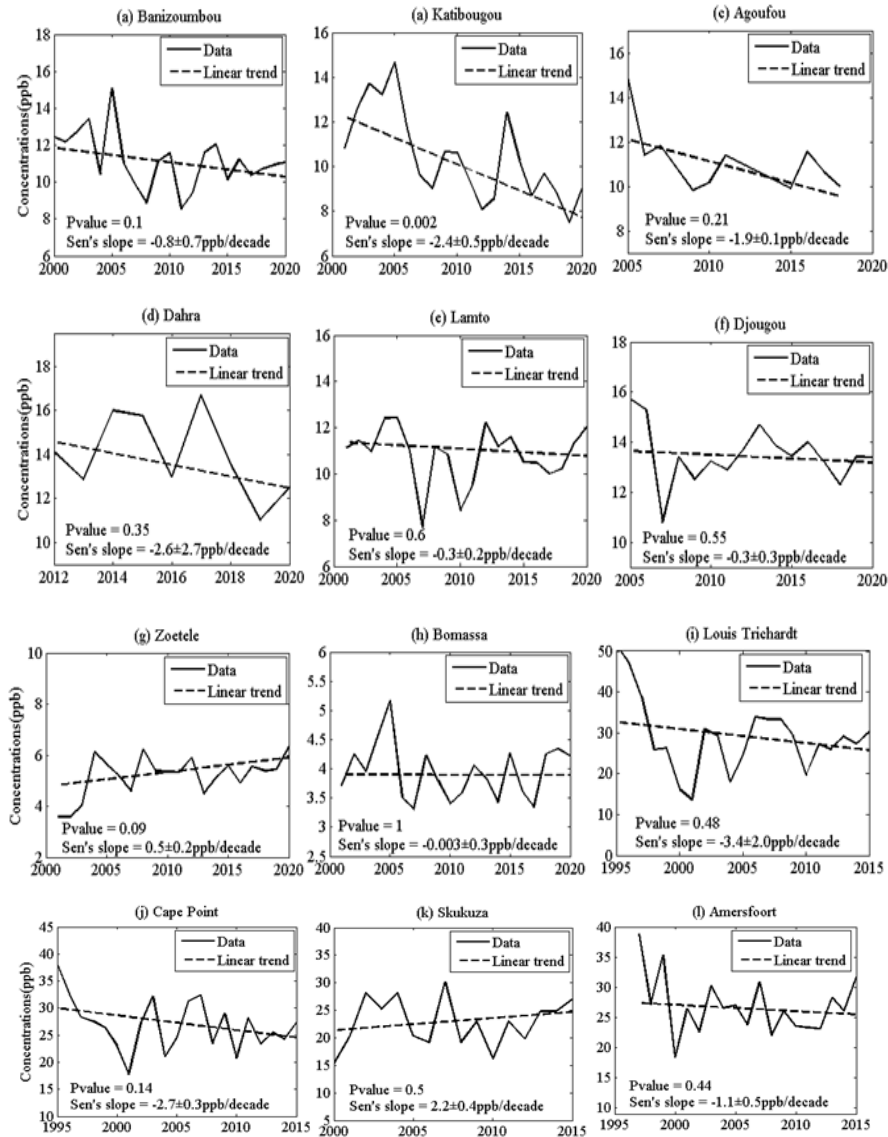
Annual trends in O<sub>3</sub> concentrations were calculated at all sites (except Bambey and Mbita which do not have 10 years of measurements) according to 95% confidence intervals in Mann-Kendall test in dry savanna, wet savanna, forest and Agricultural/semi-arid savanna (Fig. 14). At the decade scale, Katibougou site in Mali shows a decrease in O<sub>3</sub> concentrations around -2.4 ppb decade<sup>-1</sup> from 2001 to 2020 (pvalue = 0.002) at the 95% confidence level (Table 6). This trend at Katibougou is confirmed in both the dry and wet seasons. Ozone concentrations decrease by -1.8 ppb decade<sup>-1</sup> (pvalue = 0.03) in the dry season and -3.3 ppb decade<sup>-1</sup> (pvalue < 0.01) in the wet season. At the same site, the trend in nitrogen oxide (NO<sub>2</sub>) over the 1998-2020 period shows a decline in annual concentrations and annual seasonal means. Ossohou et al. (2019) observed a decrease in NO<sub>2</sub> concentrations at Katibougou in the wet season (-0.4 ppb decade<sup>-1</sup>) over the period 1998-2015. These downward trends in NO<sub>2</sub> could therefore explain the downward trends in O<sub>3</sub>. At the Banizoumbou site (Niger) a medium certainty for a decrease trend by -0.8 ppb decade<sup>-1</sup> of O<sub>3</sub> concentrations (pvalue = 0.1) is noted at a 95% confidence level (Table 6). During the dry period, this downward trend is around calculated with high certainty with O<sub>3</sub> decreasing by -1.5 ppb decade<sup>-1</sup> (pvalue = 0.04). Calculation of trends on biogenic VOCs at Banizoumbou indicate a decrease in biogenic emissions of alpha pinene ( $\tau = -0.37$ , p value = 0.020) and beta pinene ( $\tau = -0.39$ , p value = 0.01). Chen et al. (2018) indicated that trends in global tree cover from 2000 to 2015 have led to clear decreases, particularly in West Africa with a reduction of around 10% in regional BVOC emissions due to agricultural expansion. A weak indication of a downward change in ozone is observed at Agoufou (Mali). At the sites of Agoufou (Mali) and Bambey Dahra (Senegal) and, a low certainty of the O<sub>3</sub> concentrations decrease is observed (respectively pvalue = 0.21; pvalue = 0.35). In wet savanna and forests, Lamto (Cote d'Ivoire) and Djougou (Benin), sites annual ozone trends are not significant (Table 6). show a downward trend by 0.3 ppb decade<sup>-1</sup>. At 95% confidence interval, there is very low certainty that this trend will occur. In West Africa generally, we note a decrease in surface ozone concentrations even if this trend is not significant at almost all sites. On these remote sites, this decrease could be partly linked to a large decrease in burned area in tropical savannas in Africa, particularly those with low and intermediate levels of tree density (Andela et al., 2017). At Bomassa site (Congo) (pvalue = 1), we have no trend contrary to Zoetele (Cameroon) where a medium increase is recorded of O<sub>3</sub> concentrations by 0.5 ppb decade<sup>-1</sup>. is recorded, with a medium certainty. To explain the trends observed at Zoetele, we apply the Kendall rank correlation between O<sub>3</sub> concentrations and its precursors. We obtain a significant positive rank correlation at the 95% confidence level. For NO<sub>x</sub> and anthropogenic VOCs,  $\tau = 0.7$  (pvalue = 0.03) while with biogenic VOCs, the correlation varies from 0.54 to 0.69 (pvalue < 0.01). In addition, we observe increasing trends for biogenic VOCs. Isoprene increases by 18 ng.m<sup>-2</sup>s<sup>-1</sup> per decade (pvalue = 0.001), alpha pinene by 1 ng.m<sup>-2</sup>s<sup>-1</sup> per decade (pvalue < 0.001) and beta pinene by 0.4 ng.m<sup>-2</sup>s<sup>-1</sup> per decade (pvalue = 0.003). Similar trends were also observed in the wet season for alpha pinene and beta pinene, and in the dry season for isoprene. The rise in O<sub>3</sub> concentrations in Zoetele could therefore be explained by these increasing trends observed in isoprene, alpha pinene and beta pinene from one season to the other and in anthropogenic emissions in African forest regions. These results are corroborated by 18 years of satellite data (1998-2015) by Andela et al. (2017) who noted an increasing trend in burned areas close-canopy forests. In South Africa sites, at Louis Trichardt (pvalue = 0.48) and Amersfoort (pvalue = 0.44) and Skukuza, a downward no trend is reported contrary in Cape Point we observe a weak downward trend of ozone (Table 6). with a very low certainty respectively by 3.4 ppb decade<sup>-1</sup> and 1.1 ppb decade<sup>-1</sup> at scale confidence of 95%. The same negative trend is recorded at In Cape Point (pvalue = 0.14) with a low certainty (by 2.7 ppb decade<sup>-1</sup>). At Skukuza (pvalue = 0.49), an increase of O<sub>3</sub> concentrations by 2.21 ppb decade<sup>-1</sup> with no evidence of trends at a confidence threshold of 95% is observed

**Table 6.** Annual trend of ozone concentrations over the period 1995-2020 for 12 measurement sites

<u>Station name</u>	<u>Trend in ppb.decade<sup>-1</sup></u>	<u>p value</u>	<u>Analysis on annual trend values</u>
<u>Banizoumbou</u>	<u>-0.8+0.7</u>	<u>0.1</u>	<u>Medium downward trend</u>
<u>Katibougou</u>	<u>-2.4+0.5</u>	<u>0.002</u>	<u>Downward trend</u>
<u>Agoufou</u>	<u>-1.9+0.1</u>	<u>0.21</u>	<u>Weak downward trend</u>
<u>Dahra</u>	<u>-2.6+2.7</u>	<u>0.35</u>	<u>No trend</u>
<u>Lamto</u>	<u>-0.3+0.2</u>	<u>0.6</u>	<u>No trend</u>
<u>Djougou</u>	<u>-0.3+0.3</u>	<u>0.55</u>	<u>No trend</u>
<u>Zoetele</u>	<u>0.5+0.2</u>	<u>0.09</u>	<u>Medium upward trend</u>
<u>Bomassa</u>	<u>-0.003+0.3</u>	<u>1</u>	<u>No trend</u>
<u>Louis Trichardt</u>	<u>-3.4+2.0</u>	<u>0.48</u>	<u>No trend</u>
<u>Skukuza</u>	<u>2.2+0.4</u>	<u>0.5</u>	<u>No trend</u>
<u>Amersfoort</u>	<u>-1.1+0.5</u>	<u>0.44</u>	<u>No trend</u>
<u>Cape Point</u>	<u>-2.7+0.3</u>	<u>0.14</u>	<u>Weak downward trend</u>

695 The absence of annual trends at South African sites assessed with certainty confirms the results obtained by Swartz et al. (2020a, 2020b) at the Louis Trichardt, Amersfoort, Skukuza and Cape Point sites using multiple linear regression model approach. Indeed, the trend lines for the O<sub>3</sub> concentrations measured during the entire sampling periods indicate slight negative slopes at Amersfoort and Louis Trichardt and a small positive slope at Skukuza (Swartz et al., 2020a). Gaudel et al. (2020, 2024) and Wang et al. (2022) have observed that annual trends of median ozone values have increased in the tropospheric column (IAGOS, 950 to 2050 hPa) respectively around 2 nmol mol<sup>-1</sup> decade<sup>-1</sup> during 22-years (1994-2016) of measurement and of 2.4364 ± 0.4834 nmol mol<sup>-1</sup> decade<sup>-1</sup> (1994-2019) above Gulf of Guinea. Trends are confirmed by new IMO/MLS satellite data covering the period 2004-2019 at the same sites, with tropical tropospheric ozone trends indicating values of around 0.41 ± 0.80 nmol mol<sup>-1</sup> decade<sup>-1</sup> (Gaudel et al., 2024). These results are contrary to the decrease in ozone observed at the INDAAF sites in the Gulf of Guinea (Lamto and Djougou), which show no trend. To partly explain the increase of ozone in recent decades, Gaudel et al. (2020) pointed out that although NO<sub>x</sub> emissions from biomass combustion have decreased in the tropics, this decrease has been overcompensated by the increase in fossil fuel emissions. However, we believe that the discrepancy between these studies could be explained by the proximity of the measurement sites to the sources of precursor emissions. Indeed, the data measured from the commercial aircraft monitoring network used in the work of Gaudel et al. (2020, 2024) are taken at airports closer to cities, whereas INDAAF sites are rural sites, far from fossil fuel combustion sources. In addition, Gaudel et al. (2018) reported that spatially, global surface ozone trends are highly variable depending on time period, region, elevation and proximity to fresh ozone precursor emissions. The distributions of ozone annual trends in the recent two decades (2000-2019) explored by Hou et al. (2023) over six regions on the world including Africa (25°S–25°N, 17°W–51°E) showed a significant increase in these six regions of the Tropospheric Column Ozone (OMI/MLS satellite data), with the smallest value of ~0.07 DU/yr in the African while with MET+2015EMIS model, the annual trends of ozone over Africa turn to insignificant decreases (0.04 DU/yr). These trends relatively small and contrast with the changes observed at most INDAAF sites, could support that ozone surface data do not necessarily represent the free troposphere where the radiative forcing effects of ozone are concentrated. We also think that the ozone trends could be estimate more accurately in combining of the soundings and long-term surface observations is necessary. Breaks in the annual concentration data were observed at Banizoumbou and Katibougou in 2006 as a result of the Pettitt test. During the dry and wet seasons, further breaks were recorded in the annual series in 2006 (Katibougou) and 2007 (Banizoumbou) (dry season)

720 and in 2014 at Katibougou (wet season). However, no trend inversion was induced in these break years. At the other study sites, no breaks were observed.



725

**Figure 14.** Long-term annual linear trend of in situ O<sub>3</sub> concentrations over the period 1995-2020 at 95% confidence intervals calculated for 12 measurement sites representative of African dry savanna, wet savanna, forest and agricultural/semi-arid savannas and p-value for each trend.

730 **3.3.2 Seasonal trends**

Trend tests were performed on monthly mean O<sub>3</sub> concentrations using seasonal Kendall test and all trend results are presented in Fig. 15. The tests reveals a significance downward trend of -0.7 ppb decade<sup>-1</sup> at Banizoumbou (pvalue = 0.02), with high certainty at 95% confidence level. At Katibougou (pvalue <0.001), O<sub>3</sub> concentrations decrease by -2.4 ppb decade<sup>-1</sup> with very

735 ~~high certainty~~. At the other sites in West Africa, a downward trend of O<sub>3</sub> of -0.7 ppb decade<sup>-1</sup> at Agoufou, -0.6 ppb decade<sup>-1</sup> at  
Dahra ~~and~~ -0.23 ppb decade<sup>-1</sup> at Lamto ~~and -0.11 ppb decade<sup>-1</sup> at Djougou~~ are calculated. However, the ~~significance certainty~~  
is medium at Agoufou, low at Dahra and Lamto ~~at 95% confidence interval. There is no trend and very low~~ at Djougou. The  
trends in Bomassa (pvalue = 0.17) and Cape Point (pvalue = 0.13), are similar to sites of West Africa ~~with low certainty~~. At  
740 the Louis Trichardt and Amersfoort sites, the results show no ozone trend (pvalue = 0.67 and 0.93) but respectively -2.7 ppb  
and -0.1 ppb per decade decrease. In contrast, an upward trend ~~with very high certainty~~ is reported at Zoetele in Cameroon  
(Sen slope =  $\pm 0.7$  ppb decade<sup>-1</sup>; pvalue = 0.001), and at Skukuza in South Africa (Sen slope =  $\pm 3.4$  ppb decade<sup>-1</sup>; pvalue =  
0.001) at 95% confidence interval. All the annual trends observed at INDAAF sites are confirmed by Kendall's seasonal trends.  
The O<sub>3</sub> mixing ratio in the lower troposphere is slightly higher in central Africa in July than in northern Africa (in January),  
likely indicating rapid photochemical O<sub>3</sub> production by biomass burning precursors (Singh et al., 1996) during the Southern  
Hemisphere fires (Tsvilidou et al., 2023). Biomass burning air mass transport from the hemisphere where fires occur (where  
745 the highest CO is measured) to the opposite hemisphere is allowed by either the north-easterly Harmattan flow (January) or  
the southeasterly winds and monsoon flow (July) (Sauvage et al., 2005; Tsvilidou et al., 2023) and could be also explain the  
upward trend observed at Zoetele. At Skukuza, the upward trend is thought to be due to anthropogenic emissions. At the Irene  
site in the North-eastern interior of South Africa, Bencherif et al. (2020) obtained an upward trend in the tropospheric O<sub>3</sub>  
column (1998–2017) at a rate of around 2.4% per decade. At Irene an increase of tropospheric ozone is reported respectively  
750 by Thompson et al. (2014) ~~from September to November in spring~~, and Mulumba et al. (2015) ~~from December to February in~~  
~~summer~~, from ozonesonde records (1990 to 2008) and ozone tropospheric columns (1998 à 2013). An upward trend in NO<sub>2</sub>  
levels was also evident at Skukuza, signifying the influence of growing rural communities on the Kruger National Park border  
(Swartz et al., 2020a). At the South African sites, the high values of ~~NO<sub>x</sub>NO<sub>x</sub>~~ and COV fluxes are observed at Skukuza (Fig.  
11d). The population growth and the associated increase in anthropogenic activities (like domestic biomass burning and solid  
755 fuel combustion) result in high levels of pollutants in South Africa's Highveld region (Kai et al., 2022; Keita et al., 2021) and  
could therefore justify the upward trend obtained. The increase in O<sub>3</sub> in South Africa could be also explained by biomass  
burning (agriculture reason) and greenhouse (urban-industry reason) activities implemented in Africa during summer and  
spring seasons (Bencherif et al., 2020; Diab et al., 2004; Sivakumar et al., 2017). Furthermore, pollutants emissions from  
domestic biofuel, brought by long-range transport of pollution in the Southern Hemisphere have an impact at the continental  
760 scale (Thompson et al., 2014). Moreover, Thompson et al. (2021) have observed an increase mean trend of + 1.2% per decade  
(pvalue = 0.119) from 22-year SHADOZ record (1998–2019) of ozone profiles in the free tropospheric (5–15 km) at Nairobi  
in East Africa. This trend result is similar with surface ozone change observed in Skukuza. The increase in tropospheric ozone  
in the tropics, is partly of dynamic origin with the movement of air masses and not solely due to growing anthropogenic  
emissions (Thompson et al., 2021), could also explain this similarity. Balashov et al. (2014) reported from 1990 to 2007 over  
765 the South African Highveld that the sites of Palmer and Makalu exhibit statistically significant negative trends in surface ozone  
over the spring season and the month of September respectively, whereas Verkykkop and Elandsfontein show no statistically  
significant change in surface ozone. At most INDAAF sites (remote and rural) we found, as in the work of Balashov et al.  
(2014), that the surface ozone data still showed no trend. These results confirm however that surface ozone trends in Africa  
are not uniform regionally or seasonally as mentioned by Thompson et al. (2021).

770



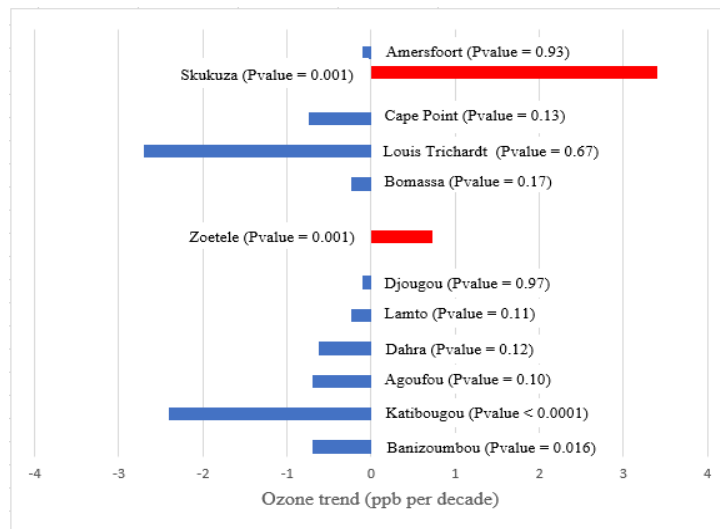


**Figure 15.** Kendall's seasonal trend of in situ O<sub>3</sub> concentrations over the period 1995-2020 at 95% confidence intervals calculated for 12 measurement sites representative of African dry savanna, wet savanna, forest and agricultural/semi-arid savannas and p-value for each trend.

775

#### 4. Conclusion

This work presents an original database of long-term O<sub>3</sub> concentrations at fourteen African sites belonging to the INDAAF program and companion projects. This database gives a better understanding of O<sub>3</sub> concentration levels at remote tropical sites representative of the major African biomes. In this study, we establish a mean annual cycle by site and ecosystem type, and investigate the seasonal variability of O<sub>3</sub> concentrations over the period 1995-2020. Our analysis of the seasonality of anthropogenic and biogenic NO<sub>x</sub> and VOC emissions then highlights the significant factors contributing to O<sub>3</sub> formation. Finally, we calculate the O<sub>3</sub> long-term trends, which provide an insight into the long-term evolution of O<sub>3</sub> levels and the local and regional dynamics of the emission sources of its precursors.

780

The results indicated that O<sub>3</sub> levels are the highest during the rainy season in dry savannas and during the dry season in wet savannas and forests. In agricultural fields, no seasonal variations of O<sub>3</sub> concentrations are observed. In the semi-arid savanna (South Africa), dry season O<sub>3</sub> levels are the highest at Louis Trichardt and Skukuza. At Cape Point and Amersfoort sites, maxima occur during the rainy season. Mean annual O<sub>3</sub> concentrations range from 10.5±5.4 to 14.8±4.3 ppb in dry savannas, from 10.8±3.3 to 13.5±4.8 ppb in wet savannas, from 3.9±1.1 to 5.2±2.1 ppb in forest ecosystems and from 19.9±4.7 to 30.8±9.4±8.04 ppb in semi-arid/agricultural savannas. BVOC (under the influence of air temperature), NO emissions (in the presence of humidity) and precipitation, are the main contributors to O<sub>3</sub> formation in dry savannas. The seasonality of O<sub>3</sub> measurements and dominant precursors confirm the important role of microbial processes leading to high NO emissions at the beginning of the wet season for O<sub>3</sub> production. Furthermore, the influence of air temperature and solar radiation on woody emissions from shrubs in the Sahel, and the presence of sparse vegetation (short grasses, forbs and dicotyledonous shrubs with perennial ground cover) in this region could be at the origin of BVOC emissions. The photochemical O<sub>3</sub> regime in savannas and rainforests (heavily vegetated areas) is strongly linked to BVOC emissions from vegetation, and to temperature, radiation and humidity. At Lamto and Zoetele, anthropogenic NO<sub>x</sub> and VOC also contribute to O<sub>3</sub> formation. The most dominant precursor species in southern Africa are mainly NO<sub>x</sub> emissions (anthropogenic and biogenic), humidity and temperature, as well as anthropogenic VOC at a few sites. They are due of Biomass and fuel combustion, large-scale transport of pollutants, domestic combustion in winter and biogenic emissions from vegetation. At INDAAF sites, which are rural sites far from many anthropogenic sources, O<sub>3</sub> concentrations are below most of the values reported in the literature. At 95% confidence intervals,

785

790

795

800

annual and seasonal ~~Mann-Kendall~~ trends (based on Mann-Kendall treatment, and low p-values) ~~at all sites~~ indicate that the Katibougou site in Mali and the Banizoubou site in Niger experience a significant decrease in O<sub>3</sub> concentrations, (around -2.4 ppb decade<sup>-1</sup> and -0.8 ppb decade<sup>-1</sup>,) respectively with a high certainty over the period 2000 to 2020. These likely results from justified by downward trends of NO<sub>2</sub> trends observed at Katibougou and reduced the BVOC emissions at Banizoubou.

805 In contrast, a significant upward trend is reported at Zoetele ( $\pm 0.7$  ppb<sub>2</sub>-decade<sup>-1</sup>) in Cameroon and Skukuza ( $\pm 3.4$  ppb<sub>2</sub> decade<sup>-1</sup>) in South Africa. ~~These trends are could be~~ attributed to the increase in BVOCs in Zoetele and increases in anthropogenic ~~and biogenic~~ emissions that affect in Skukuza.

This study described ~~in details~~ the O<sub>3</sub> levels in representative African biomes, as well as the photochemical and meteorological regimes related to seasonal concentrations and the derived trends and conditions leading to the observed concentrations. The results on regional trends variability and seasonal variations are consistent with published studies of African ozone data although in most cases, the INDAAF measurements are more rural than data taken at urban monitoring sites, including airports. The importance of developing, and maintaining long-term observations like the INDAAF project, with regular calibration and standards, cannot be overstated. In particular, for the INDAAF mostly agricultural locations, the data can be used to assess the impact of O<sub>3</sub> dry deposition fluxes on African crops and the potential crop yield losses because of O<sub>3</sub> toxicity to plants. Studies of ozone changes during the growing season can lead to action plans for achieving better food security. The ozone data provide invaluable constraints for models of chemical and climate processes in the atmosphere. With INDAAF data and improved models, there will be more confidence in future predictions of African air quality and the exposure of agriculture and the regional population to surface ozone. The results presented in this article constitute a robust database showing the importance of developing or maintaining long term observation projects and observatories. This database could be used to assess the impact of O<sub>3</sub> dry deposition fluxes on African crops and the potential yield losses because of O<sub>3</sub> absorption by crops. An assessment of the various agricultural losses during the growing season will help to better orient actions to improve crop yield and achieve food security. In addition, this documentation is invaluable for modeling chemical processes in the atmosphere and for projecting future changes in tropospheric O<sub>3</sub>. It could limit the uncertainties of these models and facilitate their validation, which is mainly based on data measured in situ.

810

815

820

825 **Data availability.** Dataset DOIs of O<sub>3</sub> observations for INDAAF sites (see complete citation in the reference list), available in the INDAAF database at <https://indaaf.obs-mip.fr> :

Banizoubou (Niger)	Katibougou (Mali)	Agoufou (Mali)	Bambey (Senegal)
<a href="https://doi.org/10.25326/608">https://doi.org/10.25326/608</a> Laouali et al. (2023)	<a href="https://doi.org/10.25326/604">https://doi.org/10.25326/604</a> Galy-Lacaux et al. (2023a)	<a href="https://doi.org/10.25326/610">https://doi.org/10.25326/610</a> Galy-Lacaux et al. (2023b)	<a href="https://doi.org/10.25326/609">https://doi.org/10.25326/609</a> Galy-Lacaux et al. (2023c)
Dahra (Senegal)	Lamto (Cote d'Ivoire)	Djougou (Benin)	Zoetele (Cameroon)
<a href="https://doi.org/10.25326/606">https://doi.org/10.25326/606</a> Galy-Lacaux et al. (2023d)	<a href="https://doi.org/10.25326/275">https://doi.org/10.25326/275</a> Galy-Lacaux et al. (2023e)	<a href="https://doi.org/10.25326/605">https://doi.org/10.25326/605</a> Akpo et al. (2023)	<a href="https://doi.org/10.25326/603">https://doi.org/10.25326/603</a> Ouafo-Leumbe et al. (2023)
Bomassa (Congo)	Mbita (Kenya)	Louis Trichardt (South Africa)	Skukuza (South Africa)
<a href="https://doi.org/10.25326/607">https://doi.org/10.25326/607</a> Galy-Lacaux et al. (2023f)	<a href="https://doi.org/10.25326/642">https://doi.org/10.25326/642</a> Galy-Lacaux et al. (2023g)	<a href="https://doi.org/10.25326/646">https://doi.org/10.25326/646</a> van Zyl et al. (2023a)	<a href="https://doi.org/10.25326/645">https://doi.org/10.25326/645</a> van Zyl et al. (2023b)
Cape Point (South Africa)	Amersfoort (South Africa)		
<a href="https://doi.org/10.25326/644">https://doi.org/10.25326/644</a> van Zyl et al. (2023c)	<a href="https://doi.org/10.25326/647">https://doi.org/10.25326/647</a> van Zyl et al. (2023d)		

830 GFED4 (~~NO<sub>x</sub>~~, COV) and MEGAN-MACC (Isoprene, pinene-a, pinene-b) data are available from  
https://eccad.sedoo.fr/#/data. ERA5 reanalysis data are available from  
https://cds.climate.copernicus.eu/cdsapp#!/dataset/reanalysis-era5-single-levels?tab=overview.

835 **Author contributions.** CGL designed the study, wrote the protocol and edited the paper. HEVD conducted data processing,  
the statistical analysis and wrote the paper. CD made conceptual contributions and edited the paper. ABA and MO contributed  
at the statistical analysis, assisted in sample collection and edited the paper. VY, DL, MO-L, ON, PGVZ assisted in sample  
collection and edited the paper. EG and MDA analysed the samples.

840 **Competing interests.** The contact author has declared that none of the authors has any competing interests.

#### Disclaimer.

845 **Acknowledgements.** The authors would like to acknowledge the INDAAF project (International Network to study Deposition  
and Atmospheric chemistry in Africa), and especially all its local technicians for their maintenance and sampling work. We  
would also like to acknowledge the "Cycle de l'Azote entre la Surface et l'Atmosphère en Afrique" (CASAQUE) project and  
the Integrated Nitrogen Management system (INMS) for providing us with data on O<sub>3</sub> concentrations at Dahra and Mbita. This  
study was supported by the INSA (Integrated Nitrogen Studies in Africa) project, which funded the research carried out for  
this paper at the "Laboratoire d'Aérodologie de Toulouse". We are indebted to the AMMA-CATCH project, the University of  
Copenhagen and the Observatoire de recherche en environnement "Bassins versants tropicaux expérimentaux" (SO BVET)  
850 for providing us with meteorological data from Niger, Benin, Senegal and Cameroon. We are also grateful to the ECCAD  
platform and the European Centre for Medium-Range Weather Forecasts (ECMWF) for biogenic and anthropogenic emissions  
and ERA5 reanalysis data.

855 **Financial support.** This study has received funding from the European Union's Horizon 2020 research and innovation  
programme under the Marie Skłodowska-Curie grant agreement no. 871944.

#### Review statement.

#### References

- 860 Abbadie, L. (Ed.), Lamto: Structure, Functioning, and Dynamics of a Savanna Ecosystem, Ecological Studies, Springer Science+Business  
Media, New York, 415pp., ISBN: 9780387948447, 2006.
- | Abiodun, B. J., Ojumu, A. M., Jenner, S., Ojumu, T. V.: The transport of atmospheric NO<sub>x</sub> and HNO<sub>3</sub> over Cape Town, Atmos. Chem. Phys.,  
14, 559–575, <https://doi.org/10.5194/acp-14-559-2014>, 2014.
- 865 Adon, M., Galy-Lacaux, C., Delon, C., Yoboue, V., Solmon, F., and Kaptue T. A, T.: Dry deposition of nitrogen compounds (NO<sub>2</sub>, NO<sub>3</sub>,  
NH<sub>3</sub>), sulfur dioxide and ozone in west and central African ecosystems using the inferential method, Atmos. Chem. Phys., 13, 11351–  
11374, 2013.
- Adon, M., Galy-Lacaux, C., Yoboué, V., Delon, C., Lacaux, J. P., Castera, P., Gardrat, E., Pienaar, J., Al Ourabi, H., Laouali, D., Diop, B.,  
Sigha-Nkamdjou, L., Akpo, A., Tathy, J. P., Lavenu, F., and Mougine, E.: Long term measurements of sulfur dioxide, nitrogen dioxide,  
ammonia, nitric acid and ozone in Africa using passive samplers, Atmos. Chem. Phys., 10, 7467–7487, doi:10.5194/acp-10-7467-2010,  
870 2010.
- Adon, M., Yoboue, V., Galy-Lacaux, C., Lioussé, C., Diop, B., Doumbia, E. H. T., Gardrat, E., Ndiaye, S. A., and Jarnot, C.: Measurements  
of NO<sub>2</sub>, SO<sub>2</sub>, NH<sub>3</sub>, HNO<sub>3</sub> and O<sub>3</sub> in West African urban environments, Atmos. Environ., 135, 31–40,  
<https://doi.org/10.1016/j.atmosenv.2016.03.050>, 2016.
- Aghedo, A. M., Schultz, M. G., and Rast, S.: The influence of African air pollution on regional and global tropospheric ozone, Atmos. Chem.  
875 Phys., 7, 1193–1212, <https://doi.org/10.5194/acp-7-1193-2007>, 2007.
- Akpo, A., Galy-Lacaux, C., Delon, C., Gardrat, E., Dias Alves, M., Lenoir, O., Halisson, J., Darakpa, C. & Darakpa, D. : Trace gases, Djougou,  
Benin, [dataset], AERIS, <https://doi.org/10.25326/605>, 2023.

- 880 Akpo, A. B., Galy-Lacaux, C., Laouali, D., Delon, C., Lioussse, C., Adon, M., Gardrat, E., Mariscal, A., Darakpa, C.: Precipitation chemistry and wet deposition in a remote wet savanna site in West Africa: Djougou (Benin), *Atmospheric Environment*, 115, 110–123, ~~2015~~, <http://dx.doi.org/10.1016/j.atmosenv.2015.04.064>, 2015.
- Alves, E. G., Jardine, K., Tota, J., Jardine, A., Yáñez-Serrano, A. M., Karl, T., et al. : Seasonality of isoprenoid emissions from a primary rainforest in central Amazonia, *Atmospheric Chemistry and Physics*, 16, 3903–3925. <https://doi.org/10.5194/acp-16-3903>, 2016
- Andela, N., Morton, C., Giglio, L., Chen, Y., van Der Werf, G., Kasibhatla, P. S., DeFries, R. S., Collatz, G. J., Hantson, S., Kloster, S., Bachelet, D., Forrest, M., Lasslop, G., Li, F., Mangeon, S., Melton, J. R., Yue, C., Randerson, J. T.: A human-driven decline in global burned area, *Science*, 356, 1356–1362, <https://doi.org/10.1126/science.aal4108>, 2017.
- 885 Bahino, J., Yoboué, V., Galy-Lacaux, C., Adon, M., Akpo, M., Lioussse, C., Gardrat, E., Chiron, C., Ossouhou, M., Gnamien, S., Keita, S., and Djossou, J.: A pilot study of gaseous pollutants' measurement (NO<sub>2</sub> HNO<sub>3</sub>, SO<sub>2</sub>, NH<sub>3</sub> and O<sub>3</sub>) in Abidjan, Côte d'Ivoire: contribution to an overview of gaseous pollution in African cities, *Atmos. Chem. Phys.*, 18, 5173-5198, <https://doi.org/10.5194/acp-18-5173-2018>, 2018.
- 890 Balashov, N. V., Thompson, A. M., Piketh, S. J., and Langerman, K. E.: Surface ozone variability and trends over the South African Highveld from 1990 to 2007, *J. Geophys. Res.-Atmos.*, 119, 4323–4342, <https://doi.org/10.1002/2013JD020555>, 2014.
- Baldy, S., Ancellet, G., Bessafi, M., Badr, A., and Luk, D. L. S.: Field observations of the vertical distribution of tropospheric ozone at the island of Reunion (southern tropics), *J. Geophys. Res.-Atmos.*, 101, 23835–23849, doi:10.1029/95jd02929, 1996.
- 895 Bakayoko, A., Galy-Lacaux, C. Véronique Yoboué, V., Hickman, J., E., Roux, F., Gardrat, E., Julien, F., and Delon, C.: Dominant contribution of nitrogen compounds in precipitation chemistry in the Lake Victoria catchment (East Africa), *Environ. Res. Lett*, 16, 1–20, doi 10.1088/1748-9326/abe25c, 2021.
- Bencherif, H., Tohir, A. M., Mbatha, N., Sivakumar V., Preez, D. J., Bègue, N., and Coetzee, G.: Ozone Variability and Trend Estimates from 20-Years of Ground-Based and Satellite Observations at Irene Station, South Africa, *Atmosphere*, 11, 1216, doi:10.3390/atmos11111216, 2020.
- 900 Bigaignon, L., Delon, C., Ndiaye, O. Galy-Lacaux, C., Serça, D., Guérin, F., Tallec, T., Merbold, L., Tagesson, T., Fensholt, R., André, S. and Sylvain Galliau, S.: Understanding N<sub>2</sub>O Emissions in African Ecosystems: Assessments from a Semi-Arid Savanna Grassland in Senegal and Sub-Tropical Agricultural Fields in Kenya, *Sustainability*, MDPI, 12, 1–26, doi:10.3390/su12218875, 2020.
- 905 Brown, F., Folberth, G. A., Sitch, S., Bauer, S., Bauters, M., Boeck, P., Cheesman, A. W., Deushi, M., Dos Santos Vieira, I., Galy-Lacaux, C. Haywood, J., Keeble, J., Mercado, L. M., O'Connor, F. M., Oshima, N., Tsigaridis, K., and Verbeecq, H.: The ozone–climate penalty over South America and Africa by 2100, *Atmos. Chem. Phys.*, 22, 12331–12352, 2022 <https://doi.org/10.5194/acp-22-12331-2022>, 2022.
- Carmichael, G.R., Ferm, M., Thongboonchoo, N., Woo, J.-H., Chan, L., Murano, K., Viet, P.H., Mossberg, C., Bala, R., Boonjawat, J., Upatum, P., Mohan, M., Adhikary, S.P., Shrestha, A.B., Pienaar, J., Brunke, E.B., Chen, T., Jie, T., Guoan, D., Peng, L.C., Dhiharto, S., Harjanto, H., Jose, A.M., Kimani, W., Kirouane, A., Lacaux, J.-P., Richard, S., Barturen, O., Cerda, J.C., Athayde, A., Tavares, T., Cotrina, J.S., Bilici, E. : Measurements of sulfur dioxide, ozone and ammonia concentrations in Asia, Africa, and South America using passive samplers, *Atmos. Environ.*, 37, 1293–1308. [https://doi.org/10.1016/S1352-2310\(02\)01009-9](https://doi.org/10.1016/S1352-2310(02)01009-9), 2003.
- 910 Carmichael, G. R., Streets, D. G., Calori, G., Amann, M., Jacobson, M. Z., Hansen, J., and Ueda, H.: Changing trends in sulfur emissions in Asia: Implications for acid deposition, *Environ. Sci. Technol.*, 36, 4707–4713, doi:10.1021/es011509c, 2002.
- 915 Camredon, M. and Aumont, B.: I-L'ozone troposphérique : production/consommation et régimes chimiques, *Pollut. Atmos.*, 193, 51–60 doi:10.4267/pollution-atmospherique.1404, 2007.
- Chang, K.-L., Petropavlovskikh, I., Cooper, I. O. R., Schultz, M. G., and Wang, T.: Regional trend analysis of surface ozone observations from monitoring networks in eastern North America, Europe and East Asia, *Elem Sci Anth*, 50, 1–22, doi: <https://doi.org/10.1525/elementa.243>, 2017.
- 920 Chen, W. H., Guenther, A. B., Wang, X. M., Chen, Y. H., Gu, D. S., Chang, M., Zhou, S. Z., Wu, L. L., Zhang, Y. Q.: Regional to global biogenic isoprene emission responses to changes in vegetation from 2000 to 2015, *Journal of Geophysical Research: Atmospheres*, 123, 3757–3771, <https://doi.org/10.1002/2017JD027934>, 2018.
- Clain, G., Baray, J. L., Delmas, R., Diab, R., Leclair de Bellevue, J., Keckhut, P., Posny, F., Metzger, J. M., and Cammas J. P.: Tropospheric ozone climatology at two Southern Hemisphere tropical/subtropical sites, (Reunion Island and Irene, South Africa) from ozone sondes, LIDAR, and in situ aircraft measurements, *Atmos. Chem. Phys.*, 9, 1723–1734, <https://doi.org/10.5194/acp-9-1723-2009>, 2009.
- 925 Cooper, O. R., Schultz, M. G., Schröder, S., Chang, K.-L., Gaudel, A., Benítez, G. C., Cuevas, E., Fröhlich, M., Galbally, I. E., Molloy, S., Kubistin, D. Lu, X., McClure-Begley, A., Nédélec, P., O'Brien, J., Oltmans, S. J., Petropavlovskikh, I., Ries, L., Senik, I. Sjöberg, K., Solberg, S., Spain, G. T., Spang, W., Steinbacher, M., Tarasick, D., Thouret V., and Xu, X.: Multi-decadal surface ozone trends at globally distributed remote locations, *Elem Sci Anth*, 8, 1–34, DOI: <https://doi.org/10.1525/elementa.420>, 2020.
- 930 Cooper, O. R., Parrish, D. D., Ziemke, J., Balashov, N. V., Cupeiro, M., Galbally, I. E., Gilge, S., Horowitz, L., Jensen, N. R., Lamarque, J.-F., Naik, V., Oltmans, S. J., Schwab, J., Shindell, D. T., Thompson, A. M., Thouret, V., Wang, Y., Zbinden, R. M.: Global distribution and trends of tropospheric ozone: An observation-based review, *Elementa*, 2, 1–28, DOI: <https://doi.org/10.12952/journal.elementa.000029>, 2014.

- Conradie, E. H., Van Zyl, P. G., Pienaar, J. J., Beukes, J. P., Galy-Lacaux, C., Venter, A. D., and Mkhathshwa, G. V.: The chemical composition and fluxes of atmospheric wet deposition at four sites in South Africa, *Atmos. Environ.*, 146, 113–131, <https://doi.org/10.1016/j.atmosenv.2016.07.033>, 2016.
- Cros, B., Fontan, J., Minga, A., Helas, G., Nganga, D., Delmas, R., Chapuis, A., Benech, B., Druilhet, A., and Andreae, M. O.: Vertical profiles of ozones between 0 and 400 meters in and above the African equatorial Forest, *J. Geophys. Res.*, 97, 12877–12887, 1992.
- Darras, S., Granier, C., Liousse, C., Doumbia, T., Keita, S., Soulie, A.: The ECCAD database: Access to a variety of inventories of emissions for greenhouse gases and air pollutants, 35ème colloque annuel de l'Association Internationale de Climatologie – AIC, France, 6–9 July 2022, 1–6, 2022.
- Debaje, S. B., Jeyakumar, S. J., Ganesan, K., Jadhav, D. B., and Seetaramayya, P.: Surface ozone measurements at tropical rural coastal station Tranquebar, India, *Atmos. Environ.*, 37, 4911–4916, <https://doi.org/10.1016/j.atmosenv.2003.08.005>, 2003.
- Delon, C., Galy-Lacaux, C., Adon, M., Liousse, C., Serça, D., Diop, B., and Akpo, A.: Nitrogen compounds emission and deposition in West African ecosystems: comparison between wet and dry savanna *Biogeosciences*, 9, 385–402, 2012. doi:10.5194/bg-9-385-2012, 2012.
- Delon, C., Galy-Lacaux, C., Boone, A., Liousse, C., Serça, D., Adon, M., Diop, B., Akpo, A., Lavenu, F., Mougou, E., and Timouk, F.: Atmospheric nitrogen budget in Sahelian dry savannas, *Atmos. Chem. Phys.*, 10, 2691–2708, <https://doi.org/10.5194/acp-10-2691-2010>, 2010.
- Delon, C., Mougou, E., Serça, D., Grippa, M., Hiernaux, P., Diawara, M., Galy-Lacaux, C., Kergoat, L.: Modelling the effect of soil moisture and organic matter degradation on biogenic NO emissions from soils in Sahel rangeland (Mali), *Biogeosciences*, 12, 3253–3272. <https://doi.org/10.5194/bg-12-3253-2015>, 2015.
- Diab, R. D., Raghunandan, A., Thompson, A. M., and V. Thouret, V.: Classification of tropospheric ozone profiles over Johannesburg based on mozaic aircraft data, *Atmos. Chem. Phys.*, 3, 713–723, <https://doi.org/10.5194/acp-3-713-2003>, 2003.
- Diab, R. D., Thompson, A. M., Mari, K., Ramsay, L., and Coetzee, G. J. R.: Tropospheric ozone climatology over Irene, South Africa, from 1990 to 1994 and 1998 to 2002, *Journal of geophysical research*, 109, 20301–203012, doi:10.1029/2004JD004793, 2004.
- Dufour, G., Hauglustaine, D., Zhang, Y., Eremenko, M., Cohen, Y., Siour, G., Lachatre, M., Bense, A., Bessagnet, B., Cuesta, J., Thouret, V., and Zheng, B., Gaudel, A., Ziemke, J.: Recent ozone trends in the Chinese free troposphere: role of the local emission reductions and meteorology. *Atmos. Chem. Phys.*, 21, 16001–16025, <https://doi.org/10.5194/acp-21-16001-2021>, 2021.
- Ferm, M.: A Sensitive Diffusional Sampler, IVL Report L91, Göteborg, Swedish Environmental Research Institute, Sweden, 12pp, ISSN 0283-877X, 1991.
- Ferm, M., Rodhe, H.: Measurements of Air Concentrations of SO<sub>2</sub>, NO<sub>2</sub> and NH<sub>3</sub> at Rural and Remote Sites in Asia, *Journal of atmospheric chemistry*, 27, 17–29, <http://dx.doi.org/10.1023/A:1005816621522>, 1997.
- Ferreira, J., Reeves, C. E., Murphy, J. G., Garcia-Carreras, L., Parker, D. J., and Oram, D. E.: Isoprene emissions modelling for West Africa: MEGAN model evaluation and sensitivity analysis, *Atmos. Chem. Phys.*, 10, 8453–8467, <https://doi.org/10.5194/acp-10-8453-2010>, 2010.
- Fleming, Z. L., Doherty, R. M., von Schneidmesser, E., Malley, C. S., Cooper, O. R., Pinto, J. P., Colette, A., Xu, X., Simpson, D., Schultz, M. G., Lefohn, A. S., Hamad, S., Moolla, R. Solberg, S., and Feng, Z.: Tropospheric Ozone Assessment Report: Present-day ozone distribution and trends relevant to human health, *Elem Sci Anth*, 6, 1–41 DOI: <https://doi.org/10.1525/elementa.273>, 2018.
- Fowler, D., Pilegaard, K., Sutton, M.A., Ambus, P., Raivonen, M., Duyzer, J., Simpson, D., Fagerli, H., Fuzzi, S., Schjoerring, J.K., Granier, C., Neftel, A., Isaksen, I.S.A., Laj, P., Maione, M., Monks, P.S., Burkhardt, J., Daemmgen, U., Neiryneck, J., Personne, E., Wichink-Kruit, R., Butterbach-Bahl, K., Flechard, C., Tuovinen, J.P., Coyle, M., Gerosa, G., Loubet, B., Altimir, N., Gruenhage, L., Ammann, C., Cieslik, S., Paoletti, E., Mikkelsen, T.N., Ro-Poulsen, H., Cellier, P., Cape, J.N., Horvath, L., Loreto, F., Niinemets, Ü., Palmer, P.I., Rinne, J., Misztal, P., Nemitz, E., Nilsson, D., Pryor, S., Gallagher, M.W., Vesala, T., Skiba, U., Brüggemann, N., Zechmeister-Boltenstern, S., Williams, J., O’ Dowd, C., Facchini, M.C., De Leeuw, G., Flossman, A., Chaumerliac, N., Erismann, J.W. : Atmospheric composition change: ecosystems-Atmosphere interactions, *Atmos. Environ.* 43, 5193–5267. <https://doi.org/10.1016/j.atmosenv.2009.07.068>, 2009.
- Frimpong, B. F., Koranteng, A., and Molkenthin, F.: Analysis of temperature variability utilising Mann–Kendall and Sen’s slope estimator tests in the Accra and Kumasi Metropolises in Ghana. *Environmental Systems Research*, 11, 1–13, <https://doi.org/10.1186/s40068-022-00269-1>, 2022.
- Galanter, M., Levy I. I., H., and Carmichael, G. R.: Impacts of biomass burning on tropospheric CO, NO<sub>2</sub>, NO<sub>x</sub>, and O<sub>3</sub>, *J. Geophys. Res.*, 105, 6633–6653, doi: 10.1029/1999JD901113, 2000.
- Galy-Lacaux, C., Delon, C., Bakayoko, A., Gardrat, E., Dias Alves, M. & Okumu, S.: Trace gases, Mbita, Kenya, [dataset], AERIS. <https://doi.org/10.25326/642>, 2023g.
- Galy-Lacaux, C., Diop, B., Orange, D., Sanogo, S., Soumaguel, N., Kanouté, C.O., Gardrat, E., Dias Alves, M., Lenoir, O., Ossouhou, M., Adon, M. & Al-Ourabi, H.: Trace gases, Katigoubou, Mali, [dataset], AERIS, <https://doi.org/10.25326/604>, 2023a.
- Galy-Lacaux, C., Dorego, G.S., Gardrat, E., Dias Alves, M., Lenoir, O., Der Ba, S., N’Diaye, G.R., Séné, M., Thiam, A., Féron, A. & Ossouhou, M.: Trace gases, Bambey, Senegal, [dataset]. AERIS. <https://doi.org/10.25326/609>, 2023c.

- Galy-Lacaux, C., Laouali, D., Descroix, L., Gobron, N., Lioussé, C.: Long term precipitation chemistry and wet deposition in a remote dry savanna site in Africa (Niger). *Atmos. Chem. Phys.*, 9, 1579–1595, <https://doi.org/10.5194/acp-9-1579-2009>, 2009.
- 990 Galy-Lacaux, C. and Modi, A.I.: Precipitation Chemistry in the Sahelian Savanna of Niger, Africa, *Journal of Atmospheric Chemistry*, 30, 319–343, 1998.
- Galy-Lacaux, C., Mougin, E., Maïga, H., Soumaguel, N., Delon, C., Gardrat, E., Dias Alves, M., Lenoir, O. & Lavenu, F.: Trace gases, Agoufou, Mali, [dataset], AERIS, <https://doi.org/10.25326/610>, 2023b.
- Galy-Lacaux, C., N'Diaye, O., Guiro, I., Ba, D., Delon, C., Gardrat, E., Dias Alves, M., Lenoir, O. & Osohou, M.: Trace gases, Dahra, Senegal, [dataset], AERIS, <https://doi.org/10.25326/606>, 2023d.
- 995 Galy-Lacaux, C., Tathy, J.-P., Opepa, C.K., Brncic, T., Gardrat, E., Dias Alves, M. & Lenoir, O.: Trace gases, Bomassa, Congo, [dataset], AERIS, <https://doi.org/10.25326/607>, 2023f.
- Galy-Lacaux, C., Yoboué, V., Osohou, M., Gardrat, E., Dias Alves, M., Lenoir, O., Konaté, I., Ki, A.F., Ouattara, A., Adon, M., Al-Ourabi, H. & Zouzou, R.: Trace gases, Lamto, Côte d'Ivoire, [dataset], AERIS, <https://doi.org/10.25326/275>, 2323e.
- 1000 García-Lázaro, J., Moreno-Ruiz, J., Riaño, D., Arbelo, M.: Estimation of burned area in the northeastern siberian boreal forest from a long-term data record (LTDR) 1982–2015 time series. *Rem. Sens.* 10, 1–15, <https://doi.org/10.3390/rs10060940>, 2018.
- [Gaudel, A., Bourgeois, I., Meng, Chang, K.-L., Ziemke, J., Sauvage, B., Stauffer, R. M., Thompson, A. M., Kollonige, D. E., Smith, N., Hubert, D., Keppens, A., Cuesta, J., Heue, K.-P., Veeffkind, P., Aikin, K., Jeff Peischl, Thompson, C. R., Ryerson, T. B., Frost, G. J., McDonald, B. C., and Cooper, O. R. : Tropical tropospheric ozone distribution and trends from in situ and satellite data, \*Atmos. Chem. Phys.\*, 24, 9975–10000, <https://doi.org/10.5194/acp-24-9975-2024>, 2024.](#)
- 1005 Gaudel, A., Cooper, O. R., Ancellet, G., Barret, B., Boynard, A., Burrows, J. P., Clerbaux, C., Coheur, P.-F., Cuesta, Cuevas, J. E., Doniki, S., Dufour, Ebojje, G. F., Foret, Garcia, G. O., Granados-Muñoz, M. J., Hannigan, J. W., Hase, F., Hassler, B., Huang, G., Hurtmans, D., Jaffe, D., Jones, N., Kalabokas, P., Kerridge, B., Kulawik, S., Latter, B., Leblanc, T., Le Flochmoën, E., Lin, W., Liu, J., Liu, X., Mahieu, E., McClure-Begley, A., Neu, J. L., Osman, M., Palm, M., Petetin, H., Petropavlovskikh, I., Querel, R., Rapp, R. N., Rozanov, A., Schultz, M. G., Schwab, J., Siddans, R., Smale, D., Steinbacher, M., Tanimoto, H., Tarasick, D. W., Thouret, V., Thompson, A. M., Trick, T., Weatherhead, E., Wespes, C., Worden, H. M., Vigouroux, C., Xu, X., Zeng, G., Ziemke, J.: Tropospheric Ozone Assessment Report: Present-day ozone distribution and trends relevant to climate and model evaluation, *Elem Sci Anth*, 6, 1–58, DOI: <https://doi.org/10.1525/elementa.291>, 2018.
- 1010 Gaudel, A., Cooper, O. R., Chang, K.-L., Bourgeois, I., Ziemke, J. R., Strode, S. A., Oman, L. D., Sellitto, P., Nédélec, P., Blot, R., Thouret, V., Granier, C.: Aircraft observations since the 1990s reveal increases of tropospheric ozone at multiple locations across the Northern Hemisphere, *Sci. Adv.*, 6, 1–11, DOI: 10.1126/sciadv.aba8272, 2020.
- 1015 Graedel, T. E., and P. J.: Crutzen.: *Atmospheric Change: An Earth System Perspective*, NY: W. H. Freeman and Company, New York, 446 pp, ISBN 0716723344, 1993.
- Guenther, A., Karl, T., Harley, P., Wiedinmyer, C., Palmer, P. I., and Geron, C.: Estimates of global terrestrial isoprene emissions using MEGAN (Model of Emissions of Gases and Aerosols from Nature), *Atmos. Chem. Phys.*, 6, 3181–3210, doi:10.5194/acp-6-3181, 2006
- 1020 Hagenbjörk, A., Malmqvist, E., Mattisson, K., Sommar, N. J., Modig, L.: The spatial variation of O<sub>3</sub>, NO, NO<sub>2</sub> and ~~NO<sub>x</sub>~~ and the relation between them in two Swedish cities, *Environ. Monit. Assess.* 189, 161–172, <https://doi.org/10.1007/s10661-017-5872-z>, 2017.
- Hamdun, A. M., and Arakaki T.: Analysis of Ground Level Ozone and Nitrogen Oxides in the City of Dar es Salaam and the Rural Area of Bagamoyo, Tanzania, *Open Journal of Air Pollution*, 4, 224–238, doi: 10.4236/ojap.2015.44019, 2015.
- 1025 Heue, K.-P., Coldewey-Egbers, M., Delcloo, A., Lerot, C., Loyola, D., Valks, P., and van Roozendaal, M., : Trends of tropical tropospheric ozone from 20 years of European satellite measurements and perspectives for the Sentinel-5 Precursor, *Atmos. Meas. Tech.*, 9, 5037–5051, 2016.
- Hirsch, R. M., Slack, J. R., Smith, R. A.: Techniques of trend analysis for monthly water quality data, *Water Resour. Res.* 18, 107–121. <https://doi.org/10.1029/WR018i001p00107>, 1982.
- 1030 Homyak P. M., Sickman, J. O., Miller, A. E., Melack, J. M., and Schimel, J. P., : Assessing N saturation in a seasonally dry chaparral watershed: Limitations of traditional indicators of N saturation, *Ecosystems*, 17: 1286–1305, <https://doi.org/10.1007/s10021-014-9792-2>, 2014.
- Hou, X.; Zhang, Y.; Lv, X.; Lee, J.: The Impact of Meteorological Conditions and Emissions on Tropospheric Column Ozone Trends in Recent Years. *Remote Sens.* 15, 5293–5305, <https://doi.org/10.3390/rs15225293>, 2023.
- 1035 Ihedike, C., Mooney, J. D., Fulton, J., and Ling, J.: Evaluation of real-time monitored ozone concentration from Abuja, Nigeria, *BMC Public Health*, 23, 1–7, <https://doi.org/10.1186/s12889-023-15327-1>, 2023.
- Jaars, K., van Zyl, P. G., Beukes, J. P., Hellén, H., Vakkari, V., Josipovic, M., Venter, A. D., Räsänen, M., Knoetze, L., Cilliers, D. P., Siebert, S. J., Kulmala, M., Rinne, J., Guenther, A., Laakso, L., and Hakola, H.: Measurements of biogenic volatile organic compounds at a grazed savannah grassland agricultural landscape in South Africa, *Atmos. Chem. Phys.*, 16, 15665–15688, 2016.
- 1040 Jaegle, L., Martin, R. V., Chance, K., Steinberger, L., Kurosu, T. P., Jacob, D. J., Modi, A. I., Yoboué, V., Sigha-Nkamdjou, L., and Galy-Lacaux, C.: Satellite mapping of rain-induced nitric oxide emissions from soils, *J. Geophys. Res.*, 109, 1–10, doi:10.1029/2004JD004787, 2004.

- Josipovic, M., Annegarn, H. J., Kneen, M. A., Pienaar, J. J. and Piketh, S. J.: Concentrations, distributions and critical level exceedance assessment of SO<sub>2</sub>, NO<sub>2</sub> and O<sub>3</sub> in South Africa, *Environmental Monitoring and Assessment*, 171, 181–196, DOI: 10.1007/s10661-009-1270-5, 2010.
- 1045 Kai, R. F., Scholes, M. C., Piketh, S. J., Scholes, R. J.: Analysis of the first surface nitrogen dioxide concentration observations over the South African Highveld derived from the Pandora-2s instrument, *Clean air journal*, 32, 1–11, <http://dx.doi.org/10.17159/caj/2022/32/1.13242>, 2022.
- Kendall, M.G.: *Rank Correlation Methods*, fourth ed. Charles Griffin, 4th Edition, Charles Griffin, London, 1975.
- 1050 Keita, S., Liousse, C., Assamoi, E.-M., Doumbia, T., N'Datchoh, E. T., Gnamien, S., Elguindi, N., Granier, C. and Yoboué, V.: African anthropogenic emissions inventory for gases and particles from 1990 to 2015, *Earth Syst. Sci. Data*, 13, 3691–3705, <https://doi.org/10.5194/essd-13-3691-2021>, 2021.
- Khoder, M. I., Diurnal, Seasonal and Weekdays-Weekends Variations of Ground Level Ozone Concentrations in an Urban Area in Greater Cairo. *Environmental Monitoring and Assessment*, 149, 349–362, <https://doi.org/10.1007/s10661-008-0208-7>, 2009.
- 1055 Kimayu, J. M., Gikuma-Njuru, P., and Musembi, D. K.: Temporal and Spatial Variability of Tropospheric Ozone in Nairobi City, Kenya, *Physical Science International Journal*, 13, 1–12, DOI: 10.9734/PSIJ/2017/31452, 2017.
- Laakso, L., Vakkari, V., Virkkula, A., Laakso, H., Backman, J., Kulmala, M., Beukes, J. P., van Zyl, P. G., Tiitta, P., Josipovic, M., Pienaar, J. J., Chiloane, K., Gilardon, S., Vignati, E., Wiedensohler, A., Tuch, T., Birmili, W., Piketh, S., Collett, K., Fourie, G. D., Komppula, M., Lihavainen, H., de Leeuw, G., and Kerminen, V.-M.: South African EUCAARI measurements: seasonal variation of trace gases and aerosol optical properties, *Atmos. Chem. Phys.*, 12, 1847–1864, <https://doi.org/10.5194/acp12-1847-2012>, 2012.
- 1060 Laakso, L., Laakso, H., Aalto, P. P., Keronen, P., Petäjä, T., Nieminen, T., Pohja, T., Siivola, E., Kulmala, M., Kgabi, N., Molefe, M., Mabaso, D., Phalatsé, D., Pienaar, K., and Kerminen, V.-M.: Basic characteristics of atmospheric particles, trace gases and meteorology in a relatively clean Southern African Savannah environment, *Atmos. Chem. Phys.*, 8, 4823–4839, <https://doi.org/10.5194/acp-8-4823-2008>, 2008.
- 1065 Laban, T. L., Van Zyl, P. G., Beukes, J. P., Mikkonen, S., Santana, L., Josipovic, M., Vakkari, Thompson, A. M., Kulmala, M. and Laakso L.: Statistical analysis of factors driving surface ozone variability over continental South Africa, *Journal of Integrative Environmental Sciences*, pp; 1–28, DOI:10.1080/1943815X.2020.1768550, 2020.
- Laban, T. L., Van Zyl, P. G., Beukes, J. P., Vakkari, V., Jaars, K., Borduas-Dedekind, N., Josipovic, M., Thompson, A. M., Kulmala, M., Laakso, L.: Seasonal influences on surface ozone variability in continental South Africa and implications for air quality, *Atmos. Chem. Phys.*, 15491–15514. <https://doi.org/10.5194/acp-18-15491-2018>, 2018.
- 1070 Lacaux, J. P., Tathy, J. P., and Sigha, L.: Acid wet deposition in the tropics: two case studies using DEBITS measurements, *IGACTivities Newsletter of the International Global Atmospheric Chemistry Project*, DEBITS Special 2, 13–18, 2003.
- Lannuque, V., Sauvage, B., Barret, B., Clark, H., Athier, G., Boulanger, D., Cammas, J.-P., Cousin, J.-M., Fontaine, A., Le Flochmoën, E., Nédélec, P., Petetin, H., Pfaffenzeller, I., Rohs, S., Smit, H. G. J., Wolff, P., and Thouret, V.: Origins and characterization of CO and O<sub>3</sub> in the African upper troposphere, *Atmos. Chem. Phys.*, 21, 14535–14555, <https://doi.org/10.5194/acp-21-14535-2021>, 2021.
- 1075 Laouali, D., Galy-Lacaux, C., Gardrat, E., Dias Alves, M., Lenoir, O., Zakou, A., Ossouhou, M., Adon, M. & Al-Ourabi, H.: Trace gases, Banizoumbou, Niger, [dataset], Aeris, <https://doi.org/10.25326/608>, 2023.
- Laville, P., Henault, C., Gabrielle, B., and Serca, D.: Measurement and modelling of NO fluxes over maize and wheat crops during their growing seasons: effect of crop management, *Nutr. Cycl. Agroecosyst.* 72, 159–171, doi: 10.1007/s10705-005-0510-5, 2005.
- 1080 Lee, J. D., Squires, F. A., Sherwen, T., Wilde, S. E., Cliff, S. J., Carpenter, L. J., Hopkins, J. R., Bauguitte, S. J., Reed, C., Barker, P., Allen, G., Bannan, T. J., Matthews, E., Mehra, A., Percival, C., Heard, D. E., Whalley, L. K., Ronnie, G. V., Seldon, S., Ingham, T., Keller, C. A., Knowland, K. E., Nisbet, E. G., and Andrews, S.: Ozone production and precursor emission from wildfires in Africa, *Environ. Sci.: Atmos.*, 1, 524–542., doi: 10.1039/D1EA00041A, 2021.
- Lefohn, A. S., Malley, C. S., Smith, L., Wells, B., and Hazucha, M.: Tropospheric Ozone Assessment Report: Global ozone metrics for climate change, human health, and crop/ecosystem research, *Elem Sci Anth*, 6, 1–39 DOI: <https://doi.org/10.1525/elementa.279>, 2018.
- 1085 Lelieveld, J., Evans, J. S., Fnais, M., Giannadaki, D., and Pozzer, A.: The contribution of outdoor air pollution sources to premature mortality on a global scale, *Nature*, 525, 367–371, <https://doi.org/10.1038/nature15371>, 2015.
- Lin, M., Horowitz, L. W., Cooper, O. R., Tarasick, D., Conley, S., Iraci, L. T., Johnson, B., Leblanc, T., Petropavlovskikh, I., and Yates, E. L.: Revisiting the evidence of increasing springtime ozone mixing ratios in the free troposphere over western North America., *Geophys Res Lett* 42, 8719–8728. DOI: <https://doi.org/10.1002/2015GL065311>, 2015.
- 1090 Liu, Y., Schallhart, S., Taipale, D., Tykkä, T., Räsänen, M., Merbold, L., Hellén, H., and Pellikka, P.: Seasonal and diurnal variations in biogenic volatile organic compounds in highland and lowland ecosystems in southern Kenya, *Atmospheric Chemistry and Physics*, 21, 14761–14787, <https://doi.org/10.5194/acp-21-14761-2021>, 2021.
- Lourens, A. S., Beukes, J. P., Van Zyl, P. G., Fourie, G. D., Burger, J. W., Pienaar, J. J., Read, C. E., and Jordaan, J. H.: Spatial and temporal assessment of gaseous pollutants in the Highveld of South Africa, *S. Afr. J. Sci.*, 107, 1–8, doi: 10.4102/sajs.v107i1/2.269, 2011.
- 1095

- Lu, X., Zhang, L., Zhao, Y., Jacob, D. J., Hu, Y., Hu, L., Gao, M., Liu, X., Petropavlovskikh, I., McClure-Begley, A., Querel, R.: Surface and tropospheric ozone trends in the Southern Hemisphere since 1990: possible linkages to poleward expansion of the Hadley circulation, *Science Bulletin*, 64, 400–409, <https://doi.org/10.1016/j.scib.2018.12.021>, 2019.
- 1100 Ludwig, J., Meixner, F. X., Vogel, B., and Forstner, J.: Soil-air exchange of nitric oxide: An overview of processes, environmental factors, and modelling studies, *Biogeochemistry*, 52, 225–257, DOI: 10.1023/A:1006424330555, 2001.
- Mari, C. H., Reeves, C. E., Law, K. S., Ancellet, G., Andres-Hernandez, M. D., Barret, B., Bechara, J., Borbon, A., Bouarar, I., Cairo, F., Commane, R., Delon, C., Evans, M. J., Fierli, F., Floquet, C., Galy-Lacaux, C., Heard, D. E., Homan, C. D., Ingham, T., Larsen, N., Lewis, A. C., Liousse, C., Murphy, J. G., Orlandi, E., Oram, D. E., Saunio, M., Serça, D., Stewart, D. J., Stone, D., Thouret, V., van Velthoven, P. and Williams, J. E.: Atmospheric composition of West Africa: highlights from the AMMA international program, *Atmos. Sci. Let.* 12, 13–18, <https://doi.org/10.1002/asl.289>, 2011.
- 1105 Martins, J. J., Dhammapala, R. S., Lachmann, G., Galy-Lacaux, C., and Pienaar, J. J.: Long-term measurements of sulphur dioxide, nitrogen dioxide, ammonia, nitric acid and ozone in southern Africa using passive samplers, *S. Afr. J. Sci.*, 103, 336–342, <https://hdl.handle.net/10520/EJC96693>, 2007.
- Mayaux, P., Bartholomé, E., Fritz, S., and Belward, A.: A new land-cover map of Africa for the year 2000: New land-cover map of Africa. *J. Biogeogr.*, 31, 861–877, <https://doi.org/10.1111/j.1365-2699.2004.01073.x>, 2004.
- 1110 Merabtene, T., Siddique, M., Shanableh, A.: Assessment of seasonal and annual rainfall trends and variability in sharjah city, UAE. *Adv. Meteorol.* 2016, 1–13, <https://doi.org/10.1155/2016/6206238>, 2016.
- Mills, G., Pleijel, H., Malley, C. S., Sinha, B., Cooper, O. R., Schultz, M. G., Neufeld, H. S., Simpson, D., Sharps, K., Feng, Z., Gerosa, G., Harmens, H., Kobayashi, K., Saxena, P., Paoletti, E., Sinha, V., and Xu, X.: Tropospheric Ozone Assessment Report: Present-day tropospheric ozone distribution and trends relevant to vegetation. *Elem Sci Anth*, 6, 1–46, DOI: <https://doi.org/10.1525/elementa.302>, 2018.
- 1115 Morakinyo, O. M., Mukhola M. S., and Mokgobu. M. I.: Ambient Gaseous Pollutants in an Urban Area in South Africa: Levels and Potential Human Health Risk. *Atmosphere*, 11, 1–14, doi:10.3390/atmos11070751, 2020.
- Monks, P. S., Archibald, A. T., Colette, A., Cooper, O., Coyle, M., Derwent, R., Fowler, D., Granier, C., Law, K. S., Mills, G. E., Stevenson, D. S., Tarasova, O., Thouret, V., von Schneidemesser, E., Sommariva, R., Wild, O., and Williams, M. L.: Tropospheric ozone and its precursors from the urban to the global scale from air quality to short-lived climate forcer, *Atmos. Chem. Phys.*, 15, 8889–8973, <https://doi.org/10.5194/acp-15-8889-2015>, 2015.
- 1120 Monks, P., Leigh, R.: Tropospheric chemistry and air pollution. In: Hewitt, C.N., Jackson, A.V. (Eds.), *Atmospheric Science for Environmental Scientists*. Wiley-Blackwell, Oxford, UK, 300 pp, ISBN 978140518542-4, 2009.
- 1125 Mulumba, J.-P., Venkataraman, S., Thomas, J. O.: Modeling Tropospheric Ozone Climatology over Irene (South Africa) Using Retrieved Remote Sensing and Ground-Based Measurement Data, *J. Remote Sens. GIS*, 4, 151, DOI:10.4172/2469-4134.1000151, 2015.
- Ngoasheng, M., Beukes, J. P., van Zyl, P. G., Swartz, J.-S., Loate, V., Krisjan, P., Mpambani, S., Kulmala, M., Vakkari, V., and Laakso, L.: Assessing SO<sub>2</sub>, NO<sub>2</sub> and O<sub>3</sub> in rural areas of the North West Provinc. *Clean air journal*, 31, 1–14, <http://dx.doi.org/10.17159/caj/2021/31/1.9087>, 2021.
- 1130 Ojumu, A.M.: Transport of Nitrogen Oxides and Nitric Acid Pollutants over South Africa and Air Pollution in Cape Town. MSc, University of South Africa, 68 pp, 2013.
- Oltmans, S. J., Lefohn, A. S., Shadwick, D., Harris, J. M., Scheel, H. E., Galbally, I., Tarasick, D. W., Johnson, B. J., Brunke, E. G., Claude, H., Zeng, G., Nichol, S., Schmidlin, F., Davies, J., Cuevas, E., Redondas, A., Naoe, H., Nakano, T., and Kawasato, T.: Recent tropospheric ozone changes-A pattern dominated by slow or no growth, *Atmos. Environ.*, 67, 331–351, <https://doi.org/10.1016/j.atmosenv.2012.10.057>, 2013.
- 1135 Oluleye, A., and Okogbue, E. C.: Analysis of temporal and spatial variability of total column ozone over West Africa using daily TOMS measurements, *Atmospheric Pollution Research*, 4, 387–397, <https://doi.org/10.5094/APR.2013.044>, 2013.
- Ossouhou M., C. Galy-Lacaux, C., V. Yoboué, V., Hickmanc, J. E., Gardrat, E., Adona, M., Darrasi, S., Laoualie, D., Akpod, A., Ouafó, M., Diopg, B., Opepah, C.: Trends and seasonal variability of atmospheric NO and HNO concentrations across three major African biomes inferred from long-term series of ground-based and satellite measurements, *Atmos. Environ.* 207, 148–66, <https://doi.org/10.1016/j.atmosenv.2019.03.027>, 2019.
- 1140 Ouafó-Leumbe, M.-R., Galy-Lacaux, C., Sigha-Nkamdjou, L., Gardrat, E., Dias Alves, M., Lenoir, O., Meka, M.Z. & Amougou, M.: Trace gases, Zoétélé, Cameroon, [dataset], Aeris, <https://doi.org/10.25326/603>, 2023.
- 1145 Petäjä, T., Vakkari, V., Pohja, T., Nieminen, T., Laakso, H., Aalto, P. P., Keronen, P., Siivola, E., Kerminen, V.-M., Kulmala, M., and Laakso, L.: Transportable Aerosol Characterization Trailer with Trace Gas Chemistry: Design, Instruments and Verification, *Aerosol Air Qual. Res.*, 13, 421–435, <https://doi.org/10.4209/aaqr.2012.08.0207>, 2013.
- Petetin, H., Bowdalo, D., Bretonnière, P.-A., Guevara, M., Armengol, J. M., Cabre, M. S., Serradell, K., Jorba, O., Soret, A., and Garcia-Pando, C. P.: Model output statistics (MOS) applied to Copernicus Atmospheric Monitoring Service (CAMS) O<sub>3</sub> forecasts: trade-offs



- 1150 between continuous and categorical skill scores, *Atmos. Chem. Phys.*, 22, 11603–11630, <https://doi.org/10.5194/acp-22-11603-2022>, 2022.
- Rummel, U., Ammann, C., Kirkman, G. A., Moura, M. A. L., Foken, T., Andreae, M. O., and Meixner, F. X.: Seasonal variation of ozone deposition to a tropical rain forest in southwest Amazonia, *Atmos. Chem. Phys.*, 7, 5415–5435, doi:10.5194/acp-7-5415-2007, 2007.
- 1155 Sadiq, M., Tai, A. P. K., Lombardozzi, D., and Martin, M. V.: Effects of O<sub>3</sub>-vegetation coupling on surface O<sub>3</sub> air quality via biogeochemical and meteorological feedbacks, *Atmos. Chem. Phys.*, 17, 3055–3066. <https://doi.org/10.5194/acp-17-3055-2017>, 2017.
- Salem, A. A., Soliman, A. A., El-Haty, I. A.: Determination of nitrogen dioxide, sulfur dioxide, ozone, and ammonia in ambient air using the passive sampling method associated with ion chromatographic and potentiometric analyses, *Air Qual Atmos Health*, 2, 133–145, doi:10.1007/s11869-009-0040-4, 2009.
- 1160 Saunois, M., Reeves, C. E., Mari, C., Murphy, J. G., Stewart, D. J., Mills, G. P., Oram, D. E., and Purvis, R. M.: Ozone budget in the West African lower troposphere during the African Monsoon Multidisciplinary Analysis (AMMA) campaign, *Atmos. Chem. and Phys.*, 9, 6135–6155, doi:10.5194/acp-9-6135-2009, 2009.
- Sauvage, B., Gheusi, F., Thouret, V., Cammas, J.-P., Duron, J., Escobar, J., Mari, C., Mascart, P., and Pont, V.: Medium-range mid-tropospheric transport of ozone and precursors over Africa: two numerical case studies in dry and wet seasons, *Atmos. Chem. Phys.*, 7, 5357–5370, <https://doi.org/10.5194/acp-7-5357-2007>, 2007.
- 1165 Sauvage, B., Thouret, V., Cammas, J.-P., Gheusi, F., Athier, G., and Nédélec, P.: Tropospheric ozone over Equatorial Africa: regional aspects from the MOZIC data, *Atmos. Chem. Phys.*, 5, 311–335, <https://doi.org/10.5194/acp-5-311-2005>, 2005.
- Saxton, J. E., Lewis, A. C., Kettlewell, J. H., Ozel, M. Z., Gogus, F., Boni, Y., Korogone, S. O. U., and Serca, D.: Isoprene and monoterpene measurements in a secondary forest in northern Benin, *Atmos. Chem. Phys.*, 7, 4095–4106, <https://doi.org/10.5194/acp-7-4095-2007>, 2007.
- 1170 Schultz, M. G., et al.: Tropospheric Ozone Assessment Report: Database and metrics data of global surface ozone observations, *Elem Sci Anth*, 5, 1–26, DOI: <https://doi.org/10.1525/elementa.244>, 2017.
- Sen P., K.: Estimates of the regression coefficient based on Kendall's tau, *J. Am. Stat. Assoc.* 63, 1379–1389, <https://doi.org/10.2307/2285891>, 1968.
- 1175 Serca, D., Guenther, A., Klinger, L., Vierling, L., Harley, P., Druilhet, A., Greenberg, J., Baker, B., Baugh, W., Bouka-Biona, C., and Loemba-Ndembu, J.: EXPRESSO flux measurements at upland and lowland Congo tropical forest site, *Tellus B*, 53, 220–234, <https://doi.org/10.3402/tellusb.v53i3.16593>, 2001.
- Silva, S. J., & Heald, C. L.: Investigating Dry Deposition of O<sub>3</sub> to Vegetation, *J. Geophys. Res. Atmos.*, 123, 559–573. <https://doi.org/10.1002/2017JD027278>, 2018.
- 1180 Sindelarova, K., Granier, C., Bouarar, I., Guenther, A., Tilmes, S., Stavrou, T., Müller, J.-F., U. Kuhn, U., P. Stefani, P., and W. Knorr, W.: Global data set of biogenic VOC emissions calculated by the MEGAN model over the last 30 years, *Atmos. Chem. Phys.*, 14, 9317–9341, <https://doi.org/10.5194/acp-14-9317-2014>, 2014.
- Singh, H. B., Herlth, D., Kolyer, R., Chatfield, R., Viezee, W., Salas, L. J., Chen, Y., Bradshaw, J. D., Sandholm, S. T., Talbot, R., Gregory, G. L., Anderson, B., Sachse, G. W., Browell, E., Bachmeier, A. S., Blake, D. R., Heikes, B., Jacob, D., and Fuelberg, H. E.: Impact of biomass burning emissions on the composition of the South Atlantic troposphere: Reactive nitrogen and ozone, *J. Geophys. Res.-Atmos.*, 101, 24203–24219, <https://doi.org/10.1029/96JD01018>, 1996.
- 1185 Sivakumar, V., Ogunniyi, J.: Ozone climatology and variability over Irene, South Africa determined by ground based and satellite observations. Part 1: Vertical variations in the troposphere and stratosphere. *Atmósfera*, 30, 337–353, <https://doi.org/10.20937/atm.2017.30.04.05>, 2017.
- Sofen, E. D., Bowdalo, D., and Evans, M. J., How to most effectively expand the global surface ozone observing network, *Atmos Chem Phys* 16, 1445–1457. DOI: <https://doi.org/10.5194/acp-16-1445-2016>, 2016.
- 1190 Stauffer, R. M., Thompson, A. M., Kollonige, D. E., Komala, N., Al-Ghazali, H. K., Risdianto, D. Y., Dindang, A., bin Jamaluddin, A. F., Sammathuria, M. K., Zakaria, N. B., Johnson, B. J., Cullis, P. D.: Dynamical drivers of free-tropospheric ozone increases over equatorial Southeast Asia, *Atmos. Chem. Phys.*, <https://doi.org/10.5194/acp-24-5221-2024>, 2024.
- Stewart, D. J., Taylor, C. M., Reeves, C. E., and McQuaid, J. B.: Biogenic nitrogen oxide emissions from soils: impact on ~~NO<sub>x</sub>~~ and ozone over west Africa during AMMA (African Monsoon Multidisciplinary Analysis): observational study, *Atmos. Chem. Phys.*, 8, 2285–2297, doi:10.5194/acp-8-2285-2008, 2008.
- Swap, R. J., Annegarn, H. J., Suttles, J. T., King, M. D., Platnick, S., Privette, J. L., Scholes, R. J.: Africa burning: a thematic analysis of the southern African regional science initiative (SAFARI 2000), *J. Geophys. Res.* 108, 1–15, <https://doi.org/10.1029/2003JD003747>, 2003
- 1200 Swartz, J.-S., van Zyl, P. G., Beukes, J. P., Galy-Lacaux, C., Ramandh, A., and Pienaar, J. J.: Measurement report: Statistical modelling of long-term trends of atmospheric inorganic gaseous species within proximity of the pollution hotspot in South Africa, *Atmos. Chem. Phys.*, 20, 10637–10665, <https://doi.org/10.5194/acp-20-10637-2020>, 2020a.
- Swartz, J.-S., Van Zyl, P. G., Beukes, J. P., Labuschagne, C., Brunke, E.-G., Galy-Lacaux, C., Pienaar, J. J., Portafaix, T.: Twenty-one years of passive sampling monitoring of SO<sub>2</sub>, NO<sub>2</sub> and O<sub>3</sub> at the Cape Point GAW station, South Africa, *Atmospheric Environment* 222, 1–17, <https://doi.org/10.1016/j.atmosenv.2019.117128>, 2020b.

- 1205 Tarasick, D., Galball, I. E., Cooper, O. R., Schultz, M. G., Ancellet, G., Leblanc, T., Wallington, T. J., Ziemke, J., Liu, X., Steinbacher, M., Staehelin, J., Vigouroux, C., Hannigan, J. W., García, O., Foret, G., Zanis, P., Weatherhead, E., Petropavlovskikh, I., Worden, H., Osman, M., Liu, J., Chang, K.-L., Gaudel, A., Lin, M., Granados-Muñoz, M., Thompson, A. M., Oltmans, S. J., Cuesta, J., Dufour, G., Thouret, V., Hassler, B., Trick T., and Neu, J. L.: Tropospheric Ozone Assessment Report: Tropospheric ozone from 1877 to 2016, observed levels, trends and uncertainties. *Elem Sci Anth*, 7, 1–72. DOI: <https://doi.org/10.1525/elementa.376>, 2019.
- 1210 Thompson, A. M., Balashov, N. V., Witte, J. C., Coetzee, J. G. R., Thouret, V., and Posny, F.: Tropospheric ozone increases over the southern Africa region: Bellwether for rapid growth in Southern Hemisphere pollution? *Atmospheric Chemistry and Physics*, 14, 9855–9869. <https://doi.org/10.5194/acp-14-9855-2014>, 2014.
- Thompson, A. M., Stauffer, R. M., Wargan, K., Witte, J. C., Kollonige, D. E., Ziemke, J. R.: Regional and seasonal trends in tropical ozone from SHADOZ profiles: Reference for models and satellite products, *J. Geophys. Res.*,  
1215 <https://agupubs.onlinelibrary.wiley.com/doi/10.1029/2021JD034691>, 2021. Thompson, A. M., Witte, J. C., Oltmans, S. J., Schmidlin, F. J., Logan, J. A., Fujiwara, M., Kirchhoff, V. W. J. H., Posny, F., Coetzee, G. J. R., Hoegger, B., Kawakami, S., Ogawa, T., Fortuin, J. P. F., and Kelder H. M.: Southern Hemisphere Additional Ozonesondes (SHADOZ) 1998–2000 tropical ozone climatology. 2. Tropospheric variability and the zonal wave-one. *Journal of Geophysical Research*, 108(D2), 1–21, <https://doi.org/10.1029/2002JD002241>, 2003b.
- 1220 Tiitta, P., Vakkari, V., Croteau, P., Beukes, J.P., Zyl, P.G.V., Josipovic, M., Venter, A.D., Jaars, K., Pienaar, J.J., Ng, N.L., Canagaratna, M.R., Jayne, J.T., Kerminen, V.M., Kokkola, H., Kulmala, M., Laaksonen, A., Worsnop, D.R., Laakso, L., Chemical composition, main sources and temporal variability of PM1 aerosols in southern African grassland. *Atmos. Chem. Phys.* 14, 1909–1927. <https://doi.org/10.5194/acp-14-1909-2014>, 2014.
- Tsivlidou, M., Sauvage, B., Bennouna, Y., Blot, R., Boulanger, D., Clark, H., Le Flochmoën, E., Nédélec, P., Thouret, V., Wolff, P., and Barret, B.: Tropical tropospheric ozone and carbon monoxide distributions: characteristics, origins, and control factors, as seen by IAGOS and IASI, *Atmos. Chem. Phys.*, 23, 14039–14063, 2023 <https://doi.org/10.5194/acp-23-14039-2023>, 2023. Vakkari, V., Beukes, J.P., Laakso, H., Mabaso, D., Pienaar, J.J., Kulmala, M., Laakso, L.: Long-term observations of aerosol size distributions in semi-clean and polluted savannah in South Africa. *Atmos. Chem. Phys.* 13, 1751–1770. <https://doi.org/10.5194/acp-13-1751-2013>, 2013.
- Vet, R., Artx, R. S., Carou, S., Shaw, M., Ro, C., Aas, W., Baker, A., Bowersox, V. C., Dentener, F., Galy-Lacaux, C., Hou, A., Pienaar, J.J., Gillet, R., Forti, M. C., Gromov, S., Hara, H., Khodzher, T., Mahowald, N. M., Nickovic, S., Rao, P. S. P., Reid, N. W.: A global assessment of precipitation chemistry and deposition of sulfur, nitrogen, sea salt, base cations, organic acids, acidity and pH, and phosphorus, *Atmos. Environ.* 93, 3–100, <https://doi.org/10.1016/j.atmosenv.2013.10.060>, 2014.
- Vitolo, C., Di Giuseppe, F., D'Andrea, M.: Caliver: an R package for CALibration and VERification of forest fire gridded model outputs, *PLoS ONE*, 13, 1–18, <https://doi.org/10.1371/journal.pone.0189419>, 2018.
- 1235 [Wang, H., Lu, X., Jacob, D. J., Cooper, O. R., Chang, K. L., Li, K., Gao, M., Liu, Y., Sheng, B., Wu, K., Wu, T., Zhang, J., Sauvage, B., Nédélec, P., R., and Fan, S.: Global tropospheric ozone trends, attributions, and radiative impacts in 1995–2017: an integrated analysis using aircraft \(IAGOS\) observations, ozonesonde, and multi-decadal chemical model simulations, \*Atmos. Chem. Phys.\*, 22, 13753–13782, 2022 <https://doi.org/10.5194/acp-22-13753-2022>, 2022.](https://doi.org/10.5194/acp-22-13753-2022)
- Williams, J. E., Scheele, M. P., van Velthoven P. F. J., Cammas, J-P., Thouret V., Galy-Lacaux, C., Volz-Thomas, A.: The influence of biogenic emissions from Africa on tropical tropospheric ozone during 2006: a global modeling study, *Atmos. Chem. Phys.*, 9, 5729–5749, <https://doi.org/10.5194/acp-9-5729-2009>, 2009.
- Young, P. J., Archibald, A. T., Bowman, K. W., Lamarque, J.-F., Naik, V., Stevenson, D.S., Tilmes, S., Voulgarakis, A., Wild, O., Bergmann, D., Cameron-Smith, P., Cionni, I., Collins, W. J., Dalsøren, S. B., Doherty, R. M., Eyring, V., Faluvegi, G., Horowitz, L. W., Josse, B., Lee, Y. H., MacKenzie, I. A., Nagashima, T., Plummer, D. A., Righi, M., Rumbold, S. T., Skeie, R. B., Shindell, D. T., Strode, S. A., Sudo, K., Szopa, S. and Zeng, G.: Corrigendum to “Pre-industrial to end 21st century projections of tropospheric ozone from the Atmospheric Chemistry and Climate Model Intercomparison Project (ACCMIP)”, *Atmos. Chem. Phys.*, 13, 2063–2090, *Atmos. Chem. Phys.*, 13, 5401–5402. DOI: <https://doi.org/10.5194/acp-13-5401-2013>, 2013.
- Young, P. J., Naik, V., Fiore, A. M., Gaudel, A., Guo, J., Lin, M. Y., Neu, J. L., Parrish, D. D., Rieder, H. E., Schnell, J. L., Tilmes, S., Wild, O., Zhang, L., Ziemke, J., Brandt, J., Delcloo, A., Doherty, R. M., Geels, C., Hegglin, M. I., Hu, L., Im, U., Kumar, R., Luhar, A., Murray, L., Plummer, D., Rodriguez, J., Saiz-Lopez, A., Schultz, M. G., Woodhouse M. T., and Zeng G.: Tropospheric Ozone Assessment Report: Assessment of global-scale model performance for global and regional ozone distributions, variability, and trends, *Elem Sci Anth*, 6, 1–49, DOI: <https://doi.org/10.1525/elementa.265>, 2018.
- 1250 Zhang, Y., Cooper, O. R., Gaudel, A., Thompson, A. M., Nédélec, P., Ogino, S.-Y. and West, J. J.: Tropospheric ozone change from 1980 to 2010 dominated by equatorward redistribution of emissions. *Nature Geoscience* 9, 875–879, DOI: <https://doi.org/10.1038/ngeo2827>, 2016.
- 1255 Zunckel M., Venjonoka K., Pienaar J. J., Brunke E. G., Pretorius O., Koosiale A., Raghunandan A., van Tienhoven A. M., Surface ozone over southern Africa: synthesis of monitoring results during the cross-border air pollution impact assessment project. *Atmos Environ.* 38:6139–6147. doi:10.1016/j.atmosenv.2004.07.029, 2004.
- van Zyl, P.G., Jaars, K., Beukes, J.P., Pienaar, J.J., Fourie, G.D., van der Walt, H.J., Mkhathshwa, G.V., van der Merwe, C. & Deacon, M.: Trace gases, Amersfoort, South Africa, [dataset], Aeris, <https://doi.org/10.25326/647>, 2024d.
- 1260

- van Zyl, P.G., Jaars, K., Beukes, J.P., Pienaar, J.J., Fourie, G.D., van der Walt, H.J., Mkhathshwa, G.V., van der Merwe, C. & James, C.: Trace gases, Louis Trichardt, South Africa, [dataset], Aeris, <https://doi.org/10.25326/646>, 2024a.
- van Zyl, P.G., Jaars, K., Beukes, J.P., Pienaar, J.J., Fourie, G.D., van der Walt, H.J., Mkhathshwa, G.V., van der Merwe, C., Govender, N., Kubheka, W., Gardiner, E. & Tleane, J.: Trace gases, Skukuza, South Africa, [dataset], Aeris, <https://doi.org/10.25326/645>, 2024b.
- 1265 van Zyl, P.G., Jaars, K., Beukes, J.P., Pienaar, J.J., Labuschagne, C., Mkololo, T., Brunke, E.-G. & Joubert, W.: Trace gases, Cape Point, South Africa, [dataset], Aeris, <https://doi.org/10.25326/644>, 2024c.